PB 185562

TRACOR Document
Number 69-579-U
Project Serial
Number 004-009
Task Number 10

APPLICABILITY OF METAL OXIDES TO THE DEVELOPMENT OF NEW PROCESSES FOR REMOVING SO_2 FROM FLUE GASES

FINAL REPORT

VOLUME I

Sections 1-7

Contract PH 86-68-68

Submitted to:

Process Control Engineering Program
National Air Pollution Control
  Administration
5710 Wooster Pike
Cincinnati, Ohio   45227

31 July 1969

TRACOR

137

TRACOR 6500 TRACOR LANE, AUSTIN, TEXAS 78721

TRACOR Document
Number 69-579-U
Project Serial
Number 004-009
Task Number 10

APPLICABILITY OF METAL OXIDES TO THE DEVELOPMENT OF NEW PROCESSES FOR REMOVING SO_2 FROM FLUE GASES

FINAL REPORT

Contract PH 86-68-68

Submitted to:

Process Control Engineering Program
National Air Pollution Control
Administration
5710 Wooster Pike
Cincinnati, Ohio 45227

31 July 1969

Approved by:

A D Thomas, Jr
A. D. Thomas, Jr., Director
Chemistry and Materials
Research Department

Donald L Davis
Donald L. Davis, Head
Chemistry Section of the
Chemistry and Materials
Research Department

Prepared by:

Terry Parsons
(Mrs.) Terry Parsons
Engineer/Scientist

Gary D. Schroeder
Gary D. Schroeder
Engineer/Scientist

David DeBerry
David DeBerry
Engineer/Scientist

ACKNOWLEDGEMENTS

Contract PH 86-68-68, under which this study was performed, was supervised by Mr. Leon Stankus of the Process Control Engineering Program of the National Air Pollution Control Administration. His suggestions and advice have been of great value.

TRACOR 6500 TRACOR LANE, AUSTIN, TEXAS 78721

CONTRIBUTING TRACOR STAFF

During the past 19 months, the Research Laboratory's staff at TRACOR has had the opportunity of investigating a method for removing SO_2 from flue gas by the use of dry metal oxides sponsored under the Process Control Engineering Program of the National Air Pollution Control Administration. I would like to take this opportunity to acknowledge the contributions of those involved in this program and to compliment them on their technical achievements.

Dr. P. S. Lowell - Planned the program and directed all phases from 1 January 1968 until 1 March 1969, with particular emphasis on thermodynamic calculations and analysis.

Mr. D. L. Davis - Directed the program from 1 March 1969 to 31 July 1969 with particular emphasis on the experimental phase of the program and compilation of the final report.

Dr. Klaus Schwitzgebel - Planned the experimental program and performed thermodynamic and kinetic studies and X-ray analysis.

Mr. Gary Schroeder - Performed the engineering calculations for the economic studies.

Mrs. Terry Parsons - Conducted thermodynamic studies, BET and X-ray diffraction experimental work, and presented the results of this study at the Contractors' Meeting.

Mr. David DeBerry - Designed experimental apparatus, performed TGA measurements and kinetic studies, and analyzed the kinetic data.

TRACOR 6500 TRACOR LANE, AUSTIN, TEXAS 78721

Appreciation is also extended to Dr. William Koehler for help in experimental set up and data analysis; Mr. Floyd Felfe for building the BET apparatus; James Johnson, Erwin Kouba, and John Nolley for assistance in the experimental work, our secretaries, Betty Danner, Drusilla Johnson, Ann Slack, and Susan Swan; and Betsy Cates and Hal Blair for programming the computer.

We are also indebted to our consultants on the program, Dr. Karl Sladek, Dr. Ray Hurd, Dr. Joseph Lagowski, and Mr. Desmond Bond for their vital contributions.

A. D. Thomas, Jr.

A. D. Thomas, Jr.
Director of the
Research Laboratory

TRACOR 6500 TRACOR LANE, AUSTIN, TEXAS 78721

ABSTRACT

This report presents the results of a study to determine the applicability of metal oxides to the development of new processes for SO_2 removal. The oxides of 48 metals were screened according to the thermodynamics of their reaction with sulfur oxides to eliminate from consideration as potential sorbents those oxides that were not capable of reducing the sulfur oxide concentration in exiting flue gas of power plants to 150 ppm. Thermodynamic studies resulted in an extensive compilation of experimentally determined and estimated thermodynamic data. The result of the thermodynamic screening process was reduction of the field of potential sorbents to the oxides of sixteen metals, most of which appear in Groups VI, VII, and VIII of the periodic table. These potential sorbents are not only thermodynamically capable of reducing the SO_2 concentration to the desired limit, but the thermodynamics of the regeneration step are also favorable.

The remaining potential sorbents were prepared in a kinetically active form and the rates of their reaction with SO_2 in a simulated flue gas atmosphere were determined using isothermal gravimetric methods. There were two results of the kinetic studies. First, the field of potential sorbents was reduced to the oxides of copper, chromium, cobalt, iron, nickel, and cerium. Second, the rate data obtained provided inputs to cost estimation calculations for the economic feasibility studies.

The economic feasibility studies consisted of equipment design and sizing and estimation of the capital investment and gross annual operating cost for a sorber-regenerator system using a fluidized bed model. The cost estimations were carried out for the three best potential sorbents. Process flowsheets including heat and material balances were also prepared. The result of the economic feasibility studies for copper and iron oxides is a preliminary estimation for a capital investment of $8 million and a gross annual operating cost of $3 million.

TABLE OF CONTENTS

Section Page

1. INTRODUCTION 1

2. THERMODYNAMIC STUDIES 4

2.1 Introduction to Thermodynamic Studies 4

2.2 Literature Survey 4

Compounds of Interest
Information of Interest
Availability of Information

2.3 Compilation of Thermodynamic Properties 5

2.3.1 Properties Tabulated 5
2.3.2 Calculations Done with Thermodynamic Data. 5
2.3.3 Consistency of Data Base 6
2.3.4 Sources of Thermodynamic Data 6

2.3.4.1 Compilations 6
2.3.4.2 Open Literature 7
2.3.4.3 Estimation Methods 7

2.4 Thermal Stability Studies 27

2.4.1 Thermal Stability of Metal Oxides 27
2.4.2 Thermal Stability of Metal Sulfites . . . 31
2.4.3 Thermal Stability of Metal Sulfates . . . 35

2.5 Catalytic Oxidation Properties of Metal Oxides . 35

2.6 Determination of Price and Availability of Metal Oxides 36

2.7 Preliminary Screening Based on Thermodynamics and Sorbent Availability 36

2.7.1 Criteria for the Screening Process 36
2.7.2 Metal Oxide Screening 38
2.7.3 Mixed Metal Oxide Screening 38

TABLE OF CONTENTS (Cont'd.)

Section Page

3. KINETIC STUDIES 49

3.1 Introduction to Kinetic Studies 49

3.2 Approach 49

3.3 Compound Preparation and Characterization . . . 50

3.3.1 Preparation Methods 50
3.3.2 Use of X-ray Diffraction 50
3.3.3 BET Surface Area Determinations 52
3.3.4 Differential Thermal Analysis 57
3.3.5 Chemical Analysis 57

3.4 Kinetic Measurements 57

3.4.1 Apparatus 57
3.4.2 Experimental Procedure 67
3.4.3 Data Analysis 68
3.4.4 Input to Economic Studies 73

3.5 Results of the Experimental Program 74

3.5.1 Rate Equation and Reaction Orders . . . 77
3.5.2 Temperature Dependence of the Reaction Rate 86
3.5.3 Physical Properties and Reactivity . . . 87
3.5.4 Conclusions 87

4. ECONOMIC FEASIBILITY STUDIES 89

4.1 Introduction to Economic Feasibility Studies . 89

4.2 Sorption Unit Design 89

4.2.1 Sorber Design 92
4.2.2 Draft Fan and Driver Design 95
4.2.3 Sorbent Fines Collector (Cyclone) Design 97

4.3 Regeneration Unit Design 101

4.3.1 Regenerator Design 101

TABLE OF CONTENTS (Cont'd.)

Section Page

    4.3.2 Draft Fan and Driver Design 102
    4.3.3 Sorbent Fines Collector (Cyclone) Design 102
4.4 Total Capital Investment Cost 102
4.5 Gross Annual Operating Cost 108
4.6 Results 108
5. SUMMARY 113
6. REFERENCES 115
7. ABSTRACTS OF TECHNICAL MEMORANDUMS 118
7.1 Technical Memorandums on Thermodynamic Studies and Preliminary Screening 118
    7.1.1 Technical Memorandums on Estimation of Heat of Formation 118
        T.M. 004-009-Ch1
        T.M. 004-009-Ch1A
    7.1.2 Technical Memorandum on Estimation of Absolute Entropy 118
        T.M. 004-009-Ch5
    7.1.3 Technical Memorandums on Estimation of Heat Capacity. 118
        T.M. 004-009-Ch4
        T.M. 004-009-Ch9
        T.M. 004-009-Ch13
        T.M. 004-009-Ch13A
    7.1.4 Technical Memorandums on the Effect of Errors in Estimated Thermodynamic Properties . . 119
        T.M. 004-009-Ch2
        T.M. 004-009-Ch4

TABLE OF CONTENTS (Cont'd.)

Section | Page

7.1.5 Technical Memorandum on Conflicting Reported Thermodynamic Data 119

T.M. 004-009-Ch18

7.1.6 Technical Memorandums on Thermal Stability Studies 119

T.M. 004-009-Ch7

T.M. 004-009-CH8

T.M. 004-009-Ch3

T.M. 004-009-Ch16

7.1.7 Technical Memorandum on the Price and Availability of Metal Oxides 120

T.M. 004-009-Ch6

7.1.8 Technical Memorandums on Preliminary Screening of Metal Oxides and Mixed Metal Oxides 120

T.M. 004-009-Ch16

T.M. 004-009-Ch22

T.M. 004-009-Ch25

7.1.9 Technical Memorandum on Computer Programs 121

T.M. 004-009-Ch23

7.2 Technical Memorandums on the Kinetic Studies Experimental Program 121

7.2.1 Technical Memorandums on Design and Operation of Experimental Equipment . . 121

T.M. 004-009-Ch10

T.M. 004-009-Ch20

T.M. 004-009-Ch24

TABLE OF CONTENTS (Cont'd.)

Section		Page
	7.2.2 Technical Memorandum on Collection of Experimental Data and Presentation of Results	122
	T.M. 004-009-Ch24	
	Bimonthly Progress Report No. 8	
7.3	Technical Memorandums on Economic Feasibility Studies	122
	7.3.1 Technical Memorandums on Equipment Design, Size and Purchase Price	122
	T.M. 004-009-Ch19	
	T.M. 004-009-Ch14	
	T.M. 004-009-Ch15	
	T.M. 004-009-Ch15A	
	T.M. 004-009-Ch 21	
	7.3.2 Technical Memorandums on the Estimation of Capital Investment and Operating Cost	123
	T.M. 004-009-Ch26	
	T.M. 004-009-Ch11	
8.	UNABRIDGED TECHNICAL MEMORANDUMS AND ASSOCIATED DATA	
8.1	Unabridged Technical Memorandums	
	8.1.1 Technical Memorandums on Thermodynamic Studies	
	8.1.2 Technical Memorandums on Kinetic Studies	
	8.1.3 Technical Memorandums on Economic Feasibility Studies	
8.2	Thermodynamic, Kinetic, and Economic Data	
	8.2.1 Data Base of Thermodynamic Properties	

TABLE OF CONTENTS (Cont'd.)

Section Page

8.2.2 Log K Plots for Sulfate Decomposition Reactions

8.2.3 Plots of the Integrated Form of the Rate Equation

8.2.4 Economic Calculations for the Best Potential Sorbents

8.2.5 Process Flowsheets Including Heat and Material Balances

8.3 References Used in Writing Technical Memorandums

LIST OF ILLUSTRATIONS

Figure 1 Periodic Arrangement of Potential Sorbents before Screening 2
Figure 2 Decomposition of Lead Oxides 32
Figure 3 Logarithm of the Equilibrium Constant for the Disproportionation of Zinc Sulfite 33
Figure 4 Logarithm of the Equilibrium Constant for the Decomposition of Zinc Sulfite 34
Figure 5 Logarithm of the Equilibrium Constant for the Decomposition Reactions for Tin, Copper, and Barium Sulfates 39
Figure 6 Periodic Arrangement of Potential Sorbents after Thermodynamic Screening . . . 47
Figure 7 X-Ray Diffraction Patterns for Different Preparations of Co_3O_4 51
Figure 8 Adsorption Isotherm for Zirconium Oxide at 77°K 53
Figure 9 Schematic Diagram of Apparatus for Determining Specific Surface Area Using the BET Method 56
Figure 10 TRACOR TGA-3C Schematic Diagram 65
Figure 11 Schematic Diagram of Gas Mixing Apparatus 66
Figure 12 Representation of Rate Data for Copper Oxide at 404°C 72
Figure 13 Rate Data for Copper Oxide 80
Figure 14 Rate Data for Iron Oxide 81
Figure 15 Rate Data for Nickel Oxide 82
Figure 16 Rate Data for Cobalt Oxide 83
Figure 17 Rate Data for Cerium Oxide 84
Figure 18 Rate Data for Chromium Oxide 85
Figure 19 Arrhenius Plot for CuO 88
Figure 20 Potential Sorbents After Kinetic Screening. . 90
Figure 21 Economic Study Concept 91
Figure 22 Cyclone Separator Proportions 99
Figure 23 Process Flowsheet for the Copper Oxide Process 112

LIST OF TABLES

Table I	Heat of Formation at 25°C	9
Table II	Deviations of Estimated Values of Absolute Entropy	20
Table III	Estimated Heat Capacities for Carbonates with Known Heat Capacities	28
Table IV	Estimated Heat Capacities for Sulfates with Known Heat Capacities	29
Table V	Estimated Heat Capacities for Sulfides with Known Heat Capacities	30
Table VI	Properties of Oxides, Sulfates, and Sulfites.	40
Table VII	Determination of Specific Surface Area by the BET Method for ZrO_2	58
Table VIII	Results of Chemical Analyses	59
Table IX	Results of Experimental Program	75
Table X	Copper Oxide Sorber Physical Dimensions . . .	96
Table XI	Copper Oxide Sorber Input Variables for Fan Cost	98
Table XII	Copper Oxide Sorber Input Parameters for Cyclone	100
Table XIII	Copper Oxide Regenerator Physical Dimensions.	103
Table XIV	Copper Oxide Regenerator Input Variables for Fan Cost	104
Table XV	Copper Oxide Regenerator Input Parameters for Cyclone	105
Table XVI	Installation Cost Factors	107
Table XVII	Components of Gross Annual Operating Cost . .	109
Table XVIII	Summary of Cost Estimation for the Copper Oxide and Iron Oxide Processes	111

1. INTRODUCTION

Studies by the Department of Health, Education and Welfare have shown that the most pressing air pollution problem is the generation of sulfur oxides during combustion of fossil fuels. Processes for preventing sulfur oxide emission have been divided by NAPCA into nine areas. One of these areas is the sorption of sulfur oxides by dry metal oxides. The work described in this report was conducted under contract PH 86-68-68 to determine the applicability and economic feasibility of the use of dry metal oxides in a sulfur oxide removal process. The three objectives for the study are given below.

The first objective was to determine which of the oxides of the metals shown in Figure 1 were thermodynamically capable of lowering the SO_2 concentration in flue gases to a specified level and had a sorption product that could be regenerated to the original metal oxide sorbent with only a small expenditure of energy. Thermodynamic screening was conducted by determining the free energy of the sorption and regeneration reactions. Knowing the standard heat of formation, the absolute entropy, and the heat capacity as a function of temperature for the products and reactants of interest, the free energy for the sorption or regeneration reaction can be calculated. These thermodynamic properties of interest which had been determined experimentally and reported in the literature were computer tabulated. Properties of interest that had not been determined experimentally were estimated using carefully selected methods. The thermodynamic studies are discussed in Section 2.

The second objective was to determine which of the oxides remaining after thermodynamic screening had favorable kinetic properties. A kinetically favorable sorbent is one which reacts fast enough to be economically feasible. This objective was achieved by conducting an experimental program, since few kinetic

PERIOD	GROUP																	
	Ia	IIa	IIIa	IVa	Va	VIa	VIIa	VIII			Ib	IIb	IIIb	IVb	Vb	VIb	VIIb	0
1	H																H	He
2	Li	Be											B	C	N	O	F	Ne
3	Na	Mg											Al	Si	P	S	Cl	Ar
4	K	Ca	Sc	Ti	V	Cr	Mn	Fe	Co	Ni	Cu	Zn	Ga	Ge	As	Se	Br	Kr
5	Rb	Sr	Y	Zr	Nb	Mo	Tc	Ru	Rh	Pd	Ag	Cd	In	Sn	Sb	Te	I	Xe
6	Cs	Ba	La	Hf	Ta	W	Re	Os	Ir	Pt	Au	Hg	Tl	Pb	Bi	Po	At	Rn
7	Fr	Ra	Ac															

LANTHANIDE SERIES	Ce	Pr	Nd	Pm	Sm	Eu	Gd	Tb	Dy	Ho	Er	Tm	Yb	Lu

ACTINIDE SERIES	Th	Pa	U	Np	Pu	Am	Cm	Bk	Cf	Es	Fm	Md		Lw

PERIODIC ARRANGEGMENT OF
POTENTIAL SORBENTS BEFORE SCREENING

TRACOR

FIGURE 1

data for the reaction of metal oxides and sulfur oxides had been reported in the literature. The program consisted of preparing the compounds in a kinetically active form, determining their physical properties, and determining their rate of reaction with SO_2 in a simulated flue gas atmosphere. An isothermal gravimetric technique was used for the collection of kinetic data. The kinetic studies are described in Section 3.

The third objective was to determine the economic feasibility of the use of the selected sorbents in a sorber-regenerator system using a fluidized bed model for the gas-solid contactor. The economic feasibility studies consisted of designing and sizing equipment, preparing flowsheets and heat and material balances, and estimating total capital investment and gross annual operating cost for the process. The capital investment was estimated on the basis of the purchase price of the major pieces of equipment to which a percent of purchase price was added to account for various installation costs. Modified Lang percentage factors, as supplied by HEW, were used. The economic studies are discussed in Section 4.

A summary of results is given in Section 5; references are given in Section 6; Section 7 contains abstracts of the technical memorandums; and, Section 8 contains the unabridged memorandums.

2. THERMODYNAMIC STUDIES

2.1 INTRODUCTION TO THERMODYNAMIC STUDIES

The work done during the thermodynamic studies phase of the contract consisted of six main tasks: (1) a literature survey, (2) compilation of thermodynamic properties, (3) determination of cost and availability of metal oxides, (4) thermal stability studies, (5) study of catalytic oxidation properties, and (6) thermodynamic screening. The first five tasks were carried out so that the screening process would be possible. The goal of the thermodynamic screening process was to select as potential sorbents oxides which met the following two criteria. First the sorbent had to be thermodynamically capable of lowering the sulfur oxide concentration to the desired limit. Second, the regeneration step had to have only a small negative free energy change so that the expenditure of a great amount of energy would not be necessary to recover the sorbent. Thermal, rather than chemical regeneration was considered to be of importance. At the same time, the oxides were screened according to price and availability.

2.2 LITERATURE SURVEY

The literature was surveyed using Chemical Abstracts as a guide to determine existing knowledge about metal oxides and mixed metal oxides; flue gas components such as sulfur oxides, oxygen, nitrogen oxides, and carbon dioxide; and the reaction products, metal sulfates, sulfites, sulfides, and carbonates The information sought was of five types: (1) thermodynamic properties, (2) physical properties, (3) compound preparation methods, (4) reaction kinetics, and (5) descriptive information such as the course of a reaction, the existence of compounds, or the stability of compounds. Much valuable information was found on thermodynamic properties, compound preparation methods, physical properties, and descriptive subjects. Little, however, was available on the kinetics of the reactions of metal oxides and flue gas components.

2.3 COMPILATION OF THERMODYNAMIC PROPERTIES

2.3.1 Properties Tabulated

The second of the six tasks in the thermodynamic studies phase was to establish a data base of thermodynamic properties for the compounds described in Section 2.2. The following thermodynamic properties were tabulated: (1) heat of formation and absolute entropy at 25°C, (2) heat capacity from 25°C to 1000°C, or the data limit, whichever is lower, and (3) the temperature, type, and heat of phase transitions. A copy of the data base is given in Section 8.2 of this report.

2.3.2 Calculations Done with Thermodynamic Data

Using the thermodynamic properties stored in the data base, calculations were made with Equations (1) through (4) to describe the extent of reactions over any temperature range for compounds

$$\Delta G^\circ_T = \Delta H^\circ_T - T\Delta S^\circ_T \tag{1}$$

$$H^\circ_T = H^\circ_{298} + \sum_{i=0}^{I} \left[\int_{298}^{T_i} Cp(T)\,dT + \Delta H_{T_i} + \int_{T_i}^{T} Cp(T)\,dT \right] \tag{2}$$

$$S^\circ_T = S^\circ_{298} + \int_{298}^{T} \frac{Cp(T)}{T}\,dT \tag{3}$$

$$\ln K = \frac{-\Delta G^\circ_T}{RT} \tag{4}$$

for which data were stored. In Equation (2) T_i is the temperature of the ith phase transition and ΔH_{T_i} is the enthalpy of the ith transition. These calculations were an important source of thermodynamic information for the screening process which is discussed in Section 2.7.1. The compilation of thermodynamic properties was also used in the economic feasibility studies to make enthalpy calculations for determining heat balances for the sorber-regenerator system. The methods are discussed further in Section 4 and in detail in T.M. 004-009-Ch26. The thermodynamic properties and the data sources were stored in a digital computer for accuracy and ease of retrieval. The program, AIRPOL, stored, retrieved, and printed the thermodynamic properties and the references from which they were taken as well as calculated the change in enthalpy, entropy and the logarithm of the equilibrium constant for reactions involving the compounds for which data were stored. For a detailed description of this program see T.M. 004-009-Ch23.

2.3.3 Consistency of Data Base

A data base should be internally consistent; that is, the value of a property should be the same for all computational paths. It should also be consistent with the measurements from which the data were derived. When published literature values of measured heats of reaction were found, they were added to values for the heats of formation of the reactants in the TRACOR data base to calculate the heat of formation of the product. Therefore, the heat of formation reported in some references cited may differ from the heat of formation given in this compilation by an amount equal to the difference in the heats of formation of the reactants used. Again, these differences are due to an attempt to establish an internally consistent compilation.

2.3.4 Sources of Thermodynamic Data

The sources of thermodynamic properties were compilations of properties, open literature, and estimation methods.

2.3.4.1 Compilations: The compilations consulted were Landolt Boernstein, Chemisch-Physikalische Tabellen (LA-001), National Bureau of Standards, Selected Values of Chemical Thermodynamic Properties (NB-003, NB-005), JANAF Thermochemical Tables (JA-001), O. Kubaschewski, Metallurgical Thermochemistry (KU-001), and the U. S.

Bureau of Mines, Contributions to the Data on Theoretical Metallurgy, Parts I through X. Occasionally several major compilations reported widely differing values for some thermodynamic property of a compound. In such cases, the original literature from which the data for the compilation were taken was consulted. In many cases the conflicts were clearly resolved. When conflicting values were reported, the reference TR-010 was given. This refers to T.M. 004-009-Ch18, which is a detailed discussion of the selected values and the reasons for their selection.

2.3.4.2 Open Literature: Another source of data for the thermodynamic properties compilation was the open literature which was surveyed through 1967 using Chemical Abstracts as a guide. Information obtained from the open literature was carefully assessed using the values reported in Chemical Abstracts as well as the original literature in many cases. The Reports of Investigations published by the U. S. Bureau of Mines were important sources of thermodynamic data from the open literature. Since thermodynamic properties for all the compounds of interest had not been determined experimentally, estimation techniques had to be employed.

2.3.4.3 Estimation Methods: Thermodynamic properties had to be estimated for about 40% of the compounds tabulated. The estimation methods were selected by first studying the methods published by various authors. Next the best method was chosen on the basis of accuracy, theory, and applicability. The accuracy was determined by comparing accepted values with those calculated by each method and computing a root mean square (RMS) error. All of the unknown thermodynamic quantities were estimated from accepted, experimentally determined values of thermodynamic data using a Univac 1108 digital computer to perform the calculations and retrieve the data previously stored in the data base.

There are several ways to estimate the standard heat of formation of inorganic compounds. It was decided on the basis of accuracy and applicability that the method of Erdös would be applied to our problem.

Erdös gave the following equation for estimating the heat of reaction ΔH^R_{ij} between base i and acid j to form, for example, a salt, ij.

$$-\Delta H^R_{ij} = B_{ij} (K_i - A_j)^{n_j} \qquad (5)$$

In Equation (5), B_{ij} is the number of ion pair bonds formed, K_i is the cation combining power, A_j is the anion combining power and n_j is the anion exponent. The heat of formation of the oxide from a_{ij} moles of cation or base and b_{ij} moles of anion or acid is given in Equation (6).

$$\Delta H^f_{ij} = a_{ij} \Delta H^f_i + b_{ij} \Delta H^f_j + \Delta H^R_{ij} \qquad (6)$$

In applying the method of Erdös the existing data were correlated to determine the values for K, A, and n for each cation or anion species of interest. Then the unknown heats of formation were estimated for all possible combinations of the cations and anions.

The accepted values, estimated values, and correlation errors for the heat of formation method are given in Table I. The root mean square (RMS) error for the correlation was 3 kcal/mole. The selection of the Erdös method as the best for our data compilation is discussed in T.M. 004-009-Chl. The mathematical details of the application of the method and the results obtained are given

TABLE I

HEAT OF FORMATION AT 25 DEG C
(KCAL/GMOLE)

COMPOUND	I	J	PAIRS OF IONIC BONDS	HEAT OF FORMATION		
				CALCULATED	ACTUAL	ERROR
(AG)2(CO3)	1	1	1.0	-1.2454+02	-1.2088+02	3.6599+00
(BA) (CO3)	2	1	1.0	-2.9000+02	-2.8716+02	2.8460+00
(CA) (CO3)	3	1	1.0	-2.8568+02	-2.8811+02	-2.4366+00
(CD) (CO3)	4	1	1.0	-1.7681+02	-1.7846+02	-1.6454+00
(CO) (CO3)	5	1	1.0	-1.7424+02	-1.7331+02	9.2835-01
(CU+2) (CO3)	6	1	1.0	-1.4221+02	-1.4210+02	1.1684-01
(FE+2) (CO3)	7	1	1.0	-1.7838+02	-1.7855+02	-1.7829-01
(K)2(CO3)	8	1	1.0	-2.7402+02	-2.7187+02	2.1538+00
(LI)2(CO3)	9	1	1.0	-2.8687+02	-2.9026+02	-3.3984+00
(MG) (CO3)	10	1	1.0	-2.5980+02	-2.6398+02	-4.1796+00
(MN+2) (CO3)	11	1	1.0	-2.0963+02	-2.1374+02	-4.1091+00
(NA)2(CO3)	12	1	1.0	-2.7001+02	-2.6972+02	2.8867-01
(NI) (CO3)	13	1	1.0	-1.6910+02	-1.6298+02	6.1260+00
(PB) (CO3)	14	1	1.0	-1.7099+02	-1.6723+02	3.7567+00
(SR) (CO3)	15	1	1.0	-2.8673+02	-2.9098+02	-4.2510+00
(ZN) (CO3)	16	1	1.0	-1.9221+02	-1.9368+02	-1.4677+00
(AL+3)2(CO3)3	17	1	3.0	-7.0703+02		
(BE) (CO3)	18	1	1.0	-2.4689+02		
(BI+3)2(CO3)3	19	1	3.0	-4.7657+02		
(CE+4) (CO3)2	20	1	2.0	-4.6801+02		
(CS)2(CO3)	21	1	1.0	-2.7257+02	-2.7447+02	-1.9008+00
(CU+1)2(CO3)	22	1	1.0	-1.4229+02		
(FE+3)2(CO3)3	23	1	3.0	-5.0266+02		
(MN+3)2(CO3)3	24	1	3.0	-5.4546+02		
(RB)2(CO3)	25	1	1.0	-2.7144+02	-2.6948+02	1.9589+00
(SB+3)2(CO3)3	26	1	3.0	-4.6809+02		
(SN+4) (CO3)2	27	1	2.0	-3.3004+02		
(TH+4) (CO3)2	28	1	2.0	-5.1962+02		
(U+4) (CO3)2	29	1	2.0	-4.7820+02		
(ZR+4) (CO3)2	30	1	2.0	-5.0261+02		
(AG)2(SO4)	1	2	1.0	-1.7082+02	-1.7036+02	4.5900-01
(BA) (SO4)	2	2	1.0	-3.4958+02	-3.4999+02	-4.0657-01
(CA) (SO4)	3	2	1.0	-3.3624+02	-3.4019+02	-1.9570+00

TABLE I (continued)

(CD) (SO4)	4	2	1.0	-2.2237+02	-2.2120+02	1.1760+00
(CO) (SO4)	5	2	1.0	-2.2048+02		
(CU+2) (SO4)	6	2	1.0	-1.8064+02	-1.8422+02	-3.5806+00
(FE+2) (SO4)	7	2	1.0	-2.2347+02	-2.2041+02	3.0621+00
(K)2(SO4)	8	2	1.0	-3.4070+02	-3.4234+02	-1.6451+00
(LI)2(SO4)	9	2	1.0	-3.4267+02	-3.4258+02	9.0534-02
(MG) (SO4)	10	2	1.0	-3.0561+02	-3.0550+02	1.1123-01
(MN+2) (SO4)	11	2	1.0	-2.5611+02	-2.5395+02	2.1601+00
(NA)2(SO4)	12	2	1.0	-3.3192+02	-3.3064+02	1.2868+00
(NI) (SO4)	13	2	1.0	-2.1287+02	-2.1350+02	-6.3629-01
(PB) (SO4)	14	2	1.0	-2.1785+02	-2.1933+02	-1.4813+00
(SR) (SO4)	15	2	1.0	-3.4302+02	-3.4497+02	-1.9566+00
(ZN) (SO4)	16	2	1.0	-2.3441+02	-2.3369+02	7.1504-01
(AL+3)2(SO4)3	17	2	3.0	-8.2135+02	-8.2038+02	9.7059-01
(BE) (SO4)	18	2	1.0	-2.8610+02	-2.8565+02	4.4514-01
(BI+3)2(SO4)3	19	2	3.0	-6.0932+02	-6.0810+02	1.2200+00
(CE+4) (SO4)2	20	2	2.0	-5.6083+02	-5.6000+02	8.2569-01
(CS)2(SO4)	21	2	1.0	-3.4119+02	-3.3900+02	2.1918+00
(CU+1)2(SO4)	22	2	1.0	-1.7981+02	-1.7951+02	3.0120-01
(FE+3)2(SO4)3	23	2	3.0	-6.1652+02	-6.1560+02	9.2418-01
(MN+3)2(SO4)3	24	2	3.0	-6.6615+02	-6.6690+02	-7.5377-01
(RB)2(SO4)	25	2	1.0	-3.3919+02	-3.4019+02	-1.0078+00
(SB+3)2(SO4)3	26	2	3.0	-5.7542+02	-5.7420+02	1.2166+00
(SN+4) (SO4)2	27	2	2.0	-3.9308+02	-3.9340+02	-3.2331-01
(TH+4) (SO4)2	28	2	2.0	-6.0807+02	-6.0726+02	8.0502-01
(U+4) (SO4)2	29	2	2.0	-5.6344+02	-5.6300+02	4.4153-01
(ZR+4) (SO4)2	30	2	2.0	-5.9801+02	-5.9701+02	9.9767-01
(AG)2(FE2O4)	1	3	1.0	-2.0553+02		
(BA) (FE2O4)	2	3	1.0	-3.5555+02	-3.5049+02	5.0564+00
(CA) (FE2O4)	3	3	1.0	-3.5924+02		
(CD) (FE2O4)	4	3	1.0	-2.5873+02		
(CO) (FE2O4)	5	3	1.0	-2.5526+02		
(CU+2) (FE2O4)	6	3	1.0	-2.3149+02	-2.3751+02	-6.0234+00
(FE+2) (FE2O4)	7	3	1.0	-2.6093+02		
(K)2(FE2O4)	8	3	1.0	-3.3105+02		
(LI)2(FE2O4)	9	3	1.0	-3.5674+02	-3.4740+02	9.3391+00
(MG) (FE2O4)	10	3	1.0	-3.4140+02	-3.4922+02	-7.8227+00
(MN+2) (FE2O4)	11	3	1.0	-2.9036+02	-2.9300+02	-2.6383+00
(NA)2(FE2O4)	12	3	1.0	-3.3280+02		
(NI) (FE2O4)	13	3	1.0	-2.5369+02	-2.5646+02	-2.7692+00
(PB) (FE2O4)	14	3	1.0	-2.5122+02		

TABLE I (continued)

(SR) (FE204)	15	3	1.0	-3.5606+02		
(ZN) (FE204)	16	3	1.0	-2.7895+02		
(AL+3)2(FE204)3	17	3	3.0	-9.7513+02		
(BE) (FE204)	18	3	1.0	-3.3585+02		
(BI+3)2(FE204)3	19	3	3.0	-7.2792+02		
(CE+4) (FE204)2	20	3	2.0	-6.2965+02		
(CS)2(FE204)	21	3	1.0	-3.2716+02		
(CU+1)2(FE204)	22	3	1.0	-2.3180+02		
(FE+3)2(FE204)3	23	3	3.0	-7.7090+02		
(MN+3)2(FE204)3	24	3	3.0	-8.1067+02		
(RB)2(FE204)	25	3	1.0	-3.2713+02		
(SB+3)2(FE204)3	26	3	3.0	-7.3707+02		
(SN+4) (FE204)2	27	3	2.0	-5.0728+02		
(TH+4) (FE204)2	28	3	2.0	-6.8728+02		
(U+4) (FE204)2	29	3	2.0	-6.5072+02		
(ZR+4) (FE204)2	30	3	2.0	-6.6104+02		
(AG)2(CR04)	1	4	1.0	-1.7180+02	-1.7237+02	-5.7195-01
(BA) (CR04)	2	4	1.0	-3.3637+02		
(CA) (CR04)	3	4	1.0	-3.3257+02	-3.2944+02	3.1271+00
(CD) (CR04)	4	4	1.0	-2.2410+02		
(CO) (CR04)	5	4	1.0	-2.2149+02		
(CU+2) (CR04)	6	4	1.0	-1.8980+02		
(FE+2) (CR04)	7	4	1.0	-2.2569+02		
(K)2(CR04)	8	4	1.0	-3.1972+02		
(LI)2(CR04)	9	4	1.0	-3.3353+02		
(MG) (CR04)	10	4	1.0	-3.0708+02		
(MN+2) (CR04)	11	4	1.0	-2.5688+02		
(NA)2(CR04)	12	4	1.0	-3.1617+02	-3.1860+02	-2.4304+00
(NI) (CR04)	13	4	1.0	-2.1648+02		
(PB) (CR04)	14	4	1.0	-2.1821+02	-2.1750+02	7.1153-01
(SR) (CR04)	15	4	1.0	-3.3336+02		
(ZN) (CR04)	16	4	1.0	-2.3965+02		
(AL+3)2(CR04)3	17	4	3.0	-8.4981+02		
(BE) (CR04)	18	4	1.0	-2.9444+02		
(BI+3)2(CR04)3	19	4	3.0	-6.1862+02		
(CE+4) (CR04)2	20	4	2.0	-5.6251+02		
(CS)2(CR04)	21	4	1.0	-3.1806+02		
(CU+1)2(CR04)	22	4	1.0	-1.8990+02		
(FE+3)2(CR04)3	23	4	3.0	-6.4546+02		
(MN+3)2(CR04)3	24	4	3.0	-6.8801+02		
(RB)2(CR04)	25	4	1.0	-3.1702+02		

TABLE I (continued)

(SB+3)2(CRO4)3	26	4	3.0	-6.1109+02		
(SN+4) (CRO4)2	27	4	2.0	-4.2563+02		
(TH+4) (CRO4)2	28	4	2.0	-6.1433+02		
(U+4) (CRO4)2	29	4	2.0	-5.7304+02		
(ZR+4) (CRO4)2	30	4	2.0	-5.9697+02		
(AG)2(V2O6)	1	5	1.0	-3.9907+02		
(BA) (V2O6)	2	5	1.0	-5.6734+02		
(CA) (V2O6)	3	5	1.0	-5.6098+02	-5.5870+02	2.2825+00
(CD) (V2O6)	4	5	1.0	-4.5132+02		
(CO) (V2O6)	5	5	1.0	-4.4877+02		
(CU+2) (V2O6)	6	5	1.0	-4.1715+02		
(FE+2) (V2O6)	7	5	1.0	-4.5287+02		
(K)2(V2O6)	8	5	1.0	-5.5466+02		
(LI)2(V2O6)	9	5	1.0	-5.6295+02		
(MG) (V2O6)	10	5	1.0	-5.3432+02	-5.2790+02	6.4164+00
(MN+2) (V2O6)	11	5	1.0	-4.8418+02		
(NA)2(V2O6)	12	5	1.0	-5.4829+02	-5.5294+02	-4.6518+00
(NI) (V2O6)	13	5	1.0	-4.4359+02		
(PB) (V2O6)	14	5	1.0	-4.4555+02		
(SR) (V2O6)	15	5	1.0	-5.6296+02		
(ZN) (V2O6)	16	5	1.0	-4.6675+02		
(AL+3)2(V2O6)3	17	5	3.0	-1.5320+03		
(BE) (V2O6)	18	5	1.0	-5.2171+02		
(BI+3)2(V2O6)3	19	5	3.0	-1.3000+03		
(CE+4) (V2O6)2	20	5	2.0	-1.0171+03		
(CS)2(V2O6)	21	5	1.0	-5.5433+02		
(CU+1)2(V2O6)	22	5	1.0	-4.1737+02		
(FE+3)2(V2O6)3	23	5	3.0	-1.3277+03		
(MN+3)2(V2O6)3	24	5	3.0	-1.3696+03		
(RB)2(V2O6)	25	5	1.0	-5.5268+02		
(SB+3)2(V2O6)3	26	5	3.0	-1.2944+03		
(SN+4) (V2O6)2	27	5	2.0	-8.8400+02		
(TH+4) (V2O6)2	28	5	2.0	-1.0686+03		
(U+4) (V2O6)2	29	5	2.0	-1.0272+03		
(ZR+4) (V2O6)2	30	5	2.0	-1.0519+03		
(AG)2(SO3)	1	6	1.0	-1.1207+02	-1.1440+02	-2.3340+00
(BA) (SO3)	2	6	1.0	-2.8148+02	-2.8260+02	-1.1171+00
(CA) (SO3)	3	6	1.0	-2.7508+02	-2.7588+02	-7.9761-01
(CD) (SO3)	4	6	1.0	-1.6412+02	-1.6390+02	2.1793-01

TABLE I (continued)

```
(    CO) (   SO3)      5   6        1.0          -1.6175+02
(  CU+2) (   SO3)      6   6        1.0          -1.2728+02
(  FE+2) (   SO3)      7   6        1.0          -1.6554+02
(     K)2(   SO3)      8   6        1.0          -2.6759+02      -2.6690+02       6.8863-01
(    LI)2(   SO3)      9   6        1.0          -2.7723+02      -2.7940+02      -2.1664+00
(    MG) (   SO3)     10   6        1.0          -2.4718+02      -2.4100+02       6.1849+00
(  MN+2) (   SO3)     11   6        1.0          -1.9722+02      -1.9737+02      -1.5163-01
(    NA)2(   SO3)     12   6        1.0          -2.6217+02      -2.6040+02       1.7728+00
(    NI) (   SO3)     13   6        1.0          -1.5586+02
(    PB) (   SO3)     14   6        1.0          -1.5869+02      -1.5700+02       1.6886+00
(    SR) (   SO3)     15   6        1.0          -2.7724+02      -2.7940+02      -2.1613+00
(    ZN) (   SO3)     16   6        1.0          -1.7848+02
(  AL+3)2(   SO3)3    17   6        3.0          -6.6191+02
(    BE) (   SO3)     18   6        1.0          -2.3221+02
(  BI+3)2(   SO3)3    19   6        3.0          -4.3728+02
(  CE+4) (   SO3)2    20   6        2.0          -4.4314+02
(    CS)2(   SO3)     21   6        1.0          -2.6671+02
(  CU+1)2(   SO3)     22   6        1.0          -1.2706+02
(  FE+3)2(   SO3)3    23   6        3.0          -4.5740+02
(  MN+3)2(   SO3)3    24   6        3.0          -5.0239+02
(    RB)2(   SO3)     25   6        1.0          -2.6532+02
(  SB+3)2(   SO3)3    26   6        3.0          -4.2064+02
(  SN+4) (   SO3)2    27   6        2.0          -2.9536+02
(  TH+4) (   SO3)2    28   6        2.0          -4.9341+02
(   U+4) (   SO3)2    29   6        2.0          -4.5100+02
(  ZR+4) (   SO3)2    30   6        2.0          -4.7852+02

(    AG)2(  TIO3)      1   7        1.0          -2.3937+02
(    BA) (  TIO3)      2   7        1.0          -3.9401+02
(    CA) (  TIO3)      3   7        1.0          -3.9548+02
(    CD) (  TIO3)      4   7        1.0          -2.9223+02
(    CO) (  TIO3)      5   7        1.0          -2.8910+02      -2.8946+02      -3.6440-01
(  CU+2) (  TIO3)      6   7        1.0          -2.6449+02
(  FE+2) (  TIO3)      7   7        1.0          -2.9417+02
(     K)2(  TIO3)      8   7        1.0          -3.7172+02
(    LI)2(  TIO3)      9   7        1.0          -3.9403+02
(    MG) (  TIO3)     10   7        1.0          -3.7502+02      -3.7150+02       3.5172+00
(  MN+2) (  TIO3)     11   7        1.0          -3.2430+02
(    NA)2(  TIO3)     12   7        1.0          -3.7199+02
(    NI) (  TIO3)     13   7        1.0          -2.8602+02      -2.8775+02      -1.7280+00
(    PB) (  TIO3)     14   7        1.0          -2.8534+02
(    SR) (  TIO3)     15   7        1.0          -3.9350+02
```

TABLE I (continued)

```
(    ZN) ( TIO3)      16   7        1.0        -3.1051+02     -3.0927+02     1.2441+00
( AL+3)2( TIO3)3      17   7        3.0        -1.0746+03
(    BE) ( TIO3)      18   7        1.0        -3.6842+02
( BI+3)2( TIO3)3      19   7        3.0        -8.2608+02
( CE+4) ( TIO3)2      20   7        2.0        -6.9746+02
(    CS)2( TIO3)      21   7        1.0        -3.6844+02
( CU+1)2( TIO3)       22   7        1.0        -2.6520+02
( FE+3)2( TIO3)3      23   7        3.0        -8.7056+02
( MN+3)2( TIO3)3      24   7        3.0        -9.0626+02
(    RB)2( TIO3)      25   7        1.0        -3.6813+02
( SB+3)2( TIO3)3      26   7        3.0        -8.3904+02
( SN+4) ( TIO3)2      27   7        2.0        -5.7714+02
( TH+4) ( TIO3)2      28   7        2.0        -7.5268+02
(  U+4) ( TIO3)2      29   7        2.0        -7.1404+02
( ZR+4) ( TIO3)2      30   7        2.0        -7.2998+02

(    AG)2(   WO4)      1   8        1.0        -2.3092+02     -2.3070+02     2.2073-01
(    BA) (   WO4)      2   8        1.0        -4.0176+02     -4.0613+02    -4.3662+00
(    CA) (   WO4)      3   8        1.0        -3.9394+02
(    CD) (   WO4)      4   8        1.0        -2.8305+02
(    CO) (   WO4)      5   8        1.0        -2.8061+02
( CU+2) (   WO4)       6   8        1.0        -2.4776+02
( FE+2) (   WO4)       7   8        1.0        -2.8452+02
(     K)2(   WO4)      8   8        1.0        -3.9084+02
(    LI)2(   WO4)      9   8        1.0        -3.9656+02
(    MG) (   WO4)     10   8        1.0        -3.6609+02     -3.7343+02    -7.3437+00
( MN+2) (   WO4)      11   8        1.0        -3.1606+02     -3.1259+02     3.4651+00
(    NA)2(   WO4)     12   8        1.0        -3.8326+02     -3.8260+02     6.6410-01
(    NI) (   WO4)     13   8        1.0        -2.7504+02     -2.7162+02     3.4174+00
(    PB) (   WO4)     14   8        1.0        -2.7749+02
(    SR) (   WO4)     15   8        1.0        -3.9667+02     -3.9270+02     3.9654+00
(    ZN) (   WO4)     16   8        1.0        -2.9795+02
( AL+3)2(   WO4)3     17   8        3.0        -1.0237+03
(    BE) (   WO4)     18   8        1.0        -3.5245+02
( BI+3)2(   WO4)3     19   8        3.0        -7.9459+02
( CE+4) (   WO4)2     20   8        2.0        -6.8082+02
(    CS)2(   WO4)     21   8        1.0        -3.9104+02
( CU+1)2(   WO4)      22   8        1.0        -2.4785+02
( FE+3)2(   WO4)3     23   8        3.0        -8.1932+02
( MN+3)2(   WO4)3     24   8        3.0        -8.6224+02
(    RB)2(   WO4)     25   8        1.0        -3.8916+02
( SB+3)2(   WO4)3     26   8        3.0        -7.8500+02
```

TABLE I (continued)

(SN+4) (WO4)2	27	8	2.0	-5.4246+02		
(TH+4) (WO4)2	28	8	2.0	-7.3163+02		
(U+4) (WO4)2	29	8	2.0	-6.8978+02		
(ZR+4) (WO4)2	30	8	2.0	-7.1602+02		
(AG)2(MOO4)	1	9	1.0	-2.1551+02	-2.1660+02	-1.0907+00
(BA) (MOO4)	2	9	1.0	-3.7704+02		
(CA) (MOO4)	3	9	1.0	-3.7541+02		
(CD) (MOO4)	4	9	1.0	-2.6785+02		
(CO) (MOO4)	5	9	1.0	-2.6521+02		
(CU+2) (MOO4)	6	9	1.0	-2.3321+02		
(FE+2) (MOO4)	7	9	1.0	-2.6945+02		
(K)2(MOO4)	8	9	1.0	-3.5690+02		
(LI)2(MOO4)	9	9	1.0	-3.7552+02		
(MG) (MOO4)	10	9	1.0	-3.5082+02		
(MN+2) (MOO4)	11	9	1.0	-3.0058+02		
(NA)2(MOO4)	12	9	1.0	-3.5583+02	-3.5405+02	1.7776+00
(NI) (MOO4)	13	9	1.0	-2.6026+02		
(PB) (MOO4)	14	9	1.0	-2.6188+02	-2.6565+02	-3.7668+00
(SR) (MOO4)	15	9	1.0	-3.7520+02		
(ZN) (MOO4)	16	9	1.0	-2.8339+02		
(AL+3)2(MOO4)3	17	9	3.0	-9.7992+02		
(BE) (MOO4)	18	9	1.0	-3.3796+02		
(BI+3)2(MOO4)3	19	9	3.0	-7.4996+02		
(CE+4) (MOO4)2	20	9	2.0	-6.4992+02		
(CS)2(MOO4)	21	9	1.0	-3.5407+02		
(CU+1)2(MOO4)	22	9	1.0	-2.3318+02		
(FE+3)2(MOO4)3	23	9	3.0	-7.7550+02		
(MN+3)2(MOO4)3	24	9	3.0	-8.1886+02		
(RB)2(MOO4)	25	9	1.0	-3.5357+02		
(SB+3)2(MOO4)3	26	9	3.0	-7.4001+02		
(SN+4) (MOO4)2	27	9	2.0	-5.0939+02		
(TH+4) (MOO4)2	28	9	2.0	-7.0189+02		
(U+4) (MOO4)2	29	9	2.0	-6.6057+02		
(ZR+4) (MOO4)2	30	9	2.0	-6.8418+02		
(AG)2(AL2O4)	1	10	1.0	-4.1364+02		
(BA) (AL2O4)	2	10	1.0	-5.6667+02		
(CA) (AL2O4)	3	10	1.0	-5.6916+02		
(CD) (AL2O4)	4	10	1.0	-4.6654+02		
(CO) (AL2O4)	5	10	1.0	-4.6337+02	-4.6653+02	-3.1633+00
RB,						

TABLE I (continued)

(CU+2) (AL204)	6	10	1.0	-4.3703+02		
(FE+2) (AL204)	7	10	1.0	-4.6852+02	-4.7440+02	-5.8829+00
(K)2(AL204)	8	10	1.0	-5.4292+02		
(LI)2(AL204)	9	10	1.0	-5.6729+02	-5.6858+02	-1.2882+00
(MG) (AL204)	10	10	1.0	-5.4932+02	-5.5100+02	-1.6829+00
(MN+2) (AL204)	11	10	1.0	-4.9856+02	-5.0109+02	-2.5334+00
(NA)2(AL204)	12	10	1.0	-5.4422+02	-5.4134+02	2.8800+00
(NI) (AL204)	13	10	1.0	-4.6044+02	-4.6332+02	-2.8810+00
(PB) (AL204)	14	10	1.0	-4.5957+02		
(SR) (AL204)	15	10	1.0	-5.6669+02	-5.5981+02	6.8826+00
(ZN) (AL204)	16	10	1.0	-4.8500+02		
(AL+3)2(AL204)3	17	10	3.0	-1.5982+03		
(BE) (AL204)	18	10	1.0	-5.4299+02		
(BI+3)2(AL204)3	19	10	3.0	-1.3493+03		
(CE+4) (AL204)2	20	10	2.0	-1.0460+03		
(CS)2(AL204)	21	10	1.0	-5.3918+02		
(CU+1)2(AL204)	22	10	1.0	-4.3971+02		
(FE+3)2(AL204)3	23	10	3.0	-1.3941+03		
(MN+3)2(AL204)3	24	10	3.0	-1.4300+03		
(RB)2(AL204)	25	10	1.0	-5.3909+02		
(SB+3)2(AL204)3	26	10	3.0	-1.3625+03		
(SN+4) (AL204)2	27	10	2.0	-9.2628+02		
(TH+4) (AL204)2	28	10	2.0	-1.1015+03		
(U+4) (AL204)2	29	10	2.0	-1.0630+03		
(ZR+4) (AL204)2	30	10	2.0	-1.0783+03		
(AG)2(CR204)	1	3	1.0	-3.0820+02		
(BA) (CR204)	2	3	1.0	-5.1632+02		
(CA) (CR204)	3	3	1.0	-4.9165+02	-4.9240+02	-7.4862-01
(CD) (CR204)	4	3	1.0	-3.6166+02		
(CO) (CR204)	5	3	1.0	-3.5232+02	-3.5064+02	1.6814+00
(CU+2) (CR204)	6	3	1.0	-3.2174+02		
(FE+2) (CR204)	7	3	1.0	-3.6022+02		
(K)2(CR204)	8	3	1.0	-5.4119+02		
(LI)2(CR204)	9	3	1.0	-5.0189+02		
(MG) (CR204)	10	3	1.0	-4.4739+02		
(MN+2) (CR204)	11	3	1.0	-3.9672+02		
(NA)2(CR204)	12	3	1.0	-5.0814+02		
(NI) (CR204)	13	3	1.0	-3.4874+02		
(PB) (CR204)	14	3	1.0	-3.5723+02		

TABLE I (continued)

```
(    SR) (CR2O4)       15   3       1.0          -5.1463+02
(    ZN) (CR2O4)       16   3       1.0          -3.7283+02
( AL+3)2(CR2O4)3       17   3       3.0          -1.2380+03
(    BE) (CR2O4)       18   3       1.0          -4.2443+02
( BI+3)2(CR2O4)3       19   3       3.0          -1.0240+03
( CE+4) (CR2O4)2       20   3       2.0          -8.3979+02
(    CS)2(CR2O4)       21   3       1.0          -5.5192+02
( CU+1)2(CR2O4)        22   3       1.0          -3.1904+02
( FE+3)2(CR2O4)3       23   3       3.0          -1.0334+03
( MN+3)2(CR2O4)3       24   3       3.0          -1.0802+03
(    RB)2(CR2O4)       25   3       1.0          -5.4497+02
( SB+3)2(CR2O4)3       26   3       3.0          -9.9712+02
( SN+4) (CR2O4)2       27   3       2.0          -6.8403+02
( TH+4) (CR2O4)2       28   3       2.0          -8.8449+02
(  U+4) (CR2O4)2       29   3       2.0          -8.3908+02
( ZR+4) (CR2O4)2       30   3       2.0          -8.7929+02



ROOT MEAN SQUARE ERROR =  3.0250+00    CALORIES/PAIR OF IONIC BONDS
```

in T.M. 004-009-Ch1A. A description of FORM, the computer program used to correlate the data and estimate the unknown heats of formation, is given in T.M. 004-009-Ch23.

Four methods for estimating absolute entropy were investigated. All of the methods were based on the concept of adding cation and anion entropy contributions and applying a correction. Latimer (LA-002) gave Equation (7) for the entropy, S, of a solid, where S_0 is a constant independent of the substance and m is the atomic weight. Equation (8) extends his method from elements to compounds with I atoms.

$$S = \frac{3}{2} R \ln m + \frac{5}{2} R \ln T - R \ln P + S_0 \qquad (7)$$

$$S^\circ_{298} = \frac{3}{2} R \sum_{i=1}^{I} \ln m_i + S_0' \qquad (8)$$

From the entropy of KCl he calculated S_0' for all elements to be -0.94 e.u.

The author subsequently amended his estimation method in light of the fact that when ionic attractions are involved in solid salts, the entropy of a large ion is increased and that of a small ion is decreased as compared to values obtained using Equation (8). Assuming a correspondence between size and atomic weight he corrected his entropy values by revising a graph of atomic weight vs entropy. He had also noticed that the entropy of a solid depends on the charge on the cation. Latimer obtained constant anion entropy values by subtracting entropies of elements forming the cation from known compound entropies.

Entropies were calculated for the TRACOR data base by determining anion entropy contributions according to the method of Latimer using Latimer's cation entropies (LA-002) and the more complete experimentally obtained entropy data from the TRACOR data base. The accepted values and correlation errors of the entropy estimation method are given in Table II. The RMS error for the correlation was 2 cal/mole °K.

The selection and application of the Latimer method for estimation of absolute entropy was discussed in detail in T.M. 004-009-Ch5. A description of ENTROP, the computer program used for estimating the average anion entropy contributions, is given in T.M. 004-009-Ch23.

There are two basic methods used in heat capacity estimation. The first, Dulong and Petit's rule, states that the heat capacity of an element is generally 6.2 - 6.5 cal/°K per atom at the temperature of the first transition. This rule may be applied to the estimation of heat capacities if the temperature or entropy of the first transition is known. Since these data are unknown for many of the compounds of interest, our estimation method was based on the second basic method, the rule of Neumann and Kopp. The rule of Neumann and Kopp states that the heat capacity of a solid is equal to the sum of the heat capacities of the constituent elements. While the rule is normally applied to compounds at room temperature, some extrapolation to other temperatures may be made.

It was found that the most accurate way of applying Kopp's rule for the compounds of interest was, for the example of a metal sulfate, to add the heat capacity of the metal oxide and the SO_3 "lattice" contribution. The method of subtracting metal oxide heat capacities from the heat capacity of another salt of the same metal and obtaining a constant contribution for the remaining lattice was found to be widely applicable. It was used for estimating the heat capacities of sulfates, sulfites, carbonates, sulfides, and mixed oxides. The selection and application of the method are discussed in detail in T.M. 004-009-Ch4, Ch9, Ch13, and Ch13A. HTCAPY and HTCAPS, the computer programs used for the calculations, are discussed in detail in T.M. 004-009-Ch23.

TABLE II

DEVIATIONS OF ESTIMATED VALUES OF ABSOLUTE ENTROPY

COMPOUND	ACCEPTED ENTROPY VALUE (e.u./gmole)	DEVIATION (e.u./gmole)
CU20	2.2521+01	-1.782+00
AG20	2.9074+01	7.708-01
LI20	9.0519+00	-6.514-01
NA20	1.6986+01	-7.176-01
K20	2.3484+01	2.381+00
RMS DEVIATION		1.441+00
SNO	1.3555+01	-1.162-01
PBO	1.5600+01	-4.713-01
BEO	3.3685+00	-1.503+00
MGO	6.4025+00	-1.769+00
CAO	9.4843+00	-3.871-01
SRO	1.2996+01	4.247-01
BAO	1.6795+01	2.523+00
CDO	1.3092+01	-3.797-01
FEO	1.4191+01	3.219+00
COO	1.2655+01	1.283+00
PDO	1.3378+01	1.070-01
NIO	9.0782+00	-1.993+00
TIO	8.3042+00	-2.067+00
MNO	1.4265+01	3.393+00
CUO	1.0187+01	-1.185+00
ZNO	1.0392+01	-1.079+00
RMS DEVIATION		1.711+00

TABLE II (continued)

DEVIATIONS OF ESTIMATED VALUES OF ABSOLUTE ENTROPY

COMPOUND	ACCEPTED ENTROPY VALUE (e.u./gmole)	DEVIATION (e.u./gmole)
B2O3	1.2865+01	2.201+00
AL2O3	1.2170+01	-4.694+00
GA2O3	2.0220+01	-3.043+00
SC2O3	1.8395+01	-1.868+00
Y2O3	2.3682+01	-1.182+00
FE2O3	2.0880+01	-7.838-01
MN2O3	2.6398+01	4.935+00
TI2O3	1.8816+01	-1.648+00
LA2O3	3.0555+01	2.092+00
CR2O3	1.9375+01	-1.889+00
BI2O3	3.6122+01	4.058+00
AS2O3	2.5586+01	1.822+00
RMS DEVIATION		2.835+00
UO2	1.8622+01	1.561+00
THO2	1.5586+01	-1.376+00
SIO2	1.0000+01	8.385-01
GEO2	1.3204+01	8.425-01
SNO2	1.2504+01	-1.657+00
PBO2	1.8262+01	1.700+00
RUO2	1.2500+01	-1.061+00
ZRO2	1.2021+01	-1.140+00
VO2	1.2100+01	9.385-01
MOO2	1.1056+01	-2.305+00
WO2	1.6006+01	-5.516-02
TIO2	1.2000+01	1.138+00
HFO2	1.4174+01	-1.688+00
MNO2	1.2686+01	1.324+00
IRO2	1.7201+01	9.393-01
RMS DEVIATION		1.336+00
NA2S	2.2480+01	-4.598-01
AG2S	3.4000+01	4.598-01
RMS DEVIATION		4.598-01

TABLE II (continued)

DEVIATIONS OF ESTIMATED VALUES OF ABSOLUTE ENTROPY

COMPOUND	ACCEPTED ENTROPY VALUE (e.u./gmole)	DEVIATION (e.u./gmole)
BES	7.4059+00	-1.916+00
MGS	1.0607+01	-2.015+00
CAS	1.3450+01	-8.722-01
SRS	1.6986+01	-3.650-02
BAS	2.1501+01	2.779+00
VS	1.4501+01	-6.211-01
MNS	1.9722+01	4.400+00
FES	1.5200+01	-2.223-01
CUS	1.5887+01	6.456-02
ZNS	1.3785+01	-2.138+00
CDS	1.6962+01	-9.604-01
SNS	1.8395+01	2.730-01
PBS	2.1788+01	1.265+00
RMS DEVIATION		1.823+00
MO2S3	2.8000+01	-1.411+00
AL2S3	2.2934+01	2.123+00
BI2S3	3.5300+01	-7.115-01
RMS DEVIATION		1.528+00
MOS2	1.5098+01	-2.223+00
RES2	1.9996+01	-2.579-02
FES2	1.2686+01	-2.736+00
CU2S	2.8883+01	2.261+00
SNS2	2.0880+01	2.758+00
RUS2	1.7487+01	-3.425-02
RMS DEVIATION		2.047+00
LI2CO3	2.1582+01	-1.446+00
K2CO3	3.6074+01	1.645+00
NA2CO3	3.2490+01	1.462+00
AG2CO3	3.9968+01	-1.661+00
RMS DEVIATION		1.557+00

TABLE II (continued)

DEVIATIONS OF ESTIMATED VALUES OF ABSOLUTE ENTROPY

COMPOUND	ACCEPTED ENTROPY VALUE (e.u./gmole)	DEVIATION (e.u./gmole)
MGCO3	1.5696+01	-3.299+00
SRCO3	2.3173+01	-2.210-01
BACO3	2.6781+01	1.686+00
MNCO3	2.0474+01	-1.221+00
FECO3	2.2194+01	3.995-01
ZNCO3	1.9685+01	-2.609+00
PBCO3	3.1272+01	4.378+00
CDCO3	2.5180+01	8.857-01
RMS DEVIATION		2.296+00
LI2SO4	3.5357+01	4.662+00
NA2SO4	3.5692+01	-3.003+00
K2SO4	4.1975+01	-1.202-01
AG2SO4	4.7756+01	-1.539+00
RMS DEVIATION		2.878+00
MGSO4	2.1900+01	-1.701+00
BESO4	1.8620+01	-1.681+00
CASO4	2.5491+01	1.894-01
SRSO4	2.9074+01	1.073+00
BASO4	3.1487+01	1.786+00
MNSO4	2.6781+01	4.794-01
COSO4	2.7067+01	4.661-01
NISO4	1.8586+01	-7.915+00
CUSO4	2.7067+01	2.661-01
ZNSO4	2.9767+01	2.866+00
CDSO4	2.9409+01	5.073-01
PBSO4	3.5166+01	3.665+00
RMS DEVIATION		2.816+00

TABLE II (continued)
DEVIATIONS OF ESTIMATED VALUES OF ABSOLUTE ENTROPY

COMPOUND	ACCEPTED ENTROPY VALUE (e.u./gmole)	DEVIATION (e.u./gmole)
LIALO2	1.2700+01	-1.000-01
NAALO2	1.6900+01	1.000-01
RMS DEVIATION		1.000-01
MGAL204	1.9250+01	-3.233+00
CAAL204	2.7300+01	3.117+00
FEAL204	2.5400+01	1.167-01
RMS DEVIATION		2.594+00
CACRO4	3.2013+01	-1.740+00
AG2CRO4	5.1794+01	1.740+00
RMS DEVIATION		1.740+00
MGCR204	2.5276+01	-1.843+00
FECR204	3.4879+01	4.961+00
COCR204	2.7000+01	-3.118+00
RMS DEVIATION		3.546+00
LIFEO2	1.8000+01	1.667+00
NAFEO2	2.1100+01	7.667-01
CUFEO2	2.1200+01	-2.433+00
RMS DEVIATION		1.759+00

TABLE II (continued)

DEVIATIONS OF ESTIMATED VALUES OF ABSOLUTE ENTROPY

COMPOUND	ACCEPTED ENTROPY VALUE (e.u./gmole)	DEVIATION (e.u./gmole)
MGFE204	2.8280+01	-9.898-01
NIFE204	3.0070+01	-2.100+00
ZNFE204	3.2180+01	-3.900-01
CAFE204	3.4449+01	3.480+00
RMS DEVIATION		2.101+00
MGMOO4	2.8400+01	5.333-01
CAMOO4	2.9300+01	-2.667-01
FEMOO4	3.0400+01	-2.667-01
RMS DEVIATION		3.771-01
LI2TIO3	2.1900+01	4.000-01
NA2TIO3	2.9100+01	-4.000-01
RMS DEVIATION		4.000-01
MGTIO3	1.7800+01	-2.708+00
CATIO3	2.2400+01	1.925-01
SRTIO3	2.5992+01	1.085+00
BATIO3	2.5777+01	-8.302-01
FETIO3	2.5276+01	1.968+00
COTIO3	2.3800+01	2.925-01
RMS DEVIATION		1.483+00

TABLE II (continued)
DEVIATIONS OF ESTIMATED VALUES OF ABSOLUTE ENTROPY

COMPOUND	ACCEPTED ENTROPY VALUE (e.u./gmole)	DEVIATION (e.u./gmole)
ZN2TI04	3.2800+01	-1.500+00
SR2TI04	3.8000+01	1.500+00
RMS DEVIATION		1.500+00
NA2TI205	4.1500+01	1.850+00
MGTI205	3.0400+01	-1.850+00
RMS DEVIATION		1.850+00
CAV206	4.2800+01	1.415+00
MGV206	3.8270+01	-1.415+00
RMS DEVIATION		1.415+00
CAW04	2.7000+01	-1.560+00
SRW04	2.8300+01	-2.960+00
BAW04	3.2000+01	-9.600-01
FEW04	3.1500+01	1.840+00
ZNW04	3.3800+01	3.640+00
RMS DEVIATION		2.398+00

The accuracy of the correlation was estimated by calculating the deviation between observed and calculated values for those compounds for which heat capacities had been determined experimentally. The accuracy was expressed as the fractional error, which is the RMS error divided by the average known heat capacity for the group of compounds of interest. This error along with the estimated heat capacity is shown in Tables III, IV, and V for the carbonates, sulfates, and sulfides, respectively.

The uncertainty in calculated log K and temperature values caused by errors in estimated thermodynamic properties was studied. It was found that the effect of errors in heat capacity and entropy was negligible compared to the effect of errors in heat of formation and that the effect was smaller at higher temperatures. The results of such investigations are described in detail in T.M.s 004-009-Ch2 and Ch4. The correlation errors for estimation methods developed at TRACOR were within the limits of experimental accuracy. The uncertainties in temperature and log K values resulting from the known correlation error in predicted ΔH values were taken into account when the log K and temperature values were used in the thermodynamic screening process.

2.4 THERMAL STABILITY STUDIES

The third task of importance for thermodynamic screening was to examine the thermal stability of metal oxides, sulfites and sulfates using information obtained from the literature survey and the compilation of thermodynamic properties.

2.4.1 Thermal Stability of Metal Oxides

For a metal having more than one oxidation state, it was necessary to determine which of its oxides was the most stable under flue gas conditions. The free energy of reaction for the oxide going from one oxidation state to another over the temperature range 20 to 800°C was calculated using the data base of thermodynamic properties from Equations (1) through (4). The free energy

TABLE III

ESTIMATED HEAT CAPACITIES FOR **CARBONATES** WITH KNOWN HEAT CAPACITIES
CAL./ GMOLE/ DEG.KELVIN
CP = CP(OXIDE) + DELTA CP

DELTA CP = 1.3058+01 + 5.8660-03*T - 5.7699+05/T**2

	METAL **CARBONATE**	A	B	D	TEMPERATURE RANGE DEGREES CENTIGRADE		**FRACTIONAL RMS** ERROR
1	AG2CO3	2.637968+01	1.290403-02	5.769911+05	2.500+01 TO	7.000+02	6.086-02
2	BACO3	2.573883+01	6.905249-03	7.752781+05	2.500+01 TO	7.000+02	3.927-02
3	CACO3	2.491211+01	6.945851-03	7.430266+05	2.270+02 TO	6.270+02	3.505-02
4	FECO3	2.471144+01	7.865626-03	6.529613+05	2.500+01 TO	1.200+03	4.737-02
5	MGCO3	2.323026+01	7.605225-03	7.248702+05	2.500+01 TO	1.727+03	1.045-02
6	MNCO3	2.415938+01	7.805961-03	5.649053+05	2.500+01 TO	1.200+03	2.378-02
7	NA2CO3	2.374835+01	1.126278-02	5.769911+05	2.500+01 TO	7.000+02	1.182-01
8	SRCO3	2.533991+01	6.986474-03	7.575995+05	2.500+01 TO	7.000+02	6.719-02

TABLE IV

ESTIMATED HEAT CAPACITIES FOR METAL SULFATES WITH KNOWN HEAT CAPACITIES
CAL./ GMOLE/ DEG.KELVIN
CP = CP(OXIDE) + DELTA CP

DELTA CP = 9.0132+00 + 1.6828-02*T - -4.6680+04/T**2

	METAL SULFATE	A	B	D	TEMPERATURE RANGE DEGREES CENTIGRADE			FRACTIONAL RMS ERROR
1	AG2SO4	2.226737+01	2.336632-02	-4.668011+04	2.500+01	TO	7.000+02	8.104-02
2	AL2(SO4)3	5.344459+01	5.482499-02	6.522597+05	2.500+01	TO	7.000+02	1.626-02
3	BASO4	2.174657+01	1.786755-02	1.516069+05	2.500+01	TO	7.000+02	8.643-02
4	BESO4	1.745331+01	2.082752-02	2.701013+05	2.500+01	TO	7.000+02	6.482-02
5	CASO4	2.035980+01	1.790816-02	1.193554+05	2.270+02	TO	6.270+02	2.111-02
6	CDSO4	1.855938+01	1.890675-02	-4.668011+04	2.500+01	TO	7.000+02	2.016-02
7	CUSO4	1.828013+01	2.162544-02	-4.668011+04	2.500+01	TO	7.000+02	8.156-02
8	MGSO4	1.918795+01	1.856752-02	1.011990+05	2.500+01	TO	1.727+03	2.573-02
9	MNSO4	2.011727+01	1.876820-02	4.123509+04	2.500+01	TO	1.200+03	3.120-02
10	NA2SO4	2.470854+01	2.222508-02	-4.668011+04	2.500+01	TO	7.000+02	6.424-02
11	PBSO4	1.960841+01	2.082752-02	-4.668011+04	2.500+01	TO	6.000+02	4.856-02
12	SRSO4	2.134760+01	1.794677-02	1.339283+05	2.500+01	TO	7.000+02	7.098-02
13	ZNSO4	2.071691+01	1.804672-02	1.711967+05	2.500+01	TO	1.200+03	4.332-02

TABLE V

ESTIMATED HEAT CAPACITIES FOR METAL SULFIDES WITH KNOWN HEAT CAPACITIES
CAL./ GMOLE/ DEG.KELVIN
CP = CP(OXIDE) + DELTA CP

DELTA CP = 1.7972+00 + -1.0570-03*T - -1.6525+04/T**2

	METAL SULFIDES	A	B	D	TEMPERATURE RANGE DEGREES CENTIGRADE	FRACTIONAL RMS ERROR
1	AG2S	1.505138+01	5.980967-03	-1.652523+04	2.500+01 TO 7.000+02	1.296-01
2	BI2S3	3.011778+01	4.824901-03	-4.957569+04	2.500+01 TO 5.000+02	8.404-03
3	CDS	1.144399+01	1.021403-03	-1.652523+04	2.500+01 TO 7.000+02	9.865-02
4	FES	1.345314+01	9.425657-04	5.944497+04	2.500+01 TO 1.200+03	1.060-01
5	MGS	1.197196+01	6.821647-04	1.313539+05	2.500+01 TO 1.727+03	1.045-01
6	MNS	1.230123+01	8.828407-04	7.138997+04	2.500+01 TO 1.200+03	4.364-02
7	NA2S	1.749055+01	4.339724-03	-1.652523+04	2.500+01 TO 7.000+02	2.380-03
8	PBS	1.239242+01	2.942159-03	-1.652523+04	2.500+01 TO 6.000+02	9.568-02
9	SB2S3	2.447974+01	1.391027-02	-4.957569+04	2.500+01 TO 9.000+02	9.250-03
10	SNS	1.134365+01	2.440469-03	-1.652523+04	2.500+01 TO 7.000+02	5.009-02
11	SNS2	2.124674+01	2.845014-04	4.827346+05	2.500+01 TO 1.200+03	4.677-02
12	TIS2	2.072594+01	-1.134565-03	3.166991+05	2.500+01 TO 1.200+03	2.217-02
13	US2	2.273525+01	-4.943126-04	3.625679+05	2.500+01 TO 1.200+03	3.686-02
14	ZNS	1.350092+01	1.613627-04	2.013516+05	2.500+01 TO 1.200+03	3.062-02

changes were used to determine which oxidation state was the most stable under flue gas conditions over the temperature range of interest. The calculations and results are given in detail in T.M. 004-009-Ch7. An example of the results for PbO and PbO_2 is given in Figure 2. Figure 2 shows that PbO_2 is the most stable oxide under flue gas conditions up to 268°C and that PbO is the most stable at higher temperatures.

2.4.2 Thermal Stability of Metal Sulfites

Thermal stability of metal sulfites was studied using both descriptive and quantitative information. From the literature survey it was found that on heating, metal sulfites either decompose, disproportionate to form sulfate and sulfide, or both disproportionate and decompose. It was found that sulfites are generally unstable at high temperatures and that the occurrence of disproportionation or decomposition depends on the thermodynamic equilibrium and the reaction kinetics. In particular if the sulfite decomposition temperature is high, disporportionation occurs to a large extent. However, for sulfites with lower decomposition temperatures, disproportionation and decomposition are competing reactions. These ideas are discussed in detail in T.M. 004-009-Ch3. The tendency towards disproportionation or decomposition was determined by calculating the equilibrium constant for the two reactions over the temperature range of interest using the program AIRPOL. These data also provided a measure of the sulfur oxide partial pressure over the reaction product. The results of these calculations, as well as the results of experimental work described in the literature, are given in detail in T.M. 004-009-Ch16. An example of the calculations is given for zinc in Figures 3 and 4. Figure 3 shows that zinc has a thermodynamic tendency to disproportionate in the temperature range of interest since the free energy (-RT ln K) is negative. Figure 4 shows that, under flue gas conditions, the sulfite would decompose around 200°C.

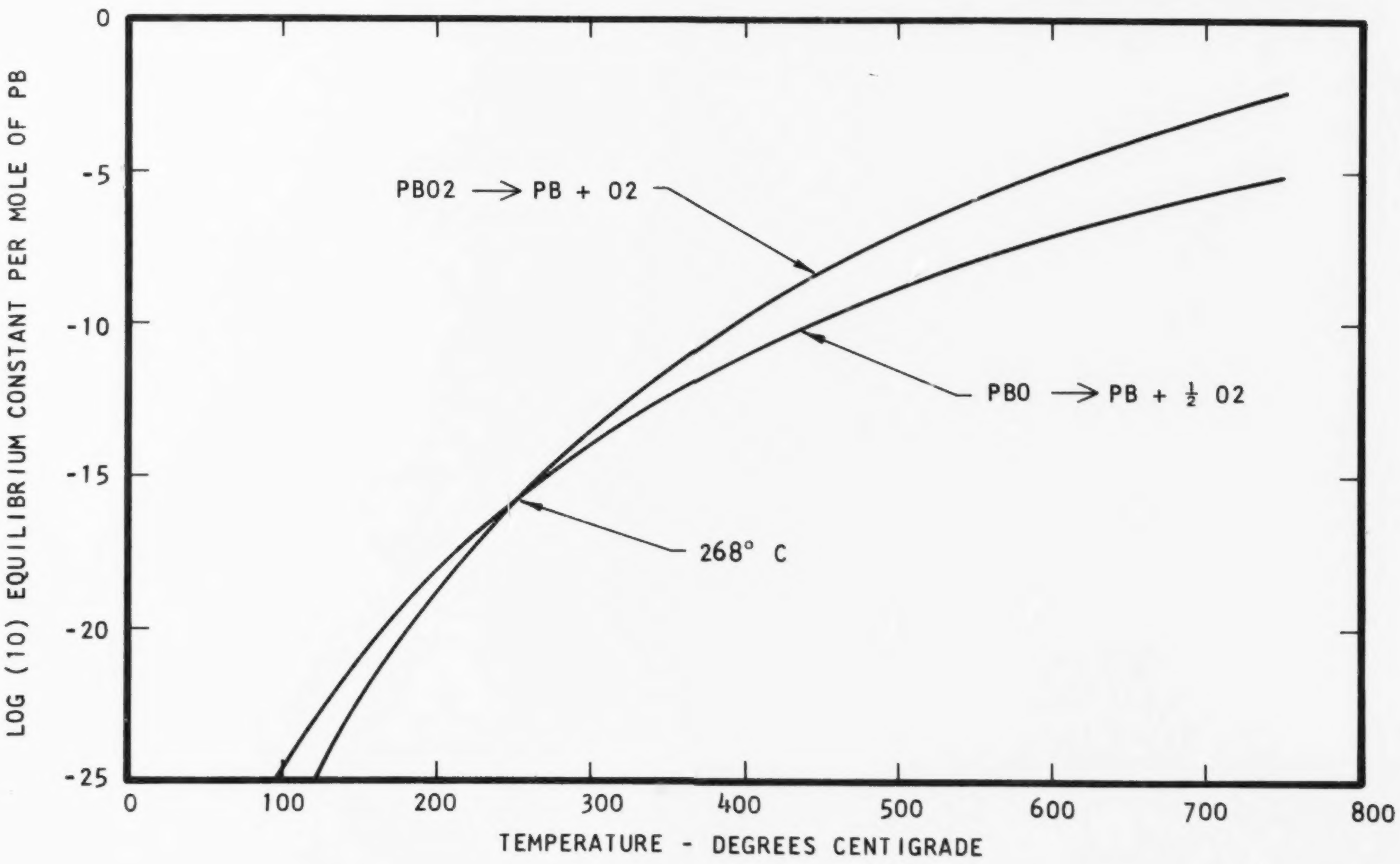

FIGURE 2 - DECOMPOSITION OF LEAD OXIDES
STANDARD STATE OF 02 IS 0.028 ATM

TRACOR DWG. A6-3-659
7/11/68
SD / SCHROEDER

LOGARITHM OF THE EQUILIBRIUM CONSTANT FOR THE DISPROPORTIONATION OF ZINC SULFITE

$4\ ZNSO_3 \rightarrow 3\ ZNSO_4 + ZNS$

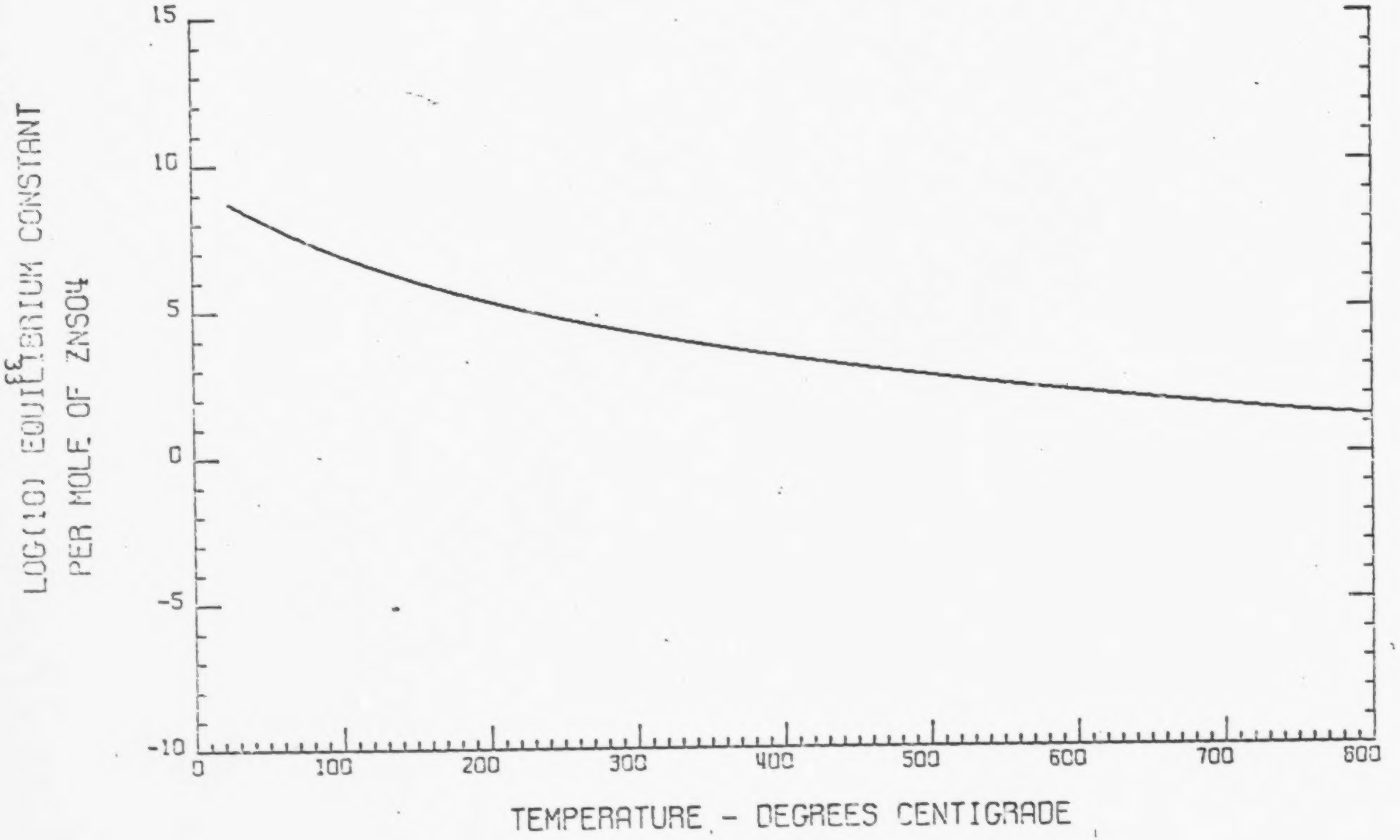

FIGURE 3

25 SEP 68

TRACOR

LOGARITHM OF THE EQUILIBRIUM CONSTANT FOR
THE DECOMPOSITION OF ZINC SULFITE

ZNSO3 → SO2 + ZNO

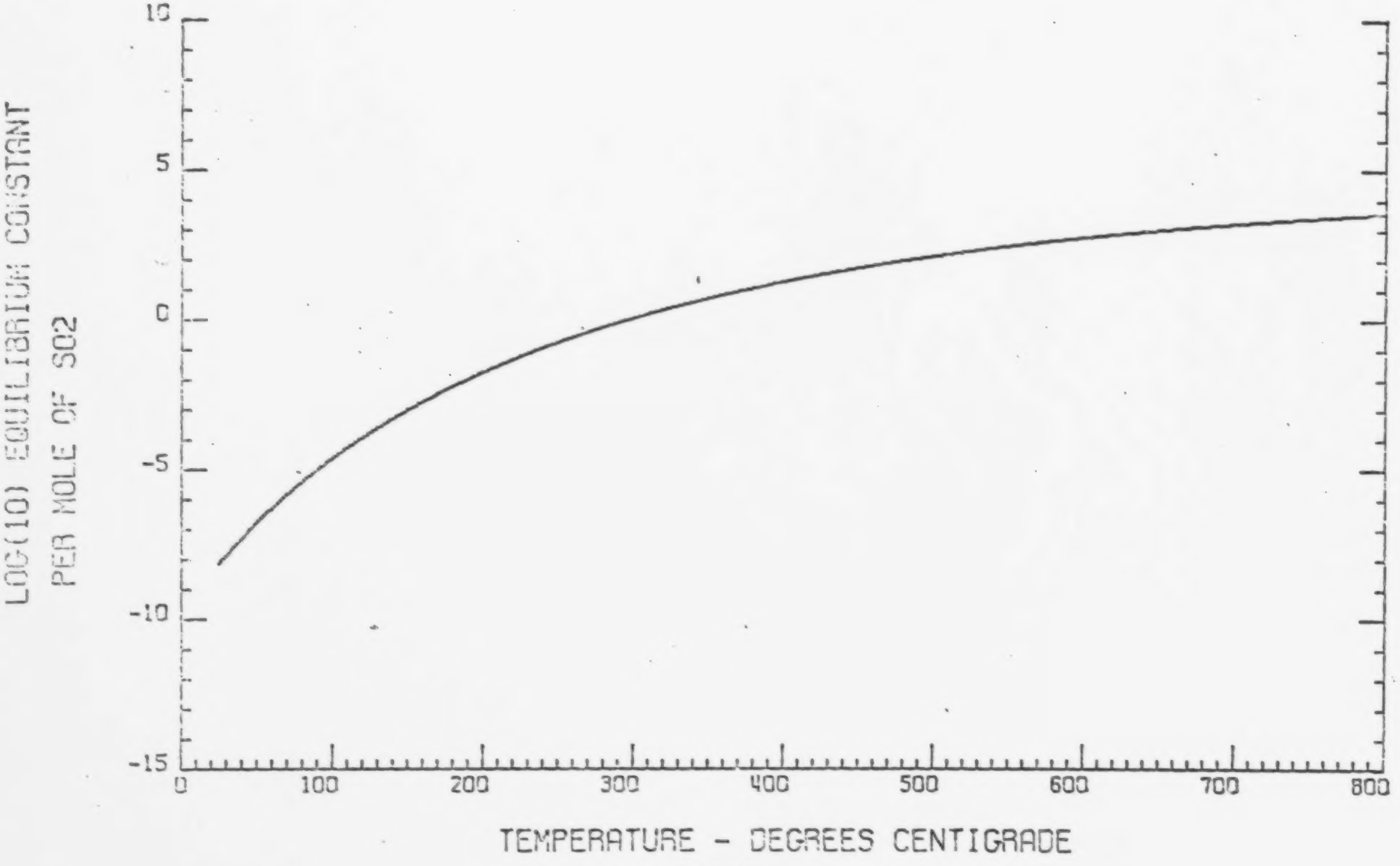

FIGURE 4

25 SEP 68

TRACOR

2.4.3 Thermal Stability of Metal Sulfates

The thermal behavior of metal sulfates was also studied using both calculated equilibrium constants and reports of experimental work described in the literature. From the literature search it was found that the sulfates can be roughly classified in four groups: (1) sulfates which show simple decomposition accompanied by the formation of the corresponding oxides; (2) sulfates which decompose to the oxides with the intermediate formation of oxysulfates; (3) sulfates which decompose with oxidation; and (4) sulfates which decompose with reduction giving the metal as the product. Naturally, this grouping is crude, since the decomposition path is influenced by the experimental conditions, especially the atmosphere. These findings are discussed in detail in T.M. 004-009-Ch8 and are summarized in Table VI on page 40.

Using the compilation of thermodynamic properties, equilibrium constants for the sulfate decomposition reactions were calculated. The sulfate decomposition reactions were written with SO_3 as the gaseous product rather than SO_2 and O_2, since the former method was the most accurate way to represent the total sulfur oxide concentration in the flue gas for the temperature range of interest. The values of log K for the decomposition reactions were plotted from 25 to 800°C by Calcomp plotter with instructions from the program AIRPOL. These plots were valuable in the thermodynamic screening process since they gave a measure of the sulfur oxide partial pressure over the sorption product and a prediction of the sulfate decomposition temperature. The plots are included in Section 8.2 of this report. Use of the equilibrium plots for thermodynamic screening is described in detail in Section 2.7.1.

2.5 CATALYTIC OXIDATION PROPERTIES OF METAL OXIDES

In order for the reaction product of sulfur oxide sorption by metal oxides to be a sulfate, either the metal sulfite must be formed and then disproportionate, or oxidation must take place. Since some metal oxides are known to be catalytically effective as SO_2 oxidation catalysts, the properties of these oxides and the oxidation reaction itself were studied in some detail. An extensive literature search revealed several ideas. An oxide that is effective as an SO_2 oxidizing catalyst is unsuitable as a sorbent in the temperature range in which it is catalytically effective, since according to the reaction mechanism proposed for catalytic oxidation, its sulfate must be unstable at that temperature. On the other hand, the oxides which are poor catalysts because of the formation of a stable sulfate are potential sorbents. Thus the main difference between catalytic effectiveness and sorption of sulfur oxide with the formation of sulfate is the partial pressure of SO_3 over the sulfate intermediate. The results of the literature search including experimentally determined catalytic activity for many oxides are discussed in detail in T.M. 004-009-Ch16 in parts III and IV.

2.6 DETERMINATION OF PRICE AND AVAILABILITY OF METAL OXIDES

The fifth task of importance for the screening process was to determine the price and availability of the potential metal oxide sorbents. In determining the availability of a sorbent, such factors as world and domestic production, consumption, and stockpiling were considered. All of the data were reported in short tons per year. The results of the survey are summarized in Table VI.

2.7 PRELIMINARY SCREENING BASED ON THERMODYNAMICS AND SORBENT AVAILABILITY

2.7.1 Criteria for the Screening Process

The goal of the preliminary screening process was to use all the thermodynamic and descriptive information obtained up to that point to reduce the field of potential sorbents. Oxides not thermodynamically capable of reducing the sulfur oxide concentration in the flue gas to the desired level were eliminated from the list of potential sorbents. The thermodynamics of the regeneration step were also considered in screening the oxides. A third consideration, though not a decisive factor, was the price or availability of the oxide. Fourth, physical properties, such as toxicity, which were a deterrent to the use of the oxide in an industrial process were also considered in screening the potential sorbents.

The data reported in the literature and calculated from thermodynamic properties on thermal behavior of the oxides, sulfites and sulfates, plus catalytic activity of the oxides, were included in the screening process. These data were used to predict the sorption products and the course of the decomposition reaction. Next, the decomposition reactions for the sorption products were written and the value of the equilibrium constant was calculated for the temperature range of interest.

Since the sulfur oxide removal process must reduce the concentration of sulfur oxides in the flue gas emitted from the largest power plants to 150 ppm, the partial pressure of SO_x in the exiting flue gas must be .00015 atmospheres when the total pressure of the flue gas is 1 atmosphere. All the other species in the sorption reaction are at unit activity (solids) so that the equilibrium constant is numerically equal to the partial pressure of SO_x in atmospheres when the reaction is written as a decomposition. Therefore, a compound will be able to reduce the sulfur oxide concentration to 150 ppm only in the temperature range where K is less than .00015 or log K is less than -3.82. The sorption temperature must also be high enough to prevent plume droop and the resulting localized pollution. Most of the oxides studied fulfilled this thermodynamic requirement.

The regeneration step imposed another thermodynamic requirement. The matter of thermal regeneration is important because chemical regeneration requires reasonably complex equipment as well as the consumption of an energetic material. A requirement of the regeneration process is that it must produce sulfur oxides in a concentration sufficient for use in a sulfur recovery process. Such a concentration of sulfur oxide must be obtainable at temperature limits imposed by materials of construction and availability of heat energy, or from 100 to 750°C. All of these requirements demand a value of log K less than -3.8 at the sorption temperature and greater than -2 at the regeneration temperature. Another way of saying this is that sorbents were sought that have only a slight negative free energy change in the sorption step, since a slight negative free energy change would be easiest to overcome in the regeneration step, whether the regeneration would be thermal or chemical. Figure 5 gives an example of how the thermodynamic requirements of the screening process were applied. The horizontal lines labeled "regeneration" and "sorption" indicate the log K values calculated as described above. As can be seen in Figure 5 the regeneration of barium sulfate would be difficult in the required temperature range. However, copper and tin oxides have favorable thermodynamic properties for both sorption and regeneration.

2.7.2 Metal Oxide Screening

Most of the data upon which the preliminary screening process was based are compiled in Table VI. The result of the preliminary screening process was a reduction of the field of potential sorbents to the oxides of the 16 metals shown in periodic arrangement in Figure 6. For the oxides of tungsten, tantalum, antimony, and niobium, not enough data were available to allow a decision to be made about their value as potential sorbents.

2.7.3 Mixed Metal Oxide Screening

It was found during the preliminary screening process that some oxides such as the alkaline earth oxides or the alkali metal oxides underwent a large negative free energy change during the sorption step. As was stated in Section 2.7.1, sorbents were sought that had only a slight negative free energy change for

LOGARITHM OF THE EQUILIBRIUM CONSTANT FOR THE DECOMPOSITION REACTIONS FOR TIN, COPPER, AND BARIUM SULFATES

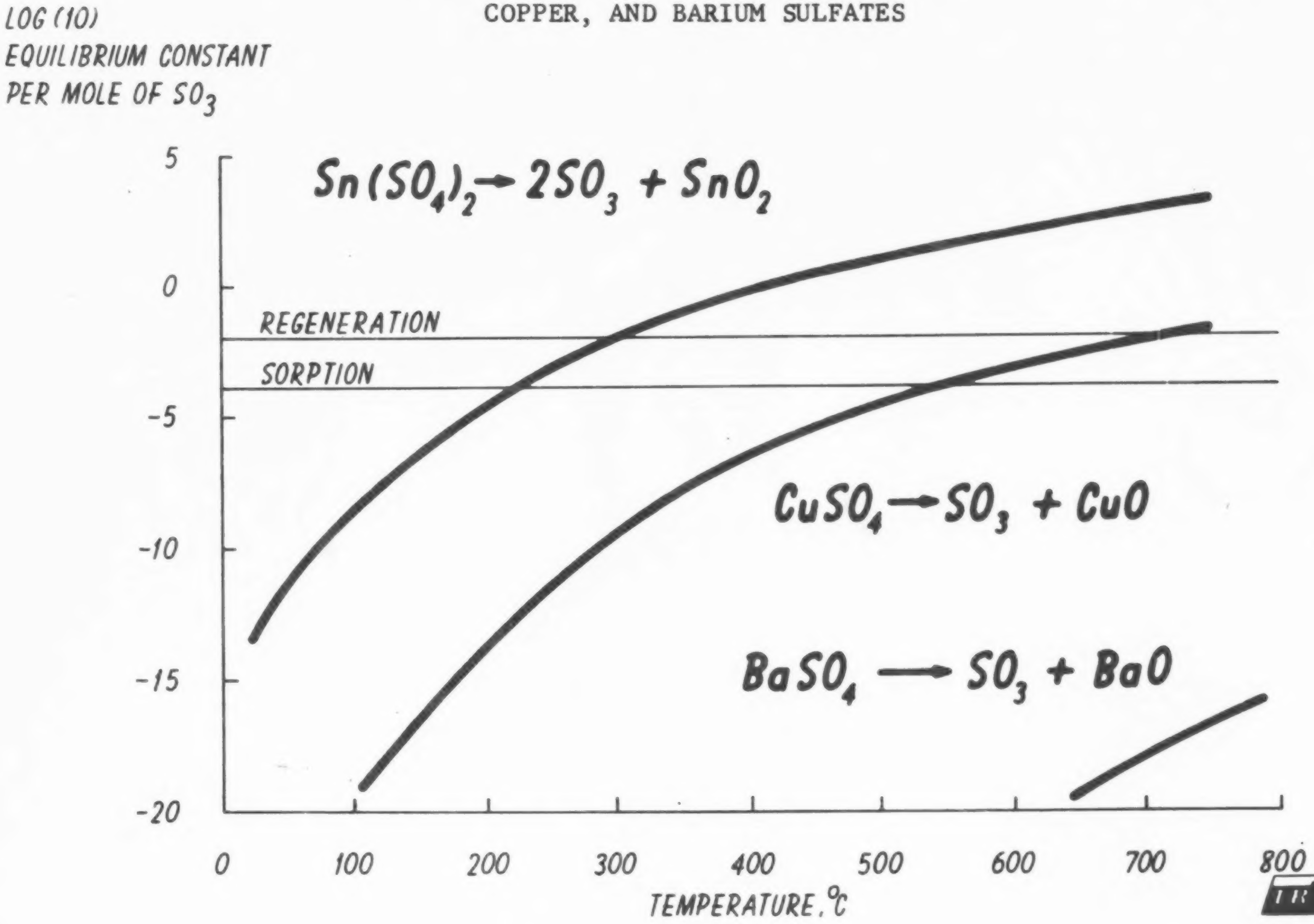

FIGURE 5

TABLE VI

PROPERTIES OF OXIDES, SULFATES, AND SULFITES

OXIDE	POSSIBLE SORPTION* RANGE WITH SULFITE FORMATION	DISPROPORTIONATION* RANGE OF SULFITE	DECOMPOSITION* TEMPERATURE OF SULFITE	DECOMPOSITION TEMPERATURE OF SULFATE	CATALYTIC BEHAVIOR OF OXIDE	PRICE DOLLARS/SHORT TON	REMARKS
1) Li_2O	25 to 800°C	Thermodynamically favored between 25-800°C. Rate becomes appreciable at 650°C.	> 800°C	> 860°C (melting point)	Inactive	Metal: 15,000 Carbonate: 850 Sulfite: 2,400	Not a potential sorbent. 1) Sulfite disproportionates. 2) Sulfate decomposition temperature is too high.
2) Na_2O	25 to 800°C	Thermodynamically favored between 25-800°C. Rate becomes appreciable at 600°C.	> 800°C	> 900°C Weight loss when held for 2 hrs. at 1200°C is 1.05%.	Inactive	Metal: 400 Carbonate: 30 Sulfate: 20	Not a potential sorbent. 1) Sulfite disproportionates. 2) Sulfate decomposition temperature is too high
3) K_2O	25 to 800°C	Thermodynamically favored between 25-800°C. Rate becomes appreciable at temperatures above 750°C.	> 800°C	> 900°C. Weight loss when held for 2 hrs. at 1200°C is 3.6%.	Inactive	Salts: 20	Not a potential sorbent. 1) Sulfite disproportionates. 2) Decomposition temperature of sulfate is too high.
4) Rb_2O	Unknown	Unknown	Unknown	> 900°C. Weight loss when held for 2 hrs. at 1200° is 6.3%.	Inactive	Metal: 1.5million Carbonate: 280,000	Not a potential sorbent. 1) Too expensive. 2) The sulfite will probably disproportionate. 3) The decomposition temp. of the sulfate is too high.
5) Cs_2O	Unknown	Unknown	Unknown	> 1036°C. Weight loss when held for 2 hrs. at 1200°C is 13.9%.	Inactive	Metal: 400,000 Carbonate: 64,000	Not a potential sorbent. 1) Too expensive. 2) Sulfite probably disproportionates. 3) The decomposition temperature is too high for the sulfate.
6) BeO	Sorption not possible at temp. greater than 25°C.	Shows no tendency to disproportionate thermodynamically.	150°C	690 to 760°C	Inactive	Metal: 130,000 Beryl(11% BeO): Buyer-Seller Basis	Not a potential sorbent. 1) Poisonous 2) Sulfite decomposition temp. too low. 3) Oxide is inactive, sorption with sulfate formation would be slow.
7) MgO	Possible at temp. less than 150°C	Thermodynamically favored between 25-800°C. The amount of sulfite converted to sulfite is 5-18% between 300 and 600°C.	350°C	Static method- ≥ 950°C Dynamic method- ≥ 871°C	Inactive	Metal: 705 Carbonate: 285	Not a potential sorbent. 1) Percent disproportionation is small but important. 2) Sulfate decomposition temperature is too high.

* Thermodynamic calculations were made only in the temperature range from 25 to 800°C.

TABLE VI (Cont'd.)

OXIDE	POSSIBLE SORPTION* RANGE WITH SULFITE FORMATION	DISPROPORTIONATION* RANGE OF SULFITE	DECOMPOSITION* TEMPERATURE OF SULFITE	DECOMPOSITION TEMPERATURE OF SULFATE	CATALYTIC BEHAVIOR OF OXIDE	PRICE DOLLARS/SHORT TON	REMARKS
8) CaO	< 590° C	Thermodynamic tendency to disproportionate from 25 to 800° C. Rate becomes appreciable at 600° C.	> 800° C	> 1227-1527° C	Inactive CaO_2: possibly high oxidation power(see Fig.65)	Metal: 4,000	Not a potential sorbent. 1) Sulfite decomposition temp. too high. 2) Disproportionation of sulfite. 3) Sulfate decomposition temp. too high.
9) SrO	25 to 800° C	Thermodynamic tendency to disproportionate from 25 to 800° C. Rate becomes appreciable at 450° C.	> 800° C	1374° C	Inactive	Sulfate: 60 Carbonate: 400-700	Not a potential sorbent. 1) Sulfate decomposition temp. too high. 2) Sulfite disproportionates. 3) Sulfite decomposition temp. is too high.
10) BaO	25 to 800° C	Thermodynamic tendency to disproportionate from 25 to 800° C. Rate becomes appreciable at 500° C.	> 800° C	> 1347 (m.pt.)	Inactive BaO_2: possibly high oxidation power(see Fig.65)	Oxide: 288 Sulfate: 20 Carbonate: 112	Not a potential sorbent. 1) Sulfite disproportionates. 2) Sulfate decomposition temperature too high. 3) Sulfite decomposition temperature too high.
11) Sc_2O_3	Unknown	Found by experiment to disproportionate from 300 to 550° C. Secondary reactions with sulfur formation at 300° C.	Decomposition should be appreciable at the same temp. as disproportionation.	780° C	Probably inactive	Oxide: 3,500,000 to 5,200,000	Not a potential sorbent. 1) Too expensive.
12) Y_2O_3	Unknown	Found by experiment to disproportionate from 500 to 800° C. Secondary reactions with sulfur formation at 700° C.	Decomposition should occur and compete with disproportionation.	1124° C. Before decomposition a basic sulfate is formed.	Probably inactive	Metal: 500,000 to 1,000,000	Not a potential sorbent. 1) Too expensive. 2) Sulfite disproportionates. 3) Sulfate decomposition temperature too high.
13) La_2O_3	Unknown	Found experimentally to disproportionate appreciably from 400 to 700° C. Secondary reactions with sulfur formation at 650° C.	Decomposition and disproportionation are are competing reactions.	> 1096° C Basic sulfate is formed before decomposition.	Probably inactive		Not a potential sorbent. 1) Probably too expensive. 2) Sulfite disproportionates. 3) Sulfate decomposition temp. too high.
14) Ce_2O_3	Unknown	Decomposition and disproportionation are expected on the basis of similarity to lanthanum and samarium.		> 650° C Decomposition product is CeO_2.	Probably active	Metal: 150,000	Potential sorbent 1) Sulfate decomposition is not too high. 2) Shows catalytic activity.
CeO_2	Unknown	Unknown	Unknown	> 860° C	1.8-13.7% conversion of SO_2 from 600 to 700° C. Some sulfate found in catalyst mass.	Oxide: 8,000	Potential sorbent 1) Sulfate decomposition is not too high. 2) Shows catalytic activity.

* Thermodynamic calculations were made only in the temperature range from 25 to 800° C.

TABLE VI (Cont'd.)

OXIDE	POSSIBLE SORPTION RANGE WITH SULFITE FORMATION	DISPROPORTIONATION RANGE OF SULFITE	DECOMPOSITION TEMPERATURE OF SULFITE	DECOMPOSITION TEMPERATURE OF SULFATE	CATALYTIC BEHAVIOR OF OXIDE	PRICE DOLLARS/SHORT TON	REMARKS
15) TiO_2	Unknown	Unknown	Unknown	430 to 600° C Basic sulfate is formed before decomposition.	Poor since reaction Ti_2O_3-TiO_2 goes too slowly.	Oxide: 120	Potential sorbent: 1) Sulfate dec position temp. seems favorable for sorption. 2) TiO_2 reacts too slowly. In catalytic experiments only small amounts of $TiOSO_4$ were found.
16) ZrO_2	Possible at temperatures below 330° C.	Unknown	600° C[1]	576 to 632° C[1] Basic sulfate formed before decomposition.	Probably inactive	Metal: 10,500 to 36,000 Oxide: 600 to 3,000	Potential sorbent 1) Sulfate decomposition temp. is favorable. 2) Oxidation power can be expected to be very low.
17) HfO_2	Unknown	Unknown	Unknown	550 to 650° C	Probably inactive	Metal: 150,000 to 276,000	Same as for ZrO_2
18) V_2O_3	Unknown	Unknown	Unknown	> 400° C Decomposition product is mixture of V_2O_4 and V_2O_5	Good catalyst. Conversion takes place from 400-700° C. Part of V_2O_5 is reduced.	V_2O_5 2,400 to 2,600	Potential sorbent: 1) Kinetics of reaction below 400° C discouraging. 2) Thermodynamically favorable.
VO_2	Unknown	Unknown	Unknown				
V_2O_5	Unknown	Unknown	Unknown				
19) Nb_2O_5	Unknown	Unknown	Unknown	Unknown	Unknown	Oxide containing ore: 2,000 to 8,000 Metal: 20,000 to 60,000	Insufficient information for decision.
20) Ta_2O_5	Unknown	Unknown	Unknown	Unknown	Unknown	Pentoxide: 15,000 to 16,000	Insufficient information for a decision.
21) Cr_2O_3	Unknown	Unknown	Unknown	Decomposition to basic sulfate 460-640°C. Sulfate decomposition temp. unknown.	SO_2 physically adsorbed on Cr_2O_3; no reaction to 400° C. Efficiency of Cr_2O_3-SnO_2 mixture is very high from 350 to 400° C.	Ore(50% Cr_2O_3): 18 to 36	Potential sorbent: 1) sulfate decomposition temperature probably favorable. 2) the reactivity with SO_2 up to 400° C is very poor.

---

[1] There seems to be a discrepancy between theoretical and experimental results. If sulfate decomposes at 576 to 632° C, the sulfite should decompose at much lower temperatures.

TABLE VI (Cont'd.)

OXIDE	POSSIBLE SORPTION RANGE WITH SULFITE FORMATION	DISPROPORTION-ATION RANGE OF SULFITE	DECOMPOSITION TEMPERATURE OF SULFITE	DECOMPOSITION TEMPERATURE OF SULFATE	CATALYTIC BEHAVIOR OF OXIDE	PRICE DOLLARS/SHORT TON	REMARKS
22) MoO_3	Unknown	Unknown	Unknown	Unknown	MoO_3 catalyst converts 45% SO_2 from 500-700° C. Catalyst mass undergoes undescribed change.	Metal: 3,200 Oxide: 2,800	Not a potential sorbent. Sublimes rapidly at 600° C.
23) WO_3	Unknown	Unknown	Unknown	Unknown	Poor: Conversion reaches a maximum of 62% at 675° C. Catalyst is partly reduced.	Metal: 35-45	No decision possible.
24) MnO	< 240° C	Thermodynamic tendency to disproportionate from 25 to 800° C	440° C	$MnSO_4$ is oxidized in O_2 containing atmosphere. Decomposition between 1090-1100° C.	Poor catalytic activity. Catalyst mass is transformed to $MnSO_4$	Metal: 590	Not a possible sorbent. 1) Shows excellent sorption behavior (especially MnO_2) with $MnSO_4$ formation. 2) Decomposition temperature of sulfate is too high. 3) Active form of sorbent difficult to regenerate.
Mn_2O_3	< 20° C	---------	130° C	1090-1100° C	Same as MnO.	Same as MnO.	Same as MnO.
MnO_2	Sorbs with formation of sulfate.	---------	-----	1090-1100° C for $MnSO_4$.	Same as MnO.	Same as MnO.	Same as MnO.
25) ReO_2	Unknown	Unknown	Unknown	Unknwon	Unknown	Metal: 1,160,000	Not a possible sorbent. 1) Too expensive.
26) FeO	< 190° C	Thermodynamic tendency to disproportionate from 25-800° C.	380° C	Oxidation takes place at 520-530° C.	Good (used as commercial catalyst)	Ore: 8.5 Oxide Pigments: 60-440	Potential sorbent: 1) Thermodynamically favorable. 2) Kinetics of the reaction below 400° C discouraging.
Fe_2O_3	Sulfite is unstable at temperatures above 60° C.	-------	60° C	Literature disagreement, probably 650° C.	Same as FeO.	Same as FeO.	Same as FeO.

TABLE VI (Cont'd.)

OXIDE	POSSIBLE SORPTION RANGE WITH SULFITE FORMATION	DISPROPORTIONATION RANGE OF SULFITE	DECOMPOSITION TEMPERATURE OF SULFITE	DECOMPOSITION TEMPERATURE OF SULFATE	CATALYTIC BEHAVIOR OF OXIDE	PRICE DOLLARS/SHORT TON	REMARKS
27) CoO	< 250°C	Thermodynamically favored from 25 to 800°C.	470°C	800-1000°C End product is Co_3O_4	No data.	Metal: 3,000-3,300 Oxide: No data.	Potential sorbent: 1) Co_xO_y can be expected to have a good oxidation power (See Figure 65). 2) Decomposition temperature of sulfate is a little too high.
28) NiO	< 180°C	Thermodynamically favored between 25 and 800°C.	410°C	About 800°C	Unknown	Metal: 1,900 Oxide: 1,800	Potential sorbent: 1) The higher oxides, Ni_xO_y, can be expected to have a high enough oxidation power for SO_2 oxidation. 2) Sulfate decomposition temperature is reasonable.
29) Rh_xO_y	Unknown	Unknown	Unknown	Unknown	Unknown	Metal: 1,200,000	Not a potential sorbent: 1) U.S. production 2 tons/yr. 2) Too expensive.
30) IrO_2	Unknown	Unknown	Unknown	Unknown	Unknown	Metal: 4,958,000 to 5,542,000	Not a potential sorbent, too expensive.
31) PdO	Unknown	Unknown	Unknown	Unknown	Unknown	Unknown	No decision possible, but probably too expensive.
32) CuO	Sulfite is unstable at temperatures higher than 110°C.	Thermodynamically favored from 25 to 800°C.	110°C	840-935°C	Poor, (sulfate formation).	Metal: 680 to 760	Potential sorbent: 1) Oxidation power may be high enough. 2) Decomposition temperature of sulfate is not too high.
Cu_2O	Sulfite is unstable at temperatures higher than 100°C.	Thermodynamically favored from 25 to 800°C.	100°C	Cu_2SO_4 is oxidized in air. Decomposes at 840-935°C.	Poor, (sulfate formation).	Same as CuO.	Same as CuO.
33) Ag_2O	< 310°C, Ag_2O is stable to 250°C.	Thermodynamically favored between 25 and 300°C.	Predicted to be > 570°C. The reaction, $2Ag_2SO_3 = 2Ag + SO_2 + Ag_2SO_4$, occurs at 100°C.	> 840°C Decomposition product is metal.	Poor, (sulfate formation).	Metal: 38,000 to 52,000	Not a potential sorbent, sulfate decomposes to metal.
34) ZnO	< [illegible] C	Thermodynamically favored between 25 and 800°C.	290°C	> 740°C Decomposition goes via oxisulfate as intermediate.	Inactive	Metal: 240-280 Oxide 300-355	Potential sorbent: 1) Disproportionation is 3% at 350°C. 2) Decomposition temperature of sulfate is low enough.

TABLE VI (Cont'd.)

OXIDE	POSSIBLE SORPTION RANGE WITH SULFITE FORMATION	DISPROPORTION-ATION RANGE OF SULFITE	DECOMPOSITION TEMPERATURE OF SULFITE	DECOMPOSITION TEMPERATURE OF SULFATE	CATALYTIC BEHAVIOR OF OXIDE	PRICE DOLLARS/SHORT TON	REMARKS
35) CdO	< 230° C	Thermodynamically favored between 25 and 800° C.	450° C	> 1065° C A basic sulfate is formed before decomposition.	Inactive	Metal: 5,160	Not a potential sorbent. 1) Since the decomposition temperature of the sulfite is higher than that for Zn disproportionation will be more extensive. 2) The resulting sulfate cannot be thermally regenerated.
36) B_xO_y	No salts are known to exist.					Element: 7,330	Not a potential sorbent.
37) Al_2O_3	Sulfite is unstable at temperatures above 70° C.	No tendency to disproportionate.	Theoretically 70° C. Literature reports 200 to 300° C.	650-950° C	Inactive	Sulfite: 44 to 76 Oxide 15 to 32	Potential sorbent: 1) Disagreement between estimated and reported decomposition temperature of sulfite. 2) No disproportionation predicted. 3) Sulfate decomposition temperature low enough.
38) Ga_2O_3	Unknown	Unknown	Unknown	Unknown	Unknown	Metal: 860,000 to 1,270,000 U.S. production: 1.12 short tons/yr.	Not a potential sorbent. 1) Price is too high. 2) Production too low.
39) SiO_2	No salts are known to exist.	-----	-----	------	-----	------	Not a potential sorbent.
40) GeO_2	Unknown	Unknown	Unknown	Unknown	Unknown	Oxide: 137,000	Not feasible, U.S. prod. 1.5 tons/yr.
41) SnO_2	Thermodynamically unstable between 25 and 800° C.	------	------	About 600° C.	Poor	Metal: 3,060	Potential sorbent: The poor oxidation power will most probably yield a very low reaction rate.
42) PbO	< 330° C	Tends to disproportionate in the entire temp. range. Rate becomes appreciable at temp. above 300° C.	> 600° C	> 800° C	Poor: It was reported that nearly all oxides(starting with PbO_2) form sulfates.	Metal: 280	Not a potential sorbent. 1) The lead oxides Pb_xO_y, especially PbO_2, show good sorption behavior. 2) Resulting sulfate cannot be thermally regenerated. 3) Poisonous.
43) As_2O_3	No salts are known.	------	-------	-------	-------	----------	Not a potential sorbent, too poisonous.
44) Sb_2O_3	Sulfite is unstable in entire temp. range.	------	-------	Unknown	Unknown	Oxide: 950 to 1,200	No decision possible. According to Fig. 65, the system Sb_2O_5/Sb_6O_{13} has a high oxidation power.

TABLE VI (Cont'd.)

OXIDE	POSSIBLE SORPTION RANGE WITH SULFITE FORMATION	DISPROPORTIONATION RANGE OF SULFITE	DECOMPOSITION TEMPERATURE OF SULFITE	DECOMPOSITION TEMPERATURE OF SULFATE	CATALYTIC BEHAVIOR OF OXIDE	PRICE DOLLARS/SHORT TON	REMARKS
45) Bi_2O_3	< 150° C	Thermodynamically favored in the entire temp. range.	310° C	≈ 860° C Basic sulfate is formed before decomposition.	Unknown	Element (refined): 6,860	Potential sorbent.
46) UO_2	< 130° C	No tendency to disproportionate.	320° C	≥ 500° C Forms basic sulfate before decomposition.	Poor, due to sulfate formation.	U_3O_8: 12,000	Potential sorbent, will sorb SO_2 probably with UO_2SO_4 formation.
47) ThO_2	< 190° C	No tendency to disproportionate.	390° C	> 800° C	Unknown	Metal Pellets: 30,000 Oxide: 12,000 to 20,000	Potential sorbent.

PERIOD	GROUP																	
	Ia	IIa	IIIa	IVa	Va	VIa	VIIa	VIII			Ib	IIb	IIIb	IVb	Vb	VIb	VIIb	0
1	H																H	He
2	**Li**	**Be**											**B**	C	N	O	F	Ne
3	**Na**	**Mg**											▨ **Al**	**Si**	P	S	Cl	Ar
4	**K**	**Ca**	**Sc**	▨ **Ti**	▨ **V**	▨ **Cr**	**Mn**	▨ **Fe**	▨ **Co**	▨ **Ni**	▨ **Cu**	▨ **Zn**	**Ga**	**Ge**	As	Se	Br	Kr
5	**Rb**	**Sr**	**Y**	▨ **Zr**	**Nb**	**Mo**	Tc	**Ru**	**Rh**	**Pd**	**Ag**	**Cd**	In	▨ **Sn**	Sb	Te	I	Xe
6	**Cs**	**Ba**	**La**	▨ **Hf**	**Ta**	**W**	**Re**	Os	**Ir**	Pt	Au	Hg	Tl	**Pb**	▨ **Bi**	Po	At	Rn
7	Fr	Ra	Ac															

LANTHANIDE SERIES	▨ **Ce**	Pr	Nd	Pm	Sm	Eu	Gd	Tb	Dy	Ho	Er	Tm	Yb	Lu
ACTINIDE SERIES	▨ **Th**	Pa	▨ **U**	Np	Pu	Am	Cm	Bk	Cf	Es	Fm	Md		Lw

PERIODIC ARRANGEMENT OF:

POTENTIAL SORBENTS BEFORE SCREENING

/// POTENTIAL SORBENTS AFTER THERMODYNAMIC SCREENING

FIGURE 6

the sorption step, since excess free energy would have to be supplied during the regeneration step. Therefore, oxides such as the alkaline earth oxides had to be eliminated as potential sorbents. However, it was further found that these oxides, as well as others, when in chemical combination with a second oxide formed a compound with more favorable thermodynamic properties for regeneration. Since little was known from the literature about the reactions which actually occurred, the following simple reaction was used for the purpose of thermodynamic calculations.

$$MeSO_4 + Me'O \rightarrow MeMe'O + SO_3 \qquad (9)$$

The thermodynamics of sulfur oxide sorption using such mixed metal oxides were studied by calculating the log of the equilibrium constant for the reaction shown in Equation (9) and determining the magnitude of the free energy change. The equilibrium constants were calculated using the data base of thermodynamic properties by the program AIRPOL. The majority of the heats of formation for the mixed metal oxides were estimated by the modified Erdös method described in T.M. 004-009-Ch1A. It was found that in many cases the free energy change was more favorable for the mixed metal oxide than for one or both of the single oxides. These studies were described in detail in T.M. 004-004-Ch22.

Preliminary screening for metal oxide pairs consisted of determining the partial pressure of sulfur oxide over the sorption product from the log of the equilibrium constant for the decomposition reaction (see paragraph 2.7.1). It was found that numerous mixed metal oxides had the desired log K values for the decomposition reaction. These compounds are listed in T.M. 004-009-Ch22. Further investigation concerning the chemistry of the so-called "mixed metal oxides" revealed that an experimental program involving these compounds would be beyond the scope of the contract. The problems involved in such a study are discussed in T.M. 004-004-Ch25.

3. KINETIC STUDIES

3.1 INTRODUCTION TO KINETIC STUDIES

This section describes the methods used to screen the sixteen metal oxides shown in Figure 6 on the basis of their rate of reaction with SO_2 in a flue gas atmosphere. Kinetic screening was essential because even the most thermodynamically capable sorbent may be impractical for SO_2 removal if it reacts too slowly to be effective or economically feasible. Kinetic measurements eliminated such sorbents and provided an input to the economic studies for determining reactor design and operating conditions.

3.2 APPROACH

The purpose of the kinetic studies was to determine which thermodynamically favorable metal oxides were most reactive with SO_2. The criteria for reactivity is the rate of reaction. The rates of noncatalytic gas-solid reactions can often depend on physical effects, such as diffusion and heat transfer, which may be a result of the conditions of the experiment or the treatment of the sample. An attempt was made to try to minimize these physical effects and thereby evaluate the inherent chemical reactivity of each candidate metal oxide. Physical effects were partially minimized by using samples with small particle size, dilution of the sample, gas flow through the diluted sample instead of around it, and isothermal conditions.

The reactivity of a metal oxide is also determined in part by physical properties that are a result of the compound preparation method. Each sample was characterized by BET surface area determination, x-ray diffraction, and chemical analysis. These measurements were useful in the comparison of reaction rate results. All of these techniques are described in detail below.

3.3 COMPOUND PREPARATION AND CHARACTERIZATION

3.3.1 Preparation Methods

The metal oxides were prepared by thermal decomposition (calcination) of suitable compounds. Compounds which could be calcined at relatively low temperatures were chosen to minimize sintering of the product oxide. The metal hydroxides or hydrous oxides were usually employed. Procedures similar to those discussed below for the hydroxide were used for all intermediates.

The metal hydroxides were prepared by precipitation. The precipitate was filtered and washed several times with large quantities of water. The moist product was dried at low temperature (60°C) for 1-3 days in a vacuum oven. It was then ground if necessary and calcined either in a muffle furnace or vacuum oven. The metal oxide product was ground, sieved, and stored in a dessicator. The -170 +325 mesh fraction was retained for BET surface area and reaction rate determinations. The actual conditions employed and the intermediates used to prepare each metal oxide are summarized in Table IX in Section 3.5.

3.3.2 Use of X-ray Diffraction

The oxides were identified from their x-ray powder diffraction patterns. The patterns were determined by using Cr K_α radiation with either a Siemens type F Diffractometer (Eg 4/22e) or a Siemens short cylindrical camera (Cat. No. 176311) for Debye-Scherrer patterns. The diffractometer was used in most cases since the peak width gave a qualitative indication of the crystallinity of the sample. The lattice spacings were calculated from the recorded diffraction angles using the Bragg equation. Observed values were compared with those listed in the ASTM Inorganic Index to the Powder Diffraction File 1967.

Figure 7 shows the diffraction patterns obtained for Co_3O_4 prepared from the nitrate (A) and the hydroxide (B). The broad peaks of B indicate that it is less crystalline or has a

NOT REPRODUCIBLE

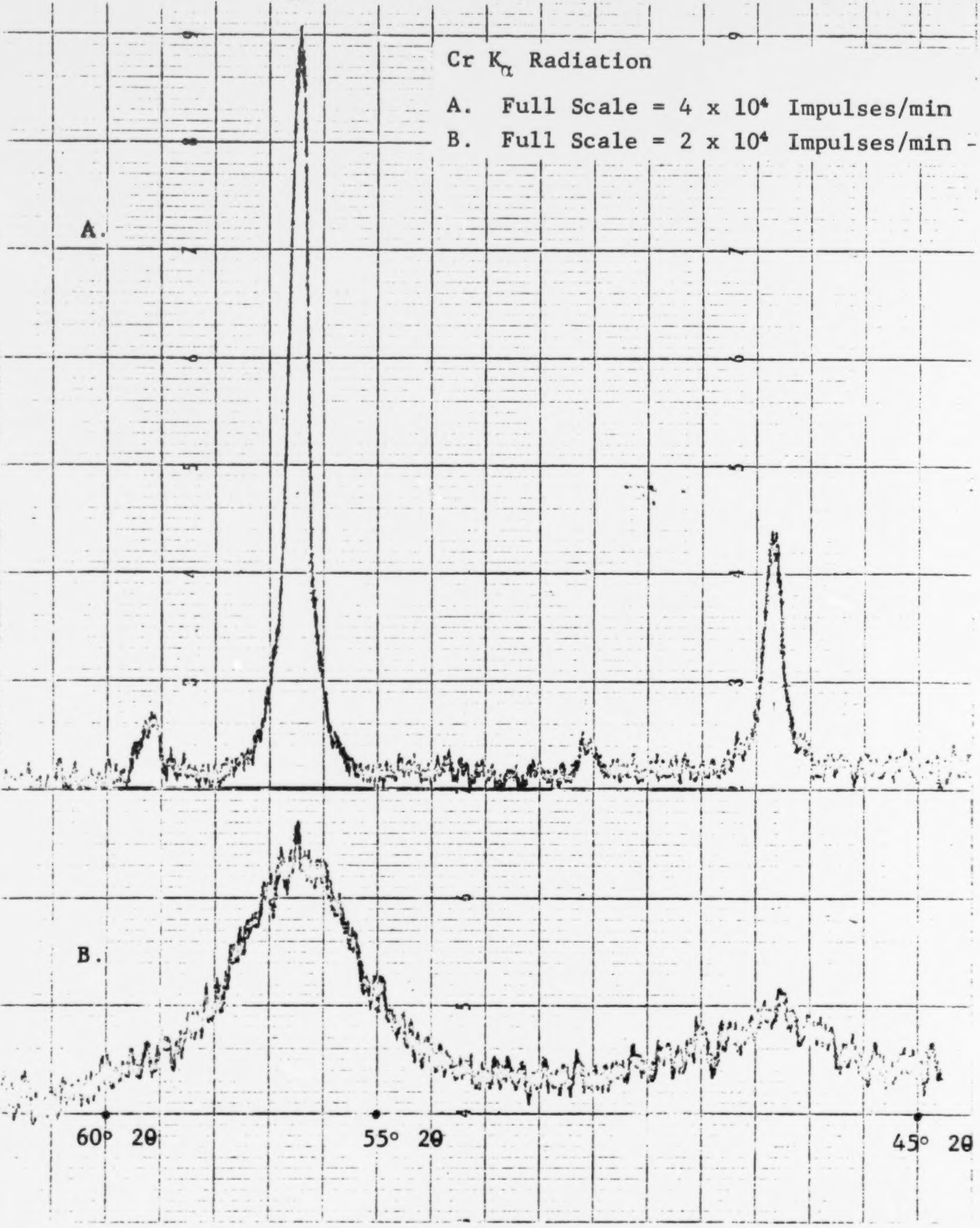

Figure 7: X-Ray Diffraction Patterns for Different Preparations of Co_3O_4

A. Surface Area 12 m²/g

B. Surface Area 169 m²/g

smaller primary particle size than A. This character is also reflected in the high surface area of B relative to A.

3.3.3 BET Surface Area Determinations

Knowledge of the surface area of a sample is an aid in characterizing its reactivity. Samples of the same metal oxide with different surface areas differ in rate of SO_2 sorption. The specific surface of metal oxide sorbents was determined using the BET method, which involves the measurement of the amount of gas (adsorbate) adsorbed on the surface of a sample (adsorbent) at a particular pressure and constant temperature. The method, apparatus, and data analysis are discussed in detail in T.M. 004-009-Ch24.

The BET method provides for calculation of the monolayer capacity, or the amount of adsorbate adsorbed in a layer one molecule thick, from the adsorption isotherm using Equation (10). An adsorption isotherm obtained at TRACOR for ziroconium oxide is shown in Figure 8.

$$\frac{P_i}{V_i(p_{o_i}-p_i)} = \frac{1}{V_m C} + \frac{C-1}{V_m C} \cdot \frac{P_i}{P_{o_i}} \qquad (10)$$

The following definitions are necessary:

V_m	Monolayer capacity in cm^3 (N.T.P.) of adsorbate per gram adsorbent
V_i	Volume of adsorbate in cm^3 (N.T.P.) adsorbed per gram sorbent at equilibrium pressure p_i (mm Hg)
P_{o_i}	The saturation vapor pressure (mm Hg) of adsorbate at the temperature of adsorption
p_i/p_{o_i}	Relative pressure

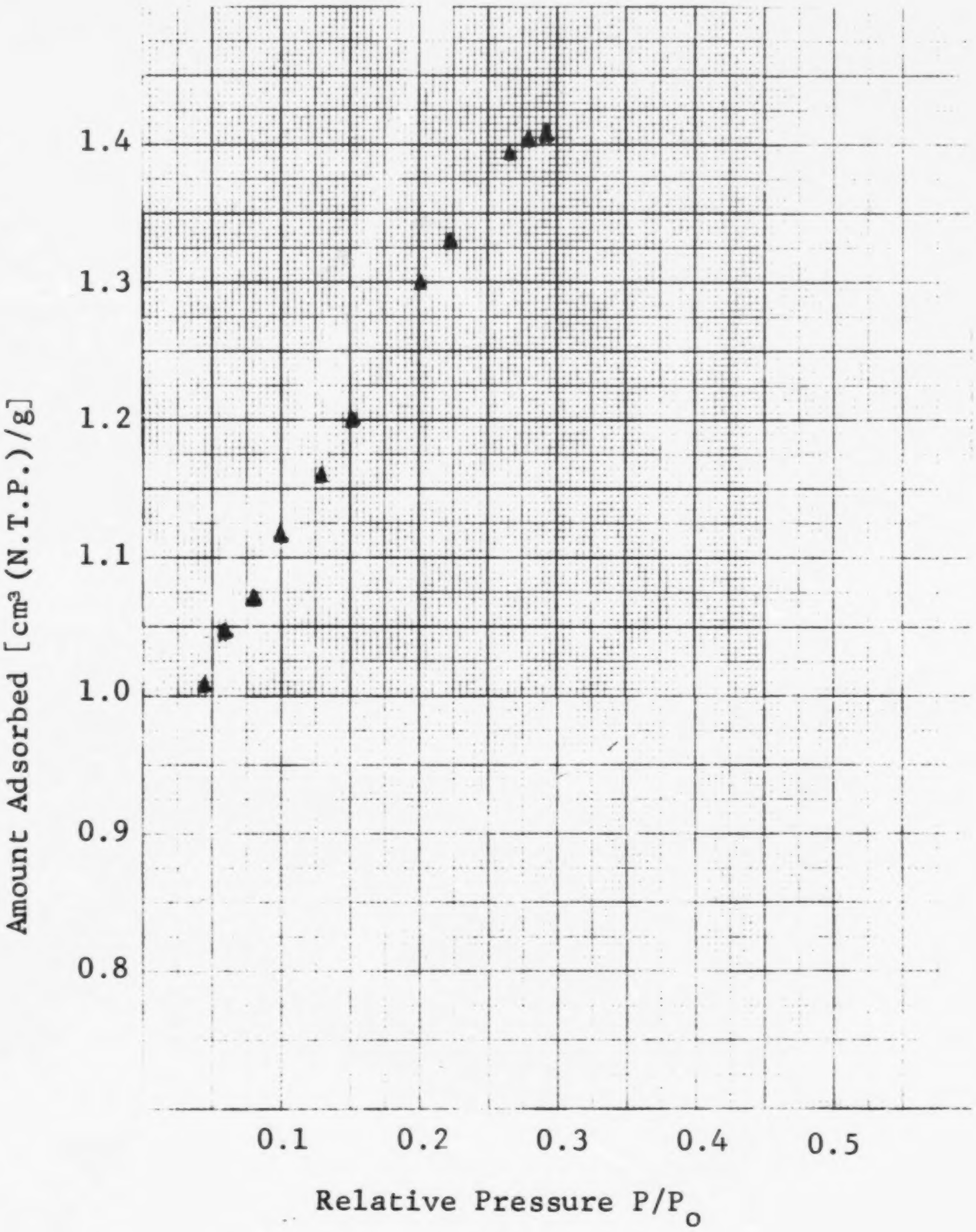

Figure 8: Adsorption Isotherm for Zirconium Oxide at 77^{o}K

From the derivation of Equation (10) (GR-002), C is defined by Equation (11).

$$C = e^{(E_1 - L)/RT} \frac{\nu_2}{\nu_1} \frac{a_1}{a_2} \qquad (11)$$

The factor, ν_1, is the frequency of oscillation of the adsorbate molecule normal to the sorbent surface and E_1 is the energy necessary for the molecule to condense or be adsorbed on the first layer. Therefore, $\nu_1 \; e^{-E_1/RT}$ is the number of molecules per second evaporating from a given site in the first layer. Similarly, the factor, $\nu_2 \; e^{-L/RT}$, is the number of molecules per second evaporating from or adsorbing on the second layer. L is the latent heat of condensation of the adsorbate.

The values of V_m and C are determined according to Equation (10) by plotting experimentally obtained values of $\frac{p_i}{V_i(p_{o_i} - p_i)}$ vs $\frac{p_i}{p_{o_i}}$ and finding the slope and intercept of the resulting straight line. The "normal" range of relative pressures for which the plot is actually linear and the BET equation is valid varies from about .05 to .35, although sometimes measurements in the 0.001-.05 range are necessary. The specific surface area S in square meters per gram is calculated from V_m using Equation (12) where V_m is the monolayer capacity in cm^3 (N.T.P.) per gram, N is Avogadro's number, and A_m is the cross-sectional area of the adsorbate molecule, 16 $Å^2$.

$$S = \frac{V_m \, N \, A_m \times 10^{-20}}{22414} \qquad (12)$$

The apparatus built and used at TRACOR for BET surface area measurements consists of a basic high vacuum system with manometer, calibrated volumetric bulbs, and thermometers. A mercury manometer is used to measure the gas pressure in the system. The temperature of the sample immersed in a liquid nitrogen bath is monitored with an argon gas thermometer. A schematic diagram of the apparatus is shown in Figure 9.

The procedure followed to determine the necessary temperature, pressure, and volume data was to introduce a known amount of gaseous adsorbate to the sample enclosed in a known volume, allow the sample to adsorb the gas until equilibrium pressure was reached, and measure the pressure. Since the temperature and volume of the system were known, it was possible to calculate the amount of adsorbate present after equilibrium had been reached using ideal gas laws. Then the amount adsorbed at the measured pressure could be determined from the difference between the known, original amount of adsorbate and the amount remaining unadsorbed at that particular equilibrium pressure. This procedure was repeated for several different values of pressure such that the reduced or relative pressure (equilibrium pressure divided by saturation vapor pressure) varied in the range of .001 to .35.

The metal oxides were dried in a vacuum oven, and the samples to be determined were weighed by difference using a Mettler Type B6 analytical balance. The samples were weighed into sample tubes constructed so that bumping of the sample during outgassing would not cause it to be blown into other parts of the system. The samples were outgassed overnight until the system pressure, as measured with an ion gage (NRC Model 741), was about 10^{-5} torr.

A computer program, SSAREA, was written at TRACOR to calculate V_i, p_i, and p_{o_i} from input pressure, temperature, and volume data and, using a least squares technique, to find the best straight line with ordinate $y_i = \frac{p_i}{V_i(p_{o_i}-p_i)}$ and abscissa

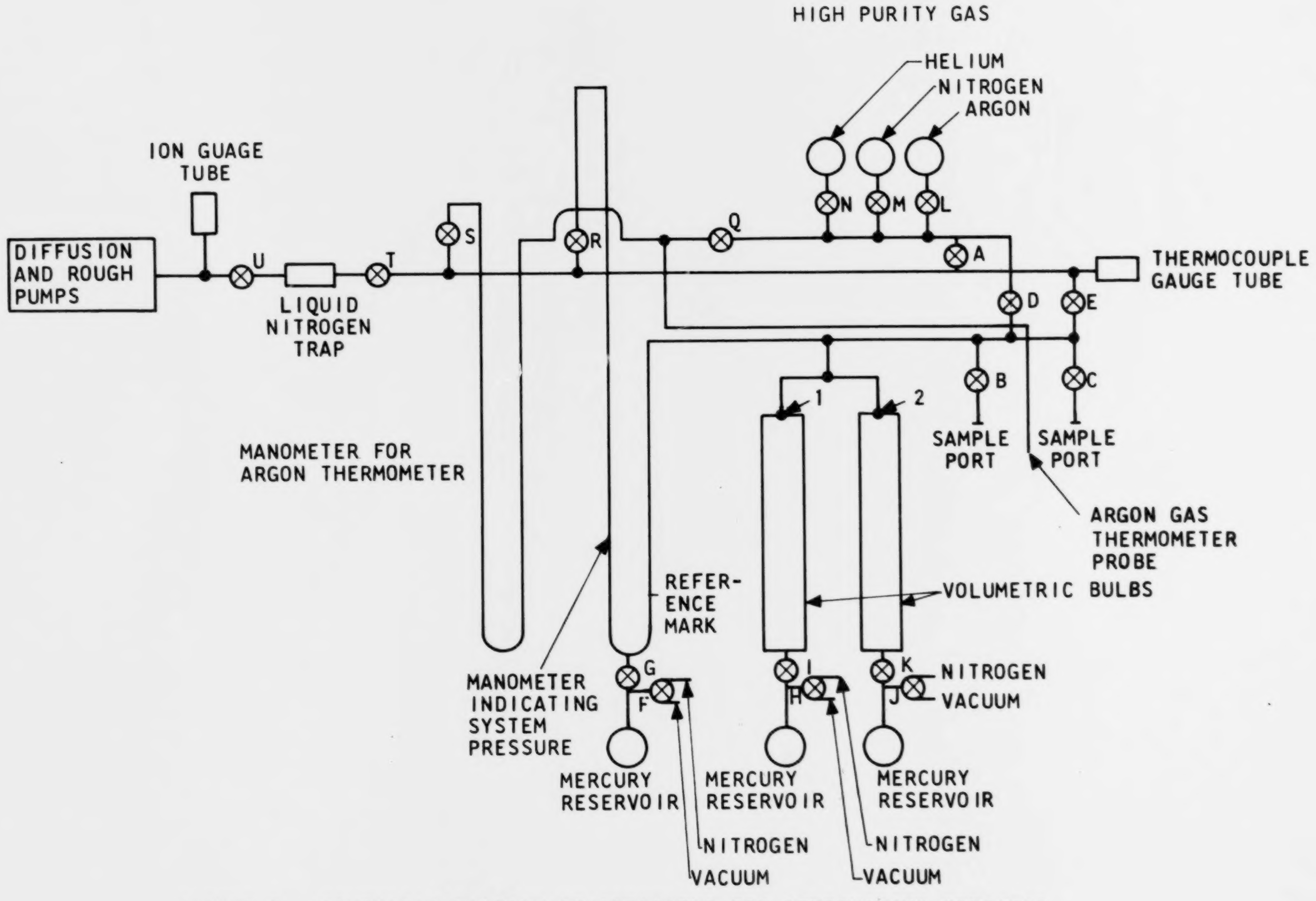
HIGH PURITY GAS
HELIUM
NITROGEN
ARGON
ION GUAGE TUBE
DIFFUSION AND ROUGH PUMPS
U
LIQUID NITROGEN TRAP
T
S
R
Q
N
M
L
A
D
E
THERMOCOUPLE GAUGE TUBE
B
C
1
2
SAMPLE PORT
SAMPLE PORT
ARGON GAS THERMOMETER PROBE
MANOMETER FOR ARGON THERMOMETER
VOLUMETRIC BULBS
REFER-ENCE MARK
MANOMETER INDICATING SYSTEM PRESSURE
G
F
I
H
K
J
NITROGEN
VACUUM
MERCURY RESERVOIR
MERCURY RESERVOIR
MERCURY RESERVOIR
NITROGEN
VACUUM
NITROGEN
VACUUM

FIGURE 9 - SCHEMATIC DIAGRAM OF APPARATUS FOR DETERMINING SPECIFIC SURFACE AREA USING THE BET METHOD

$x_i = \frac{p_i}{p_{o_i}}$. An cxample of the output for ziroconium oxide, whose adsorption isotherm was given in Figure 8, is shown in Table VII.

3.3.4 Differential Thermal Analysis

Differential thermal analysis (DTA) was used to determine the calcination temperature of intermediate compounds if the temperature was not already known. It was also used in some instances to check for completeness of calcination of an intermediate compound.

A TRACOR LB-202 Recorder-Controller and JP-202 Furnace Platform were used to make the measurements. The results obtained were in the form of difference in temperature between sample and an inert reference (alumina) as a function of system temperature. The decomposition reactions of interest appeared as endothermic peaks.

3.3.5 Chemical Analysis

The metal oxide samples were analyzed by atomic absorption and emission spectroscopy to determine the impurities present. The analyses were done by Southern Spectrographic Laboratory in Dallas, Texas.

The results are summarized in Table VIII, which has been reprinted by permission of Southern Spectrographic Laboratory. The only compound having significant impurities was aluminum oxide with about 1.2% zinc. The impurity was probably only a physical mixture of ZnO with the Al_2O_3 caused by incomplete cleaning of the sieve.

3.4 KINETIC MEASUREMENTS

3.4.1 Apparatus

A TRACOR TGA-3C thermal balance was used to make the isothermal kinetic measurements. In this instrument the sample holder is suspended from a spring. A photocell detector activates a servo motor and linear actuator to maintain a null condition

TABLE VII

DETERMINATION OF SPECIFIC SURFACE AREA BY THE B E T METHOD

AMPLE DESCRIPTION ZRO2 634-63-1
170-325 MESH, OUT GASSED AT 65C

B E T EQUATION: P/V(PO-P) = ((C-1)/VM*C)P/PO + 1/VM*C

SAMPLE TEMPERATURE (DEG. K)	REDUCED PRESSURE P/PO (MM HG)	VOLUME ADSORBED PER GRAM SAMPLE AT STP (ML/G)		P/V(PO-P) (G/ML)		NORMALIZED WEIGHTING FUNCTION
		OBSERVED	CALCULATED	OBSERVED	CALCULATED	
77.5	.046	1.006	1.040	.04815	.04660	1.00
77.5	.059	1.047	1.061	.05944	.05867	1.00
77.4	.080	1.073	1.092	.08093	.07947	1.00
77.4	.101	1.117	1.123	.10082	.10028	1.00
77.5	.127	1.160	1.159	.12496	.12512	1.00
77.4	.143	1.207	1.192	.14532	.14723	1.00
77.4	.200	1.300	1.270	.19174	.19636	1.00
77.4	.224	1.330	1.310	.21645	.21978	1.00
77.4	.265	1.393	1.386	.25925	.26061	1.00
77.4	.279	1.406	1.412	.27516	.27393	1.00
77.4	.292	1.411	1.440	.29288	.28705	1.00

VOLUME ABSORBED PER GRAM SAMPLE IN MOLECULAR MONOLAYER (VM) = 1.02 ML/G

RELATIVE LIFETIMES OF MOLECULES IN FIRST AND HIGHER LAYERS (C) = 677.24

CORRELATION ERROR FOR P/V(PO-P) = .00268 C-1/VM*C = .9768 1/VM*C = .00144

RMS ERROR FOR VOLUME ADSORBED = .02 ERROR IN C-1/VM*C = .0093

ERROR IN 1/VM*C = .00175 ERROR IN VM = .01

SPECIFIC SURFACE AREA = 4.35 * VM

SPECIFIC SURFACE AREA = 4.45 SQUARE METERS/GRAM

ERROR IN SPECIFIC SURFACE AREA = .04

PHONE FEDERAL 1-3243

TABLE VIII: RESULTS OF CHEMICAL ANALYSIS

Southern Spectrographic Laboratory
P. O. BOX 6014
2824 N. WESTMORELAND
DALLAS, TEXAS 75222

May 8, 1969

Tracor
6500 Tracor Lane
Austin, Texas 78721

SSL#69-AA-68
P.O. #1149

Sample: Nine Oxides

	ZnO	Cr_2O_3	SnO_2	Co_3O_4	NiO	Fe_2O_3	Al_2O_3	Sb_2O_5	CuO
Cu	37	18	74	146	32	458	88	119	X
Ni	10*	10*	525	1,170	X	126	10*	280	10*
Sn	10*	127	X	10*	10*	90	90	10*	10*
Co	327	10*	10*	X	127	72	10*	10*	10*
Al	10*	10*	835	20	75	10*	X	10*	10*
Zn	X	17.6	47	57	39	118	12,200	44	50
Ag	---	---	43	---	---	---	---	---	---
Sb	10	10	---	---	765	---	---	X	---
Fe	---	43	48	40	15	X	76	272	270
Mn	---	---	---	11	---	1,595	---	---	---
Mg	---	---	---	---	---	---	727	14	---
K	---	---	---	---	2,350	---	---	---	---
Cr	10*	X	10*	10*	10*	10*	10*	10*	10*

Note: All Values ppm
* - less than

SOUTHERN SPECTROGRAPHIC LABORATORY

Donald L McAlpin

Don McAlpin

TABLE VIII (Cont'd.)

SOUTHERN SPECTROGRAPHIC LABORATORY

P. O. BOX 6014 • 2824 N. WESTMORELAND • DALLAS, TEXAS 75222
FEderal 1-3243

Page 1 of 4

Tracor
6500 Tracor Lane
AustingTexas 78721

Re: P.O.# 1149

Report of Semi-quantitative Analysis No. 69-196 Date: 5/8/69

	No. ZnO	No. CuO	No. Cr_2O_3
Over 10%	Zn	Cu	Cr
1-10%	---	---	---
0.1-1.0%	---	---	Sn
0.01-0.1%	Co	---	---
0.001-0.01%	Sb, Pb, Cu	Si, Pb, Cu, Fe	Sb, Pb, Cu, Fe
less than 0.001%	Si, Mg, Sn, Al, Ag, Ni, Fe, Ca, Cr	Mg, Sn, Al, Ag, Zn, Ca, Cr	Si, Mg, Al, Ag, Ni, Ca

Semi-quantitative analysis is a preliminary, low-cost supplement to more refined methods. The basic definition of semi-quantitative is a "factor of three", denoting that the reported concentration may be one-third to three times the amount present. SOUTHERN SPECTROGRAPHIC LABORATORY reports in "ranges of ten". This indicates an accuracy exceeding the basic definition, reflects the greater accuracy attainable at low concentrations, and relates the increased deviation with increased concentration.

SOUTHERN SPECTROGRAPHIC LABORATORY

Chief Spectrographer

This report, or any part thereof, does not imply an endorsement, and may not be reproduced or used for advertising, unless expressly permitted by Southern Spectrographic Laboratory.

TABLE VIII (Cont'd.)

SOUTHERN SPECTROGRAPHIC LABORATORY

P. O. BOX 6014 • 2824 N. WESTMORELAND • DALLAS, TEXAS 75222
FEderal 1-3243

Page 2 of 4

Tracor

Re: P.O. #1149

Report of Semi-quantitative Analysis No. 69-196 Date: 5/8/69

	No. SnO_2	No. Co_3O_4	No. NiO
Over 10%	Sn	Co	Ni
1-10%	---	---	---
0.1-1.0%	---	Ni	K
0.01-0.1%	Sn, Al, Ni	Cu	Sb
0.001-0.01%	Si, Pb, Zn, Fe, Cu, Ag	Fe, Si, Pb, Al, Ag, Zn, Mn	Fe, Si, Pb, Al, Cu, Zn
less than 0.001%	Sb, Mg, Ca, Cr	Mg, Sn, Ca, Cr	Sn, Ag, Co, Ca, Cr

Semi-quantitative analysis is a preliminary, low-cost supplement to more refined methods. The basic definition of semi-quantitative is a "factor of three", denoting that the reported concentration may be one-third to three times the amount present. SOUTHERN SPECTROGRAPHIC LABORATORY reports in "ranges of ten". This indicates an accuracy exceeding the basic definition, reflects the greater accuracy attainable at low concentrations, and relates the increased deviation with increased concentration.

SOUTHERN SPECTROGRAPHIC LABORATORY

Chief Spectrographer

This report, or any part thereof, does not imply an endorsement, and may not be reproduced or used for advertising, unless expressly permitted by Southern Spectrographic Laboratory.

TABLE VIII (Cont'd.)

SOUTHERN SPECTROGRAPHIC LABORATORY

P. O. BOX 6014 • 2824 N. WESTMORELAND • DALLAS, TEXAS 75222 ~~XXXXXX~~ Page 3 of 4
FEderal 1-3243

Tracor ReP.O. #1149

Report of Semi-quantitative Analysis No. 69-196 Date: 5/8/69

	No. Sb_2O_5	No. Fe_2O_3	No. Al_2O_3
Over 10%	Sb	Fe	Al
1-10%	---	---	Zn
0.1-1.0%	---	Mn	Mg
0.01-0.1%	Si, Cu, Ni, Fe	Cu	---
0.001-0.01%	As, Mg, Zn, Pb, Ag	Pb, Zn, Ni, Sn	Si, Pb, Cu, Fe, Sn
less than 0.001%	Sn, Al, Co, Ca, Cr	Si, Al, Ag, Co, Ca, Cr	Ag, Ca, Cr

Semi-quantitative analysis is a preliminary, low-cost supplement to more refined methods. The basic definition of semi-quantitative is a "factor of three", denoting that the reported concentration may be one-third to three times the amount present. SOUTHERN SPECTROGRAPHIC LABORATORY reports in "ranges of ten". This indicates an accuracy exceeding the basic definition, reflects the greater accuracy attainable at low concentrations, and relates the increased deviation with increased concentration.

SOUTHERN SPECTROGRAPHIC LABORATORY

Chief Spectrographer

This report, or any part thereof, does not imply an endorsement, and may not be reproduced or used for advertising, unless expressly permitted by Southern Spectrographic Laboratory.

TABLE VIII (Cont'd.)

SOUTHERN SPECTROGRAPHIC LABORATORY

P. O. BOX 6014 • 2824 N. WESTMORELAND • DALLAS, TEXAS 75222
FEderal 1-3243

Page 4 of 4

Tracor

Re:**P.O. #1149**

Report of Semi-quantitative Analysis No. **69-196** Date: **5/8/69**

	No. CeO_2	No. ZrO	No.
Over 10%	Ce	Zr	
1-10%	---	---	
0.1-1.0%	---	Zn	
0.01-0.1%	---	Ni	
0.001-0.01%	Sr, Sb, Cu, Fe, Mn	Si, Pb, Sn, Cu, Fe	
less than 0.001%	Mg, Ag, Cr	Al, Ag, Co, Ca, Cr	

Semi-quantitative analysis is a preliminary, low-cost supplement to more refined methods. The basic definition of semi-quantitative is a "factor of three", denoting that the reported concentration may be one-third to three times the amount present. SOUTHERN SPECTROGRAPHIC LABORATORY reports in "ranges of ten". This indicates an accuracy exceeding the basic definition, reflects the greater accuracy attainable at low concentrations, and relates the increased deviation with increased concentration.

SOUTHERN SPECTROGRAPHIC LABORATORY

Chief Spectrographer

This report, or any part thereof, does not imply an endorsement, and may not be reproduced or used for advertising, unless expressly permitted by Southern Spectrographic Laboratory.

whenever a weight change occurs. The linear actuator movement causes the displacement of the core of a linear variable differential transformer (LVDT). This displacement results in a signal which is displayed as the weight change. The instrument is shown schematically in Figure 10.

The most important feature of the TGA-3C for this type of rate measurement is that the gas is forced past the solid. The gas enters the hollow connecting rod between the spring and sample holder and passes down through the sample exiting from a porous frit or 400 mesh stainless steel screen at the bottom of the sample holder. Thus the gas composition actually surrounding the solid particles is known. The measured reaction rate is not limited by the rate of diffusion of the gas through the bulk solid.

The temperature was measured with a Pt-Pt/10% Rh thermocouple placed about 1 mm from the sample holder. The cylindrical Inconel sample holder is 1.3 cm in diameter and 2.8 cm long.

A TRACOR LB-202 Recorder-Controller was used with the TGA-3C to control and record the temperature and to amplify and record the weight change signal The weight gain _vs_ system temperature was recorded on a Moseley X-Y recorder. The 0°C reference point was set electronically. A Hewlitt-Packard model 17504 A strip chart recorder provided the isothermal weight gain _vs_ time record.

The gas mixing and control apparatus used to supply the simulated flue gas to the sample has been described in T.M. 004-009-Ch20. This apparatus is capable of producing a wide range of gas compositions. Flows and pressures are reproducible and can be obtained without affecting the flow through the thermal balance system. Gas analysis equipment is included to provide an independent means of determining compositions and can be used without disturbing the flow to the experimental equipment. A schematic diagram of the gas mixing apparatus is given in Figure 11.

TRACOR TGA-3C SCHEMATIC DIAGRAM

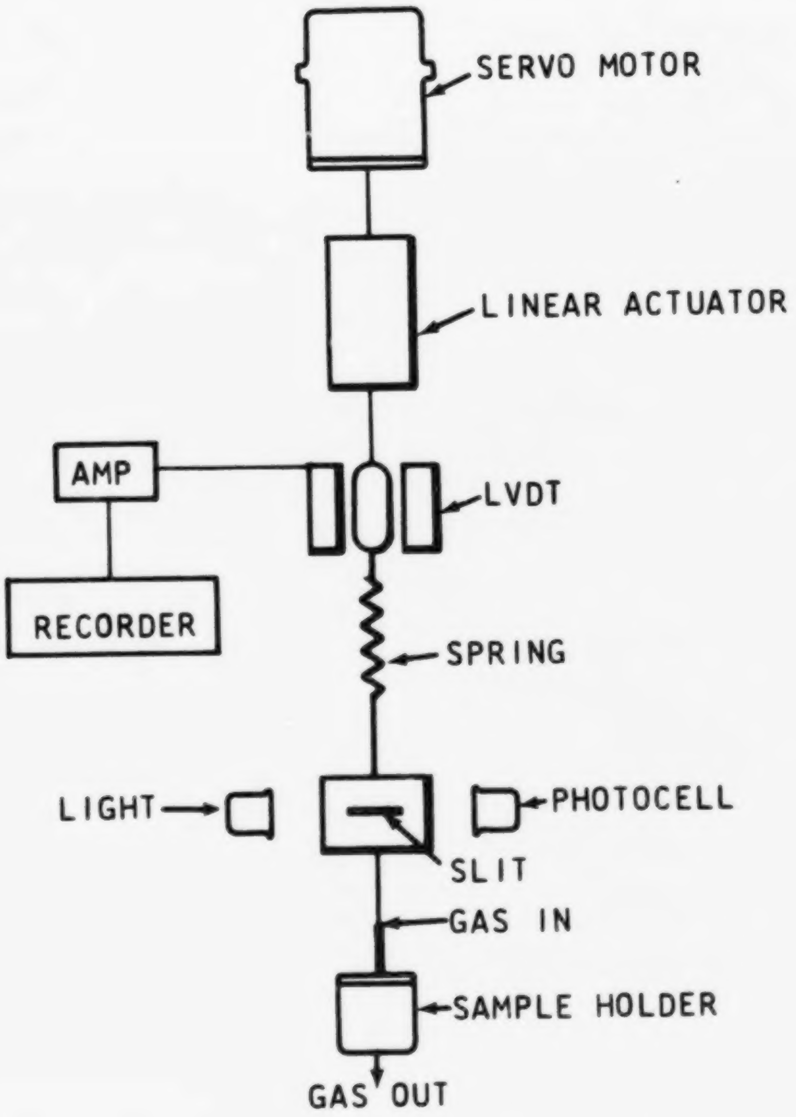
SERVO MOTOR
LINEAR ACTUATOR
AMP
LVDT
RECORDER
SPRING
LIGHT
PHOTOCELL
SLIT
GAS IN
SAMPLE HOLDER
GAS OUT

FIGURE 10

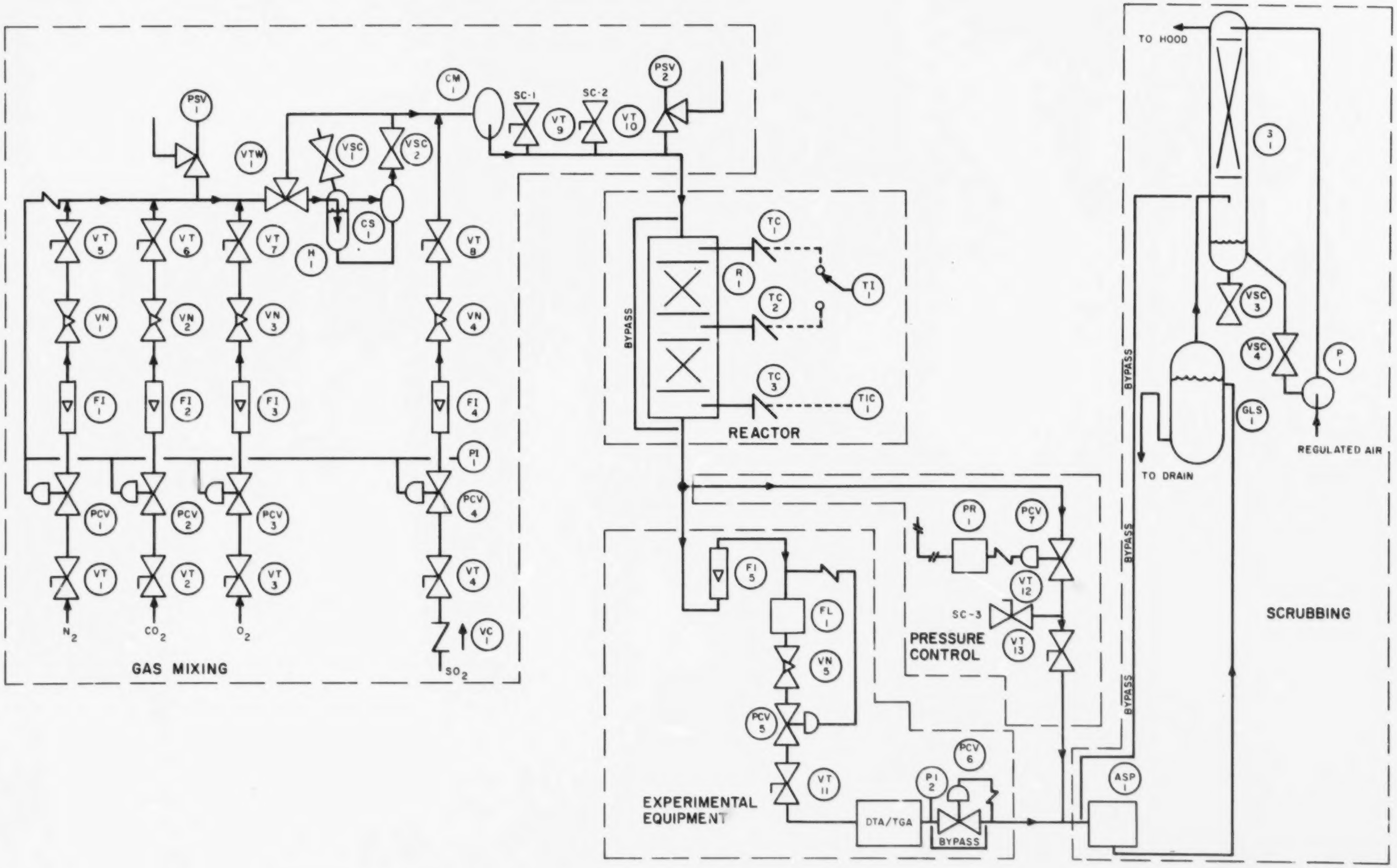
GAS MIXING
N2
CO2
O2
SO2
VT 1
VT 2
VT 3
VT 4
PCV 1
PCV 2
PCV 3
PCV 4
PI 1
FI 1
FI 2
FI 3
FI 4
VN 1
VN 2
VN 3
VN 4
VT 5
VT 6
VT 7
VT 8
VC 1
PSV 1
VTW 1
H 1
CS 1
VSC 1
VSC 2
CM 1
SC-1
VT 9
SC-2
VT 10
PSV 2
REACTOR
BYPASS
R 1
TC 1
TC 2
TC 3
TI 1
TIC 1
EXPERIMENTAL EQUIPMENT
FI 5
FL 1
VN 5
PCV 5
VT 11
DTA/TGA
PI 2
PCV 6
BYPASS
PRESSURE CONTROL
PR 1
PCV 7
VT 12
SC-3
VT 13
ASP 1
BYPASS
BYPASS
BYPASS
SCRUBBING
TO HOOD
3 1
VSC 3
VSC 4
P 1
GLS 1
TO DRAIN
REGULATED AIR

FIGURE 11 - SCHEMATIC DIAGRAM OF GAS MIXING APPARATUS

TRACOR DWG 86-164-5
2/17/69 JM / LOWELL

3.4.2 Experimental Procedure

The particle size of all of the samples studied was -170 +325 mesh (44-88 microns). Usually a 10-50 mg sample was mixed well with 1.0-1.1 g of inert alumina in the sample holder. The weight of sample and alumina were determined by difference using a Mettler Type B6 analytical balance. The alumina used as an inert had been fired and did not react with SO_2. Dilution of the sample kept the particles separated and thus provided good gas-solid contact and thermal homogeneity.

The average total flow to the sample was 250 cm^3/min. The sample size was kept small enough that the reaction rate was not limited by the rate of SO_2 supply. The experimental conditions used corresponded to a differential reactor.

The temperature range of interest for each compound was determined by making a linear temperature programmed run using a simulated flue gas atmosphere. The composition of the atmosphere is shown below.

Component	Mole Per Cent
SO_2	0.3
CO_2	14.3
O_2	3.4
H_2O	2.0
N_2	balance

The sample was heated at 10°C/min until a measurable weight gain occurred. This experiment indicated at what temperature the reaction of the metal oxide with SO_2 "started", or became fast enough to give a measureable weight gain, and at what temperature the product began to decompose.

Two or more isothermal runs were then made at temperatures within the range as determined above. The thermal balance was mass calibrated before each run by hanging known weights on the sample holder and adjusting the amplifier. A fresh sample was used for each run. The sample was heated in a nitrogen atmosphere at 20°C/min until the chosen temperature was reached. The temperature was then held constant by the Recorder-Controller. After thermal equilibrium was established, H_2O, CO_2, and O_2 were admitted to the gas stream. When a straight baseline (zero weight change) was obtained on the strip chart recorder, SO_2 was added to the gas mixture. The atmosphere thus obtained was the same as that given above. This procedure ensured that the weight gain measured would be due to sulfite or sulfate formation rather than carbonate or hydroxide formation or oxidation of the metal oxide.

Zero time for the reaction was taken as the point at which the weight gain began. The run was continued until there was little or no further weight gain. The temperature range of the reaction was recorded on the X-Y recorder as a horizontal of the weight change vs temperature graph. In most cases there was no more than ± 1°C variation in temperature. The SO_2 concentration of the stream was determined during each run by titration of a known amount of iodine (Reich's test).

The procedure used for the determination of the rate dependence on the partial pressure of SO_2 was the same as above except that the SO_2 concentration was set at 0.12 mole % rather than 0.3 mole %.

3.4.3 Data Analysis

The data obtained from these kinetic measurements were in the form of weight gain, w, as a function of time. The extent of reaction can be better represented as the fractional conversion $\alpha \equiv w/w_0$. Ideally w_0 is the theoretical stoichiometric weight gain. In practice it was found that often the stoichiometry of the reaction was unknown or that the reaction rate became very slow before the stoichiometric weight gain was reached. In these cases the highest ratio of maximum weight gain to initial sorbent weight, m_o, observed for a given compound was used to calculate w_o. The calculations for the other runs of the same compound were then based on the ratio w_o/m_o which is given in Table IX in Section 3.5.

The rate of product formation can be defined as $\frac{d\alpha}{dt}$. In isothermal conditions the reaction rate should depend only upon the fraction reacted and the partial pressure of SO_2. This is expressed in Equation (13) where k is the rate constant and $g(P_{so_2})$ is the

$$\frac{\partial\alpha}{\partial t} = k\ f(\alpha)\ g(P_{so_2}) \tag{13}$$

dependence on SO_2 partial pressure. Equation (13) can be written as Equation (14), since P_{so_2} was constant in the experiments.

$$\frac{d\alpha}{dt} = k'\ f(\alpha) \tag{14}$$

The analytical form of $f(\alpha)$ depends upon the mechanism of the reaction. For our purposes the general form

$$f(\alpha) = (1-\alpha)^n \tag{15}$$

has been most often used. In Equation (15), n is the order of reaction with respect to the solid reactant. The values 0, 1/3, 1/2, 2/3, 1, 3/2, and 2 have been used for n. The form derived by assuming that the rate is controlled by diffusion of the gaseous reactant through the solid product to the unreacted core has also been used. This form, given in Equation (16), is referred to as DCE for Diffusion Controlled Equation.

$$f(\alpha) = \frac{(1-\alpha)^{1/3}}{1 - (1-\alpha)^{1/3}} \tag{16}$$

The basis for these various forms of $f(\alpha)$ will be discussed in Section 3.5.

The rate equation was applied to the data in its integrated form. The integrated form of $f(\alpha)$ is given in Equation (17).

$$I(\alpha) = \int_0^{\alpha} \frac{d\alpha}{f(\alpha)} = k' t \qquad (17)$$

The integrated forms of $f(\alpha)$ are listed below for each value of n.

n	$I(\alpha)$
0	α
1/3	$3/2\left[1 - (1-\alpha)^{2/3}\right]$
1/2	$2\left[1 - (1-\alpha)^{1/2}\right]$
2/3	$3\left[1 - (1-\alpha)^{1/3}\right]$
1	$-\ln (1-\alpha)$
3/2	$2\left[\frac{1}{(1-\alpha)^{1/2}} - 1\right]$
2	$\frac{\alpha}{1-\alpha}$
DCE	$1/2\left[1 - 3(1-\alpha)^{2/3}\right] + (1-\alpha)$

The $I(\alpha)$ which corresponds to the proper or "best" $f(\alpha)$ should yield a straight line with slope k' when plotted versus time. The Univac 1108 computer was used to calculate the values of $I(\alpha)$ for each value of n from the weight gain data. About

50-100 weight gain-time points were taken from the strip chart recording for each isothermal run.

The computer first plotted the values of each form of $I(\alpha)$ versus t. The value of n which gave the best straight line was determined by inspection. The slope k' of the least squares regression line for the "best" n was computer calculated and the data and line were again plotted by the Calcomp plotter. An example for copper oxide with n = 1/3 is given in Figure 12. The plots of $I(\alpha)$ versus t for each of the compounds investigated are given in Section 8.2.3.

It was found that the SO_2 partial pressure dependence of the reaction rate could be satisfactorily represented by Equations (18) and (19).

$$g(P_{so_2}) = P^m_{so_2} \tag{18}$$

or

$$\frac{\partial\alpha}{\partial t} = k\ f(\alpha)\ P^m_{so_2} \tag{19}$$

The exponent m is the reaction order with respect to SO_2. This quantity was determined by calculating k' for two runs at the same temperature but different SO_2 partial pressures and noting that

$$k_i' = k\ P^m_{i_{so_2}} \tag{20}$$

where $m = \dfrac{\log\ (k_1'/k_2')}{\log\left(P_{1_{so_2}} \middle/ P_{2_{so_2}}\right)}$.

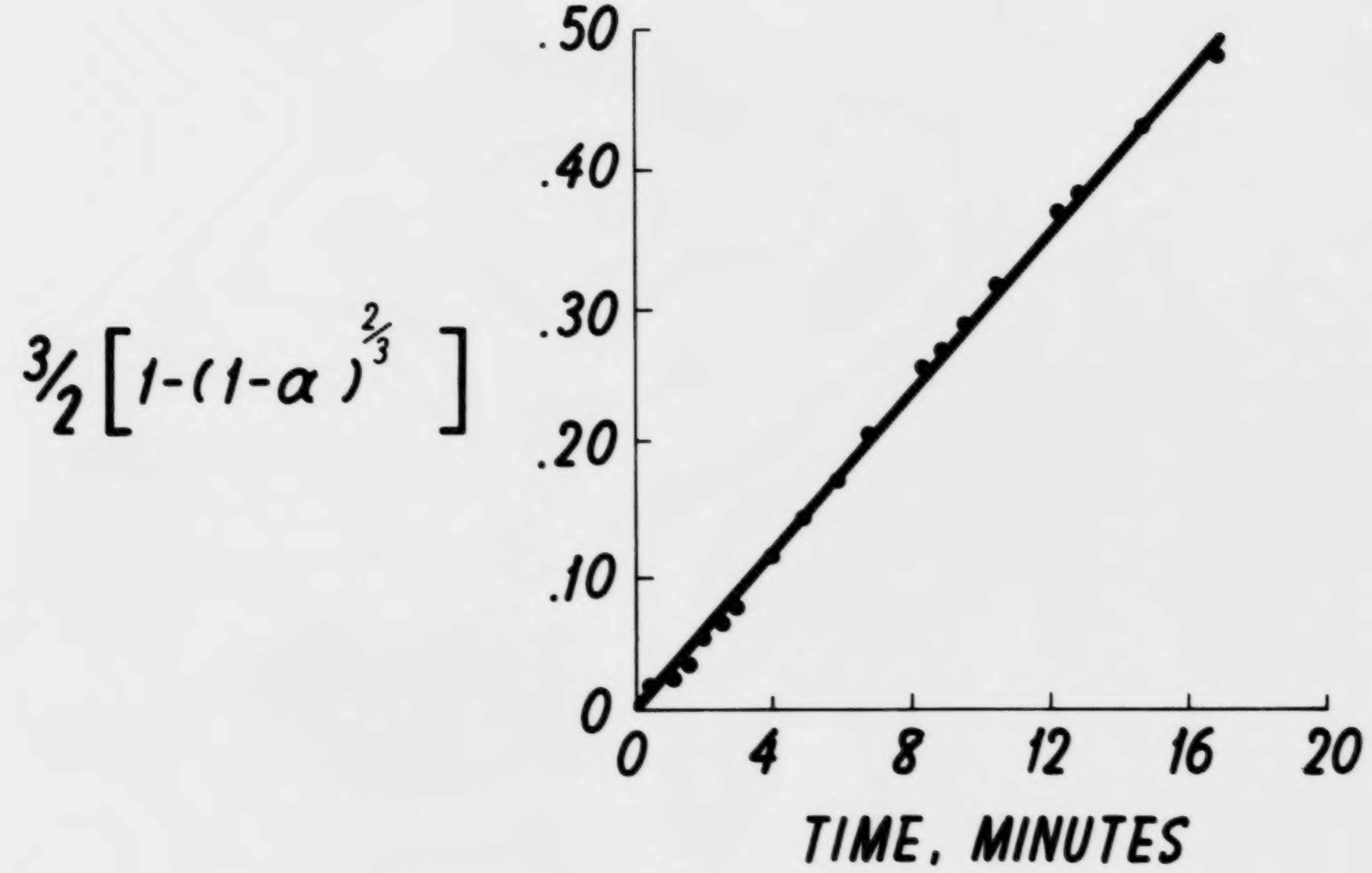

REPRESENTATION OF RATE DATA FOR COPPER OXIDE AT 404°C
SLOPE = RATE CONSTANT (k)

FIGURE 12

Once m was known, k was easily calculated from Equation (20). In these experiments P_{SO_2} (in atm) was numerically equal to the measured concentration of SO_2 since the sample holder was at atmospheric pressure.

3.4.4 Input to Economic Studies

The data obtained from kinetic studies must be used to describe the reaction rate in the fluidized bed model used for economic calculations. The rate quantity of interest in the fluidized bed calculations is the rate at which the SO_2 concentration can be lowered to a specified level as the flue gas passes through the bed at a specified flow rate. This rate will be a function of the steady-state degree of conversion or loading of the well-mixed solids in the bed. Thus the fluid bed design was based on the following equation for the rate of SO_2 removal given by Kunii and Levenspiel (KU-007).

$$-\frac{1}{V_s}\frac{d\,N_{SO_2}}{dt} = K_r\,C_{SO_2} \tag{21}$$

In Equation (21), V_s is the volume of sorbent, N_{SO_2} is the number of moles of SO_2 removed, C_{SO_2} is the concentration of SO_2 in the flue gas, and K_r is the rate constant which is a function of the extent of sorbent conversion. Dependence on SO_2 concentration was found to be linear from the experimental studies.

The rate constant K_r in Equation (21) can be related to the experimentally determined rate constant k by noting that the amount of SO_2 removed from the flue gas equals the amount sorbed by the solid where M is the molecular weight of SO_3 and w is the

$$-\frac{d\,N_{SO_2}}{dt} = \frac{1}{M}\frac{dw}{dt} = V_s\,K_r\,C_{SO_2} \tag{22}$$

weight gain of SO_3 (for sulfate formation). If we substitute P_{SO_2}/RT for C_{SO_2}, Equation (21) becomes

$$\frac{dw}{dt} = M\ V_s\ K_r\ \frac{P_{SO_2}}{RT}\ . \tag{23}$$

The rate equation used in the experimental studies is given in Equation (24).

$$\frac{d\alpha}{dt} = \frac{1}{w_o}\ \frac{dw}{dt} = k\ f(\alpha)\ P_{SO_2} \tag{24}$$

Combining Equations (23) and (24), noting that $V_s = m_o/\rho_s$, and converting k from min^{-1} to sec^{-1} with the factor 60 yields the required expression for K_r.

$$K_r = \frac{k\ f(\alpha)\ \rho_s\ RT\ w_o}{60\ M\ m_o} \tag{25}$$

In Equation (25) m_o, w_o, and $f(\alpha)$ have been defined in Section 3.4.3, ρ_s is the density of the sorbent (g/cm^3), R is the gas constant (cm^3 atm mole^{-1} °K^{-1}), and T is the temperature (°K). The value for the extent of conversion (α) used in $f(\alpha)$ for the K_r calculation was determined by inspection of the kinetic data. A large value of α is desirable for obtaining low sorbent recirculation rates and for efficiency. However, the reaction rate often decreases drastically at higher values of α. Thus an α was chosen which was just below the region in which the reaction rate became slow.

In summary, the values input to the Economic Studies were the rate constant K_r, temperature of reaction, and extent of conversion (sorbent loading).

3.5 RESULTS OF EXPERIMENTAL PROGRAM

The quantitative results of the experimental program are given in Table IX. A discussion of these results and the qualitative findings is given in the following paragraphs.

TABLE IX: RESULTS OF THE EXPERIMENTAL PROGRAM

COMPOUND	PREPARATION METHOD	X-RAY DIFFRACTION PATTERN	BET SURFACE AREA m^2g^{-1}	KINETIC DATA FOR SO_2 SORPTION									SO_2 SORPTION PRODUCTS FROM X-RAY DIFFRACTION
				n	$\frac{W_s}{W_o}$	T(°C)	k'^a	m	$P_{SO_2}{}^b$	k^c	E^d	A^e	
COPPER OXIDE 634-47-1	THE OXIDE WAS PREPARED BY PRECIPITATION OF THE HYDROXIDE FROM THE SULFATE. THE HYDROXIDE WAS HEATED IN THE VACUUM OVEN AT 55°C FOR 44.5 HOURS.	THE PATTERN AGREED WITH THAT OF CuO. THE PEAKS WERE BROAD, INDICATING SMALL CRYSTAL SIZE OR AMORPHOUS CHARACTER.	52.04	1/3	1.01	325	0.00209	1	0.313	0.668	26.9	4.27×10^{8}	$CuSO_4 . CuO$ $CuSO_4 . 3H_2O$ (PROBABLY FORMED ON COOLING SAMPLE AFTER RUN).
						352	0.00642		0.299	2.15			
						355	0.00473		0.316	1.50			
						376	0.01140		0.308	3.70			
						404	0.02850		0.306	9.31			
						482	0.11100		0.314	35.4			
						404	0.01120		0.122	9.18			
COBALT OXIDE 634-43-1	THE OXIDE WAS PREPARED BY CALCINATION OF THE NITRATE FOR 3 HOURS AT 350°C AND 3 HOURS AT 100°C IN VACUO.	THE PATTERN AGREED WELL WITH THAT FOR Co_3O_4. THE PEAKS WERE SHARP AND WELL DEFINED.	12.05	1	0.380	453	0.0200	1	0.318	6.29	19.4	4.36×10^{8}	β-$CoSO_4$ Co_3O_4
						544	0.0916		0.326	28.1			
						453	0.00864		0.129	6.70			
				1	0.931	453	0.00671		0.318	2.11	19.2	1.24×10^{8}	
						544	0.0302		0.326	9.26			
COBALT OXIDE 634-71-2	CoO OH WAS PRECIPITATED FROM $Co(NO_3)_2$ SOLUTION AND CALCINED FOR 2.5 HR AT 160°C IN VACUO.	THE PEAKS WERE BROAD AND NOT WELL DEFINED. THE PATTERN AGREED WELL WITH THAT FOR Co_3O_4.	169.1	1	0.931	359	0.00566	1	0.321	1.76	13.9	1.6×10^{8}	β-$CoSO_4$ Co_3O_4
						430	0.0175		0.325	5.38			
TIN OXIDE 634-55-1	THE HYDROXIDE WAS PRECIPITATED FROM $SnCl_4$ AND HEATED IN THE VACUUM OVEN FOR 31 HOURS AT 60°C. THE OXIDE WAS CALCINED AT 150°C FOR 3 HOURS.	NO DIFFRACTION PATTERN WAS OBTAINED USING THE DIFFRACTOMETER.	4.04										
ZINC OXIDE 634-51-1	ZINC HYDROXIDE WAS PRECIPITATED FROM THE SULFATE AND HEATED IN THE VACUUM OVEN FOR 23 HOURS AT 60°C. THE OXIDE WAS CALCINED FOR 1.5 HR. AT 145°C AND 1 HOUR AT 100°C.	DIFFRACTION PATTERN AGREED WELL WITH THAT FOR ZnO. PEAKS WERE SHARP AND WELL DEFINED.	16.46										
NICKEL OXIDE 634-41-1	THE OXIDE WAS PREPARED BY CALCINING THE NITRATE FOR 1 HOUR AT 300°C AND 45 MINUTES AT 380°C	DIFFRACTION PATTERN AGREED WELL WITH THAT FOR NiO. PEAKS WERE SHARP AND WELL DEFINED.	7.02										
NICKEL OXIDE 634-65-2	THE OXIDE WAS PREPARED BY PRECIPITATING THE HYDROXIDE FROM THE NITRATE. THE HYDROXIDE WAS HEATED FOR 18 HOURS AT 70°C IN VACUO, THEN HEATED IN AIR AT 330°C FOR 2 HOURS.	THE DIFFRACTION PAT. AGREED WELL WITH THAT OF NiO. THE PEAKS WERE BROAD.	63.44	1/2	1.07	380	0.000764	1	0.322	0.232	13.5	7.81×10^{7}	$NiSO_4$ NiO
						500	0.00391		0.333	1.17			
						501	0.00157		0.124	1.27			
IRON OXIDE 634-45-1	THE OXIDE WAS PREPARED BY PRECIPITATION OF THE HYDROXIDE FROM THE CHLORIDE. THE HYDROXIDE WAS HEATED AT 55°C IN VACUO FOR 39 HOURS, AT 120°C IN VACUO FOR 1.5 HOURS AND AT 170°C IN VACUO FOR 2 HOURS.	THE PATTERN HAD VERY BROAD, UNEASILY DISTINGUISHED PEAKS. PROBABLY Fe_3O_4.	225.56	1/3	0.833	342	0.00572	1	0.309	1.85	9.16	3.34×10^{7}	PATTERN OBTAINED WITH DIFFRACTOMETER INCONCLUSIVE. PEAKS BROAD AND NOT WELL DEFINED. REGENERATION PRODUCT CONTAINED Fe_3O_4.
						400	0.0108		0.306	3.53			
						400	0.00368		0.120	3.07			
ALUMINUM OXIDE 634-53-1	THE OXIDE WAS PREPARED BY PRECIPITATION OF THE HYDROXIDE FROM THE CHLORIDE. PRODUCT WAS DRIED IN VACUO FOR 50 HOURS AT 60°C. THE OXIDE WAS CALCINED FOR 3 HOURS AT 280°C.	THE PATTERN OBTAINED WITH THE DIFFRACTOMETER HAD NO PEAKS.	322.54										
ZIRCONIUM OXIDE 634-63-1	THE OXIDE WAS PREPARED BY PRECIPITATING THE HYDROXIDE FROM THE SULFATE. THE HYDROXIDE WAS DRIED IN THE VACUUM OVEN AT 60°C FOR 24 HOURS AND THE OXIDE WAS CALCINED AT 400°C FOR 2 HOURS.	THE PATTERN OBTAINED WITH THE DIFFRACTOMETER HAD NO PEAKS.	4.45										
ANTIMONY OXIDE 634-67-1	THE HYDROXIDE WAS PRECIPATED FROM THE PENTACHLORIDE, DRIED AT 70°C FOR 15 HOURS AND CALCINED AT 275°C FOR 2 HOURS.	THE PATTERN AGREED WELL WITH THAT OF Sb_2O_5. THE PEAKS WERE BROAD AND NOT WELL DEFINED.	18.28										

UNITS: a min^{-1} b atm $\times 10^{2}$ c $min^{-1}\,atm^{-m}$ d kcal/mole e $min^{-1}\,atm^{-m}$

CA-100-67

TABLE IX: EXPERIMENTAL RESULTS (CONTINUED)

COMPOUND	PREPARATION METHOD	X-RAY DIFFRACTION PATTERN	BET SURFACE AREA m^2g^{-1}	KINETIC DATA FOR SO SORPTION									SO_2 SORPTION PRODUCTS FROM X-RAY DIFFRACTION
				n	$\frac{w_s}{m_0}$	T(°C)	k'^{a}	m	$P_{SO_2}{}^{b}$	k^{c}	E^{d}	A^{e}	
CERIUM OXIDE 634-37-1	THE HYDROXIDE WAS PRECIPITATED FROM AMMONIUM HEXANITRATE CERATE $[(NH_4)_2Ce(NO_3)_6]$ AND DRIED IN VACUO AT 60°C.	THE DIFFRACTION PATTERN WAS QUITE BROAD AND THE PEAKS ALMOST UNDEFINED. IT AGREED WITH THAT OF CeO_2.	192.66	2	0.251	194 194 196 238 262	0.0426 0.0122 0.0166 0.0345 0.0504	1	0.315 0.127 0.190 0.318 0.320	13.5 9.60 8.74 10.8 15.8	7.89	2.56X10^{4}	PEAKS BROAD, NOT WELL DEFINED. CeO_2 PRESENT, POSSIBLY $Ce(SO_4)_2 \cdot 4H_2O$ EVIDENCE INCONCLUSIVE
CHROMIUM OXIDE 634-59-2	THE OXIDE WAS PREPARED BY CALCINATION OF $(NH_4)_2CrO_4$ AT 180°C FOR 15 MINUTES.	THE PATTERN AGREED WELL WITH THAT OF Cr_2O_3. THE PRODUCT WAS ALMOST AMORPHOUS AS INDICATED BY THE BROAD PEAKS.	66.52	DCE	0.106	335 390 336	0.00257 0.00481 0.00105	1	0.319 0.312 0.122	0.806 1.54 0.861	9.43	1.89X10^{3}	DIFFRACTION PATTERN OBTAINED WITH DIFFRACTOMETER INCONCLUSIVE. THE PRODUCT APPEARS TO BE AMORPHOUS.
TITANIUM OXIDE 634-69-1	HYDROLYSIS OF $TiCl_4$ WITH $(NH_4)_2SO_4$ SOLUTION. CALCINATION AT 1) 350°C 2 HR. 2) 500°C 2.5 HR. 3) 600°C 3 HR.			A TEMPERATURE PROGRAMMED TGA WAS MADE IN FLUE GAS ATMOSPHERE AFTER EACH CALCINATION BUT NO REACTION OCCURRED.									
VANADIUM OXIDE 634-73-1	NH_4VO_3 SOLUTION + DIL. H_2SO_4 THEN 1) DRYING AT 90°C IN VACUO FOR ~15 HR. 2) HEATING AT 450°C FOR 2 HR.			SEE COMMENT FOR TITANIUM OXIDE									
TUNGSTEN OXIDE 634-61-1	CALCINATION OF H_2WO_4 AT 1) 200°C - 2 HR. 2) 300°C - 3 HR.			SEE COMMENT FOR TITANIUM OXIDE									

UNITS a min^{-1} b $atm \times 10^{2}$ c $min^{-1}atm^{-m}$ d kcal/mole e $min^{-1}atm^{-m}$

With the exception of CeO_2, the metal oxides studied showed low reactivity with SO_2 below a temperature of about 325°C. In this case "low reactivity" means that the time necessary to achieve a significant conversion would be on the order of hours rather than minutes. CeO_2 was unique because sorption was rapid even at 190°C. The behavior of CeO_2 was anomalous in other ways which will be discussed later.

Either the reaction rates of the metal oxides other than CuO, Fe_2O_3, CeO_2, Co_3O_4, Cr_2O_3, and NiO were very low or the oxide did not react at all. The unreactive oxides studied were Al_2O_3, SnO_2, ZrO_2, ZnO, TiO_2, Sb_2O_5, W_xO_y, and V_2O_5. These oxides could possibly be prepared in more active forms than the forms resulting from our preparations. For those unreactive oxides which had low specific surface areas, kinetics experiments were made with large amounts of sample to give about the same surface area as for the reactive compounds. Even under these conditions, the reaction rates were very low. In most cases the reaction rates were too low to make meaningful kinetic calculations. For these reasons attention was concentrated on the reactive oxides and little data are given for many of the others.

3.5.1 Rate Equation and Reaction Orders

A relationship was sought between the reaction rate and the extent of sorbent conversion and SO_2 partial pressure. Equation (26) was chosen for its flexibility, general applicability, and simple representation of the reaction rate (see Section 3.4.3).

$$\frac{\partial\alpha}{\partial t} = k\ (1-\alpha)^n\ P^m_{SO_2} \qquad (26)$$

An alternate approach would have been to attempt to fit the data for each of the metal oxides to each of the many equations arising from idealized solid-gas reaction models. Even this method often does not indicate which is the true reaction mechanism since some of the equations obtained from these models give similar results. The actual reaction mechanism may be intermediate between several reaction models. In view of the difficulties involved Wen (WE-002) has pointed out that there is no reason why simple rate equations which fit the data should not be used as long as no extrapolation beyond the reaction conditions investigated is allowed.

Equation (26) corresponds to several models depending on the value of the reaction order. When surface phenomenon controls the rate of a solid-gas reaction, the order can be shown to vary from zero to two depending on whether the gas reactant is strongly or weakly adsorbed. For $n = 2/3$, $m = 1$, Equation (26) represents the unreacted-core-shrinking spherical particle with constant radius model with the rate controlled by the chemical reaction. For $n = 1/3$, $m = 1$, the equation represents the unreacted-core-shrinking spherical particle with constant radius model with the rate controlled by fluid film resistance (WE-002). For $n = 1$, $m = 1$, Equation (26) represents the continuous reaction for which diffusion of the gaseous reactant into a particle is rapid enough compared with chemical reaction rate that the solid reactant is consumed uniformly throughout the particle. The values for n of 0, 1/2, 1, and 2 have been considered by different authors for gas-solid decomposition reactions (PR-002). In addition to the $n + m$ order rate equation, calculations were also made for the form of $f(\alpha)$ which corresponds to the unreacted-core-shrinking spherical particle with constant radius model with the rate controlled by gaseous diffusion through the porous product layer as shown in Equation (27).

$$f(\alpha) = \frac{(1-\alpha)^{1/3}}{1 - (1-\alpha)^{1/3}} \qquad (27)$$

In most cases the data were well represented by Equation (26). The reaction rates were in general linear ($m = 1$) with respect to SO_2 partial pressure under flue gas conditions (0.1 - 0.3% SO_2). The data for CeO_2 indicated a higher value of m (~1.4), but the evidence was not conclusive. Therefore to maintain consistency with the other metal oxides, the values for CeO_2 were calculated using m = 1. The value of n or f(α) which gave the best fit was found to depend on the metal oxide. This is to be expected since the reaction mechanism may be dependent on physical properties and chemical reactivities which vary from one metal oxide to another. In some cases the "best" apparent reaction order varied with the extent of conversion of the sorbent. This is also to be expected since the rate controlling process may change during the course of reaction. For example the initial rate of reaction may be limited by the rate of chemical reaction. But after a layer of inert reaction product is formed, the rate may be controlled by diffusion of the SO_2 through this barrier. A value of n was chosen which gave the best fit up to a conversion which would be sufficient for use in an SO_2 removal process. Since the true reactivity is best shown in the initial stages of the sorption process, using the value of n and the rate constants obtained for the early stages of the experiments allows a good comparison of the chemical reactivity of the oxides studied.

CuO, Fe_2O_3, and NiO had "low" reaction orders of 1/3, 1/3, and 1/2 respectively. Once again this does not indicate a particular model since the data could have been represented almost as well for these compounds by n = 1/3 to 2/3. It does suggest that the reaction rate was controlled either by chemical reaction or fluid film diffusion or both. For Co_3O_4 the rate was linear (n = 1) with respect to extent of conversion. The reaction rate for ceric oxide, with n = 2, was more strongly dependent on extent of sorbent conversion than the other rates. The data for Cr_2O_3 fit the diffusion controlled Equation (27) after a very brief rapid initial sorption step. The reaction became very slow after a small extent of conversion. Examples of the rate plots obtained are given in Figures 13-18.

RATE DATA FOR COPPER OXIDE
CUO 634-47-1
ISO TGA 4 TEMP = 352 DEG C

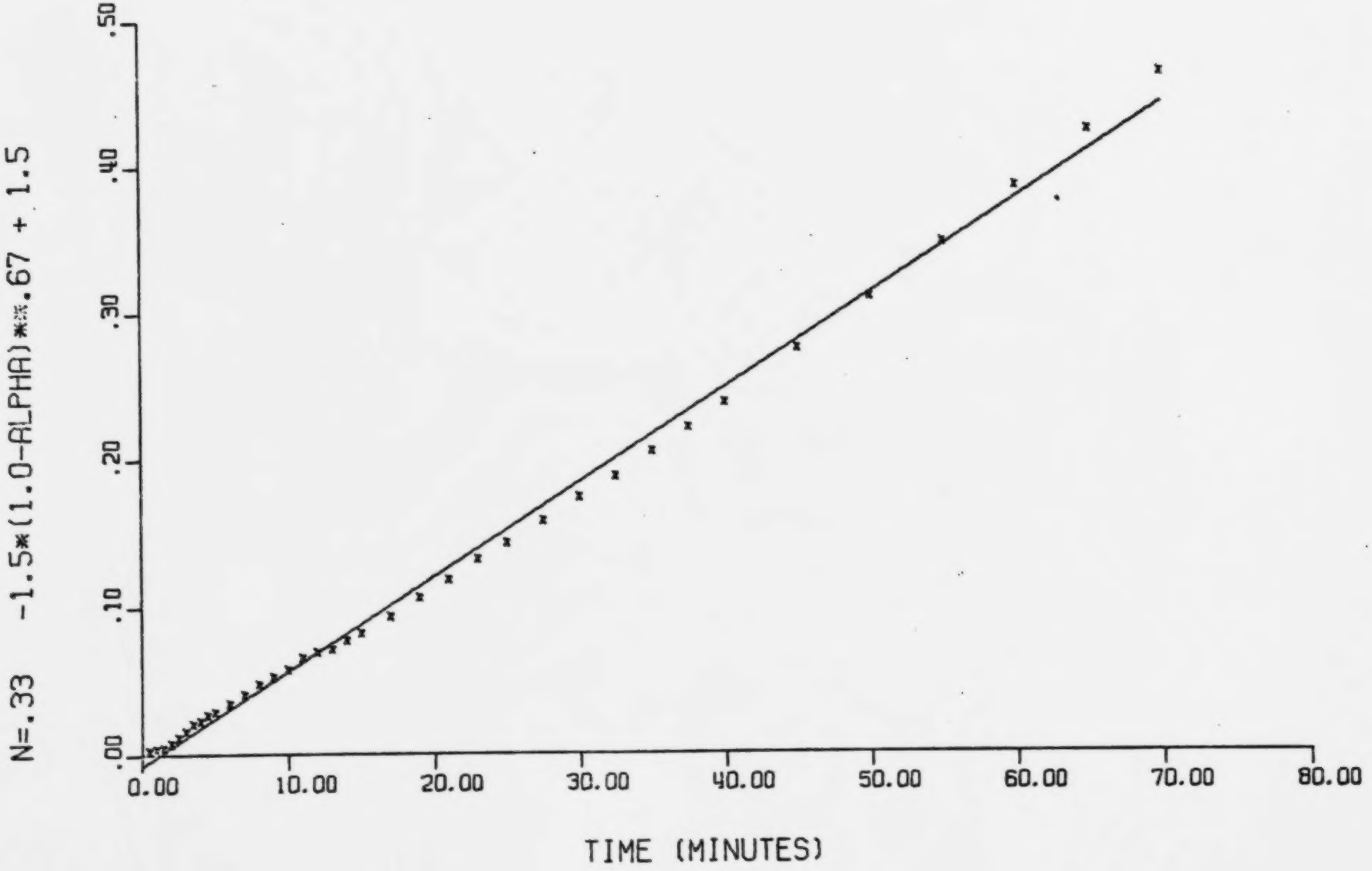

Figure 13

18 APR 69

RATE DATA FOR IRON OXIDE

FE203 634-45-1
ISO-TGA 4 TEMP = 342 DEG C

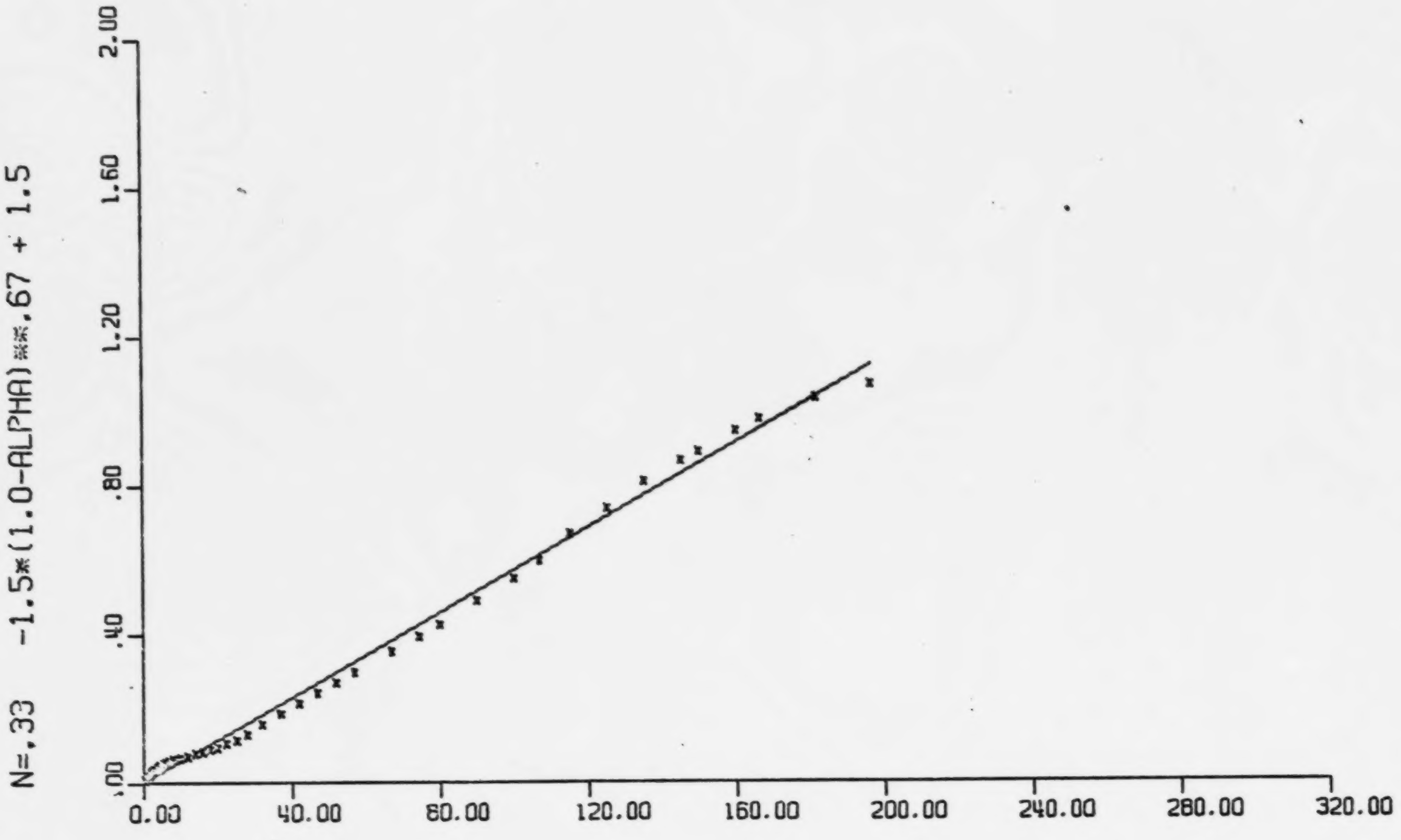

Figure 14

4 JUN 69

RATE DATA FOR NICKEL OXIDE

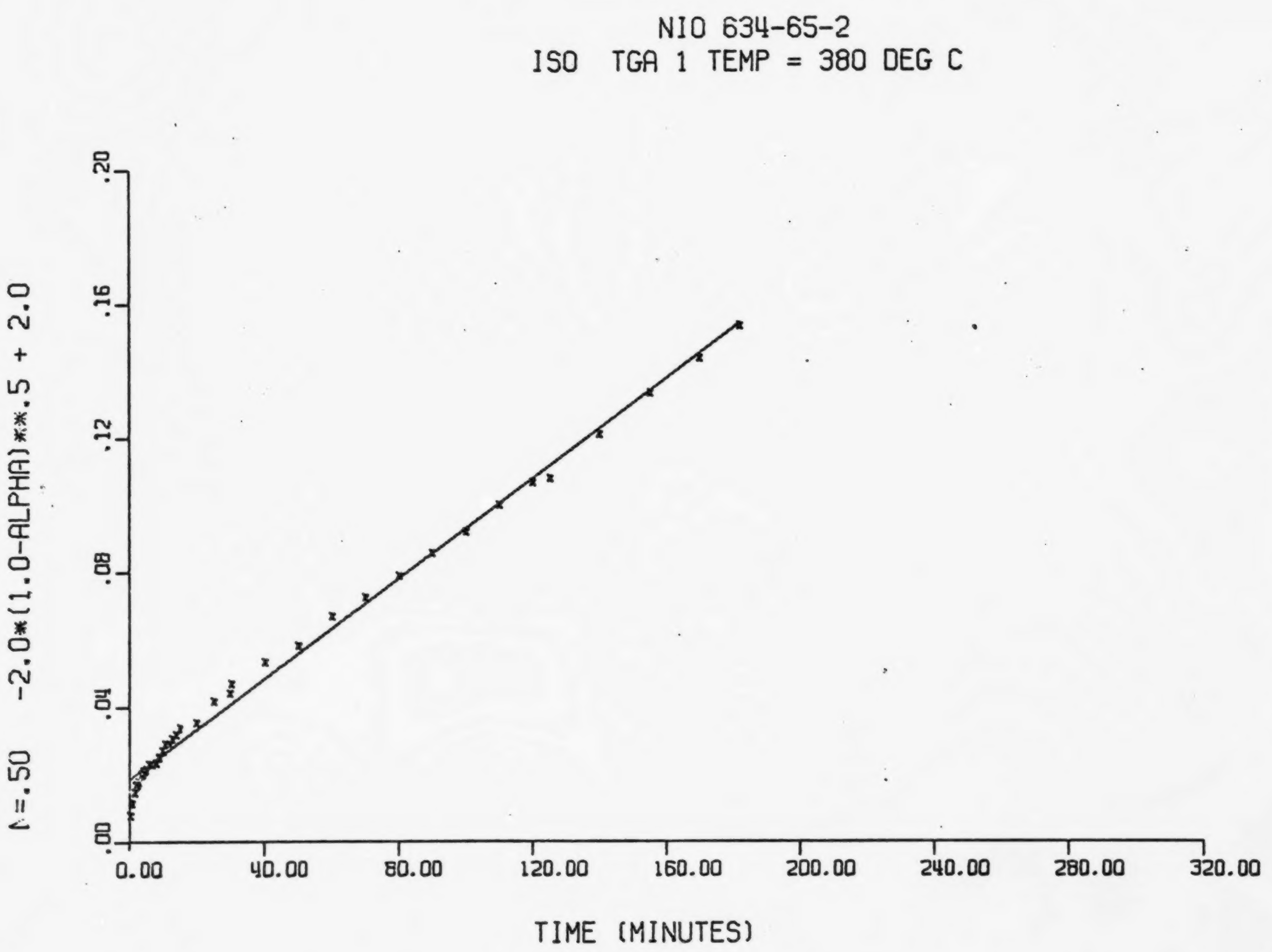

Figure 15

TRACOR

RATE DATA FOR COBALT OXIDE

C0304 634-71-2
ISO TGA 1 TEMP = 359 DEG C

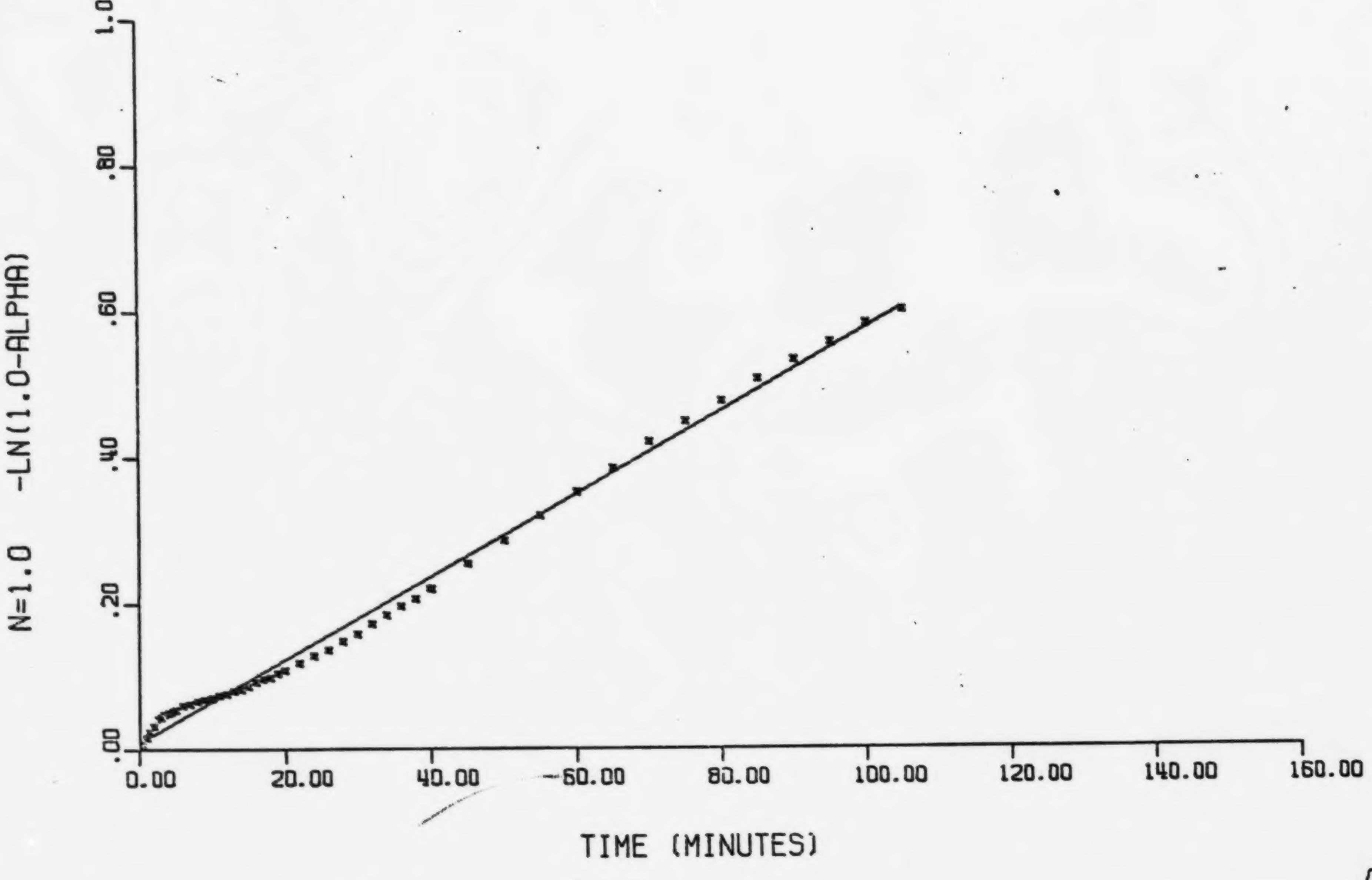

20 MAY 69

Figure 16

TRACOR

RATE DATA FOR CERIUM OXIDE
CEO2 634-37-1
ISO TGA 3 TEMP = 191 DEG C

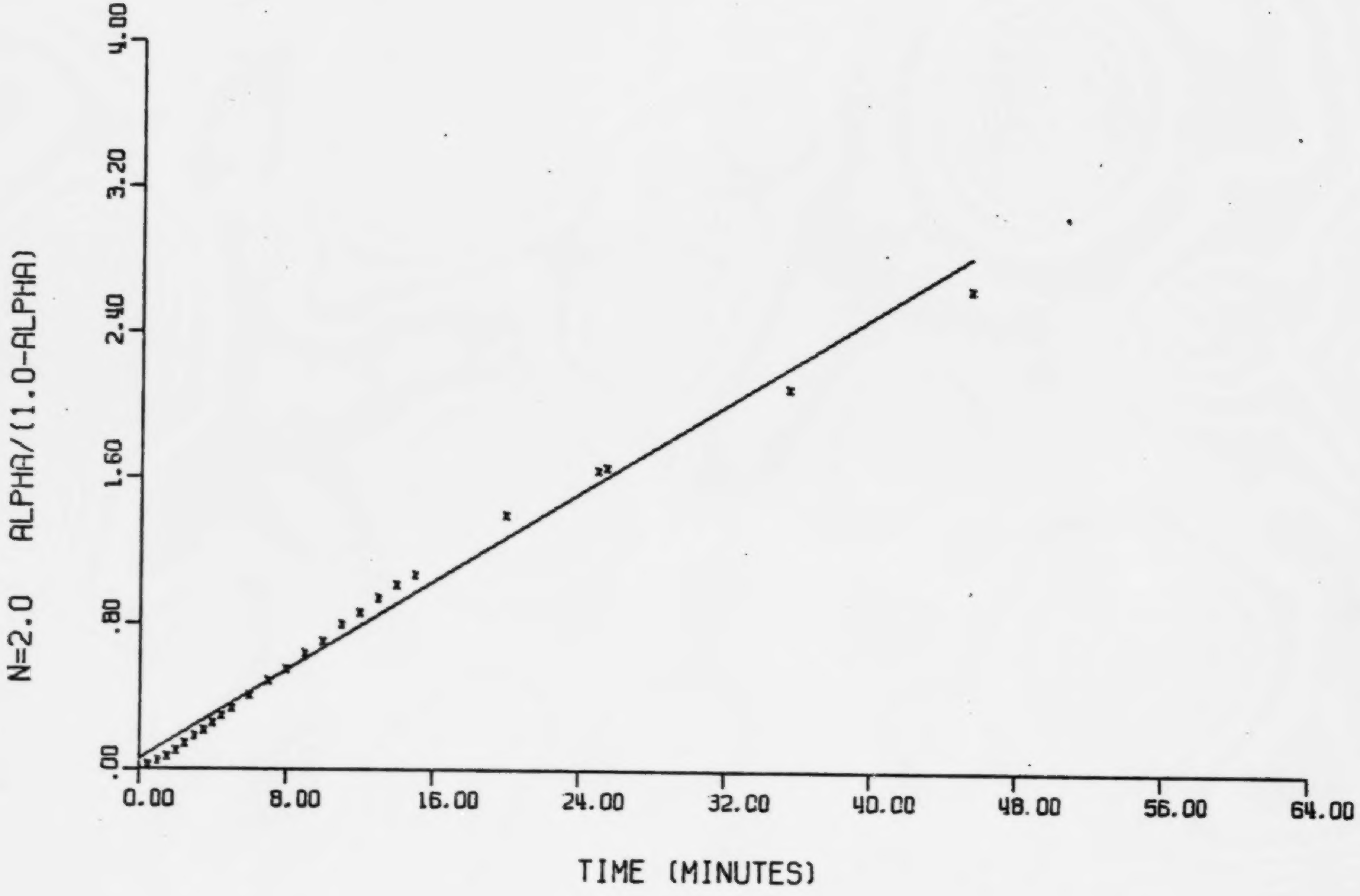

Figure 17

18 APR 69

RATE DATA FOR CHROMIUM OXIDE

CR203 634-59-2

ISO-TGA-2 TEMP = 335 DEG C.

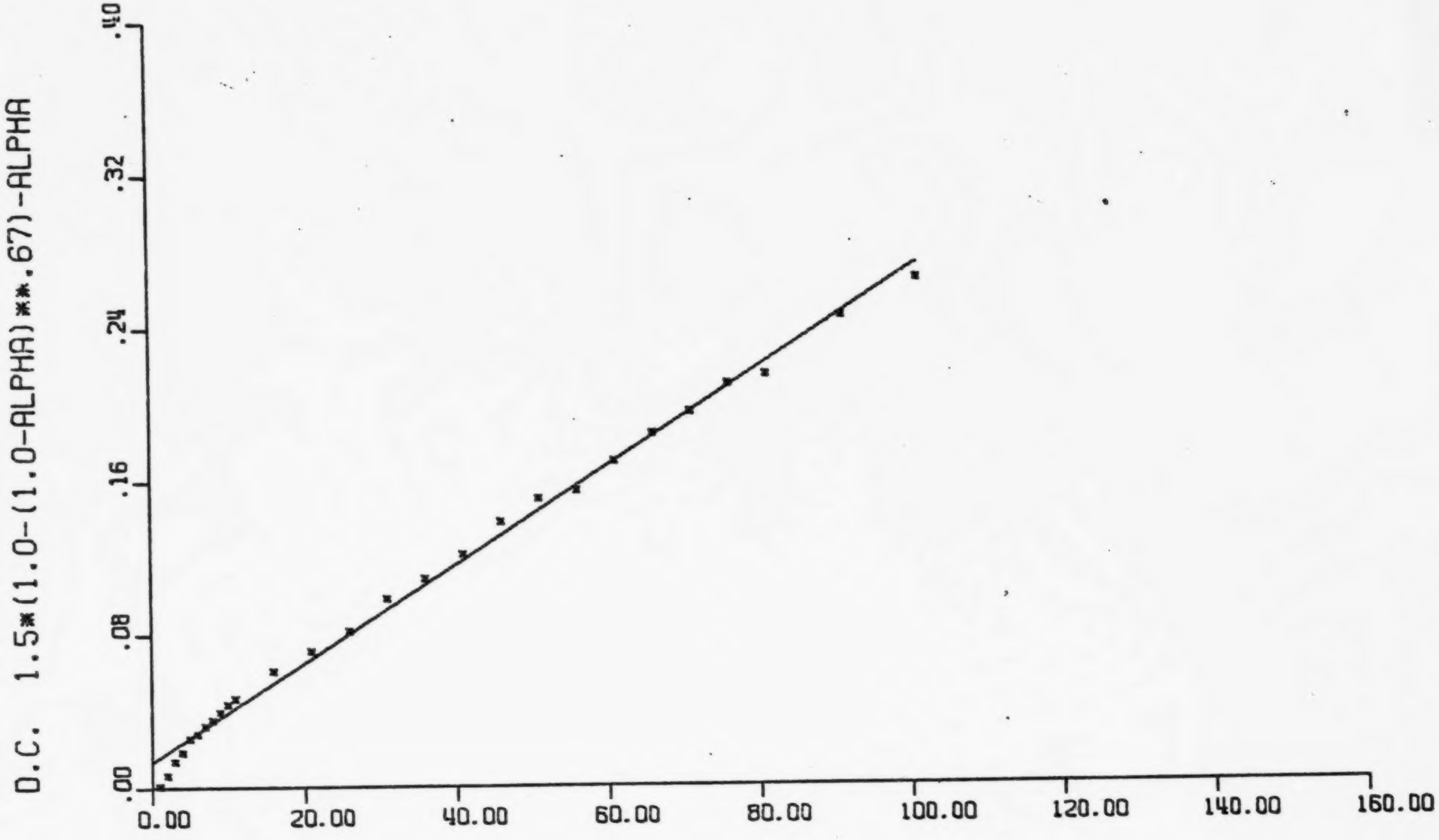

TIME (MINUTES)

Figure 18

14 APR 69

TRACOR

The rate plots are given in Section 8.2.3. The plots used to obtain the rate constants are given along with the plots for each f(α) at a single temperature. For Co_3O_4 prepared by nitrate decomposition, plots are given both for $w_o/m_o = 0.38$, which represents saturation conversion, and for $w_o/m_o = 0.931$, which represents the theoretical conversion for $CoSO_4$ formation. Some of the plots seem to oscillate regularly about the least squares regression line. No attempt was made to study this behavior, but it may be of interest to future investigators. As mentioned above, several of the plots show initial rapid SO_2 uptake immediately followed by a slower continuous weight gain. This is probably due either to initial chemisorption or reaction of a thin outer layer of solid.

3.5.2 Temperature Dependence of the Reaction Rate

The temperature dependence of the reaction rate was another quantity of interest for design purposes. The form of this relationship depends upon whether the reaction rate is limited by the chemical reaction or by mass transfer (diffusion). The Arrhenius Equation (28) can be used when there appears to be strong temperature dependence.

$$k = Ae^{-E/RT} \tag{28}$$

In this equation k is the rate constant, A is the frequency or pre-exponential factor, and E is the activation energy. Due to our incomplete knowledge of the reaction mechanisms, the use of this equation must be interpreted for the present simply as an empirical means of describing the temperature dependence. If the rate controlling step is pore diffusion or bulk diffusion of the gas into the solid, the rate should vary as $T^{1/2}$ and $T^{3/2}$ depending on which diffusion mechanism predominates.

The relative importance of chemical reaction and mass transfer temperature dependence effects may change with temperature and the effects may not always be separable. Therefore, the situation may become very complex. The sorption temperatures used for economic calculations were the same as those at which one of the kinetic runs had been made so that the measured rate constant could also be used. The temperature dependence was strongest for CuO, Co_3O_4, and NiO. The activation energies are all small (less than 27 kcal/mole), however. An Arrhenius plot for CuO is given in Figure 19. The deviation at high temperature may be due to a transition from chemical reaction to diffusion limitation of the reaction rate. Several runs for CeO_2 at about 190°C gave higher rates than those obtained for 240°C. The reaction may be occuring via different paths at different temperatures. The temperature dependence tabulated is for the 240-260°C temperature range only. The temperature dependence for the six metal oxides is summarized in Table IX.

3 5.3 Physical Properties and Reactivity

The effect of compound preparation and resulting physical properties on reactivity of a metal oxide with SO_2 was studied briefly. The surface area and crystallinity of a sample provide a good guide to relative reactivity of different preparations of the same metal oxide. A Co_3O_4 sample prepared by calcination of the nitrate had a surface area of 12 m^2/g and was fairly crystalline, while a sample prepared from CoO·OH had a surface area of 169 m^2/g and was nearly amorphous (see Figure 7, Section 3.3.2). The high surface area, nearly amorphous preparation had a reaction rate nearly three times that of the nitrate preparation. Such comparisons between different compounds must be done with care, however. High surface area and amorphous character do not guarantee reactivity. The Al_2O_3 sample had a surface area of 322 m^2/g and was nearly amorphous according to the X-ray diffraction pattern, but it was nevertheless a poor SO_2 sorbent.

3.5.4 Conclusions

One of the aims of the experimental program was to select the "best" metal oxides on the basis of their chemical reactivity.

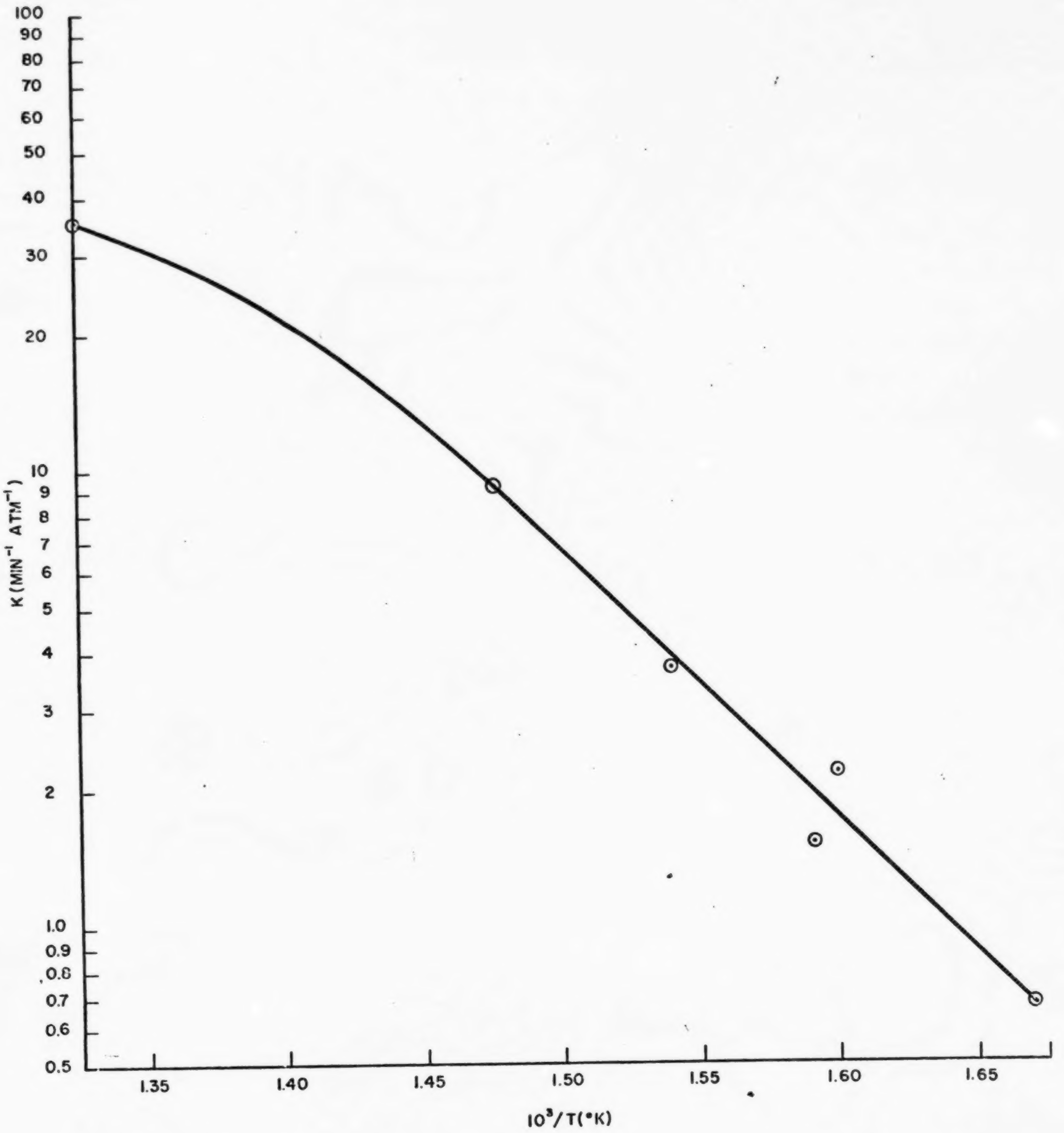

ARRHENIUS PLOT FOR CuO

Figure 19

The six reactive compounds are given in Figure 20. Of these, Cr_2O_3 and NiO can be eliminated for the time being due to their slow reaction rate once a thin layer of reaction product has formed. Thus, these two have only a small practical SO_2 capacity. Co_3O_4 has a fairly high reaction rate and SO_2 capacity. It was found, however, that the reaction product was $CoSO_4$ which is not well suited for thermal regeneration since its SO_3 partial pressure is fairly low even at 800°C. The SO_2 capacity of CeO_2 was low, but its low sorption temperature makes it attractive in that respect. The reaction products could not be identified, however, and more research is needed before it can be recommended. CuO and Fe_2O_3 are both potential sorbents. CuO has a high reaction rate and SO_2 capacity. The reaction stoichiometry is well defined. Fe_2O_3 is somewhat slower and our preparation had a lower SO_2 capacity than CuO. More work is needed also to define the stoichiometry of the reaction.

4. ECONOMIC FEASIBILITY STUDIES

4.1 INTRODUCTION TO ECONOMIC FEASIBILITY STUDIES

The economic feasibility studies involved equipment design, equipment sizing and cost estimation. Process flowsheets including heat and material balances were also prepared. The estimation scheme for determining the total capital investment and gross annual operating cost is shown in Figure 21. The dry metal oxide sulfur oxide removal process is composed of three steps: 1) sorption, 2) regeneration, and 3) sulfur recovery. TRACOR estimated the cost of the sorption and regeneration steps using a fluidized bed contactor model with computer calculated parameters. Cost information for the sulfur recovery step is to be supplied by HEW.

4.2 SORPTION UNIT DESIGN

The major pieces of equipment used in the sorption step are the sorber (see T.M. 004-009-Ch19), draft fan (see T.M. 004-009-Ch12), and sorbent fines collector (see T.M. 004-009-Ch15A).

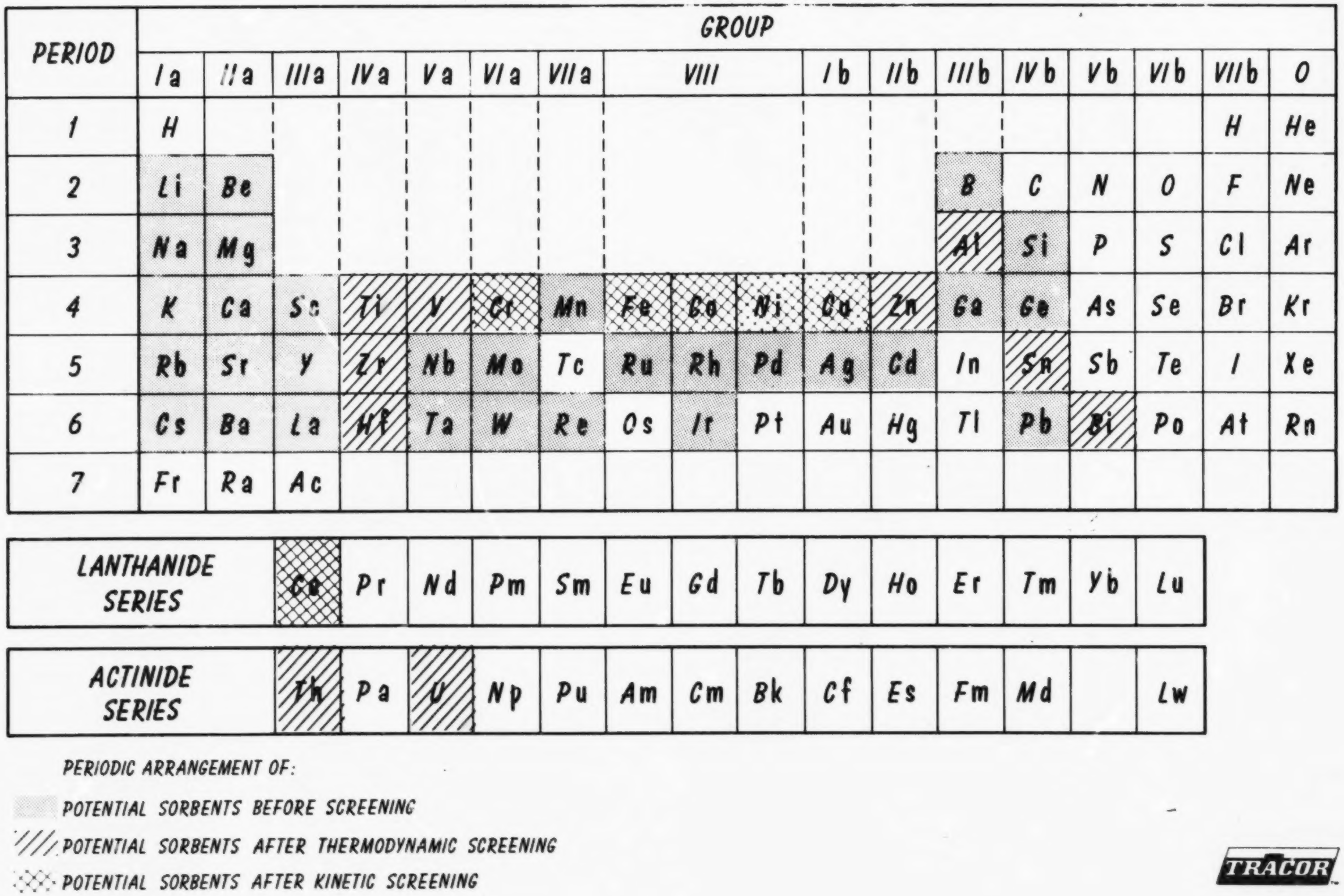

PERIOD	GROUP																	
	Ia	IIa	IIIa	IVa	Va	VIa	VIIa	VIII			Ib	IIb	IIIb	IVb	Vb	VIb	VIIb	0
1	H																H	He
2	Li ▒	Be ▒											B ▒	C	N	O	F	Ne
3	Na ▒	Mg ▒											Al ▨	Si ▒	P	S	Cl	Ar
4	K ▒	Ca ▒	Sc ▒	Ti ▨	V ▨	Cr ▩	Mn ▒	Fe ▩	Co ▩	Ni ▩	Cu ▩	Zn ▨	Ga ▒	Ge ▒	As	Se	Br	Kr
5	Rb ▒	Sr ▒	Y ▒	Zr ▨	Nb ▒	Mo ▒	Tc	Ru ▒	Rh ▒	Pd ▒	Ag ▒	Cd ▒	In	Sn ▨	Sb	Te	I	Xe
6	Cs ▒	Ba ▒	La ▒	Hf ▨	Ta ▒	W ▒	Re ▒	Os	Ir ▒	Pt	Au	Hg	Tl	Pb ▒	Bi ▨	Po	At	Rn
7	Fr	Ra	Ac															

LANTHANIDE SERIES	Ce ▩	Pr	Nd	Pm	Sm	Eu	Gd	Tb	Dy	Ho	Er	Tm	Yb	Lu
ACTINIDE SERIES	Th ▨	Pa	U ▨	Np	Pu	Am	Cm	Bk	Cf	Es	Fm	Md		Lw

PERIODIC ARRANGEMENT OF:

▒ POTENTIAL SORBENTS BEFORE SCREENING

▨ POTENTIAL SORBENTS AFTER THERMODYNAMIC SCREENING

▩ POTENTIAL SORBENTS AFTER KINETIC SCREENING

TRACOR

FIGURE 20

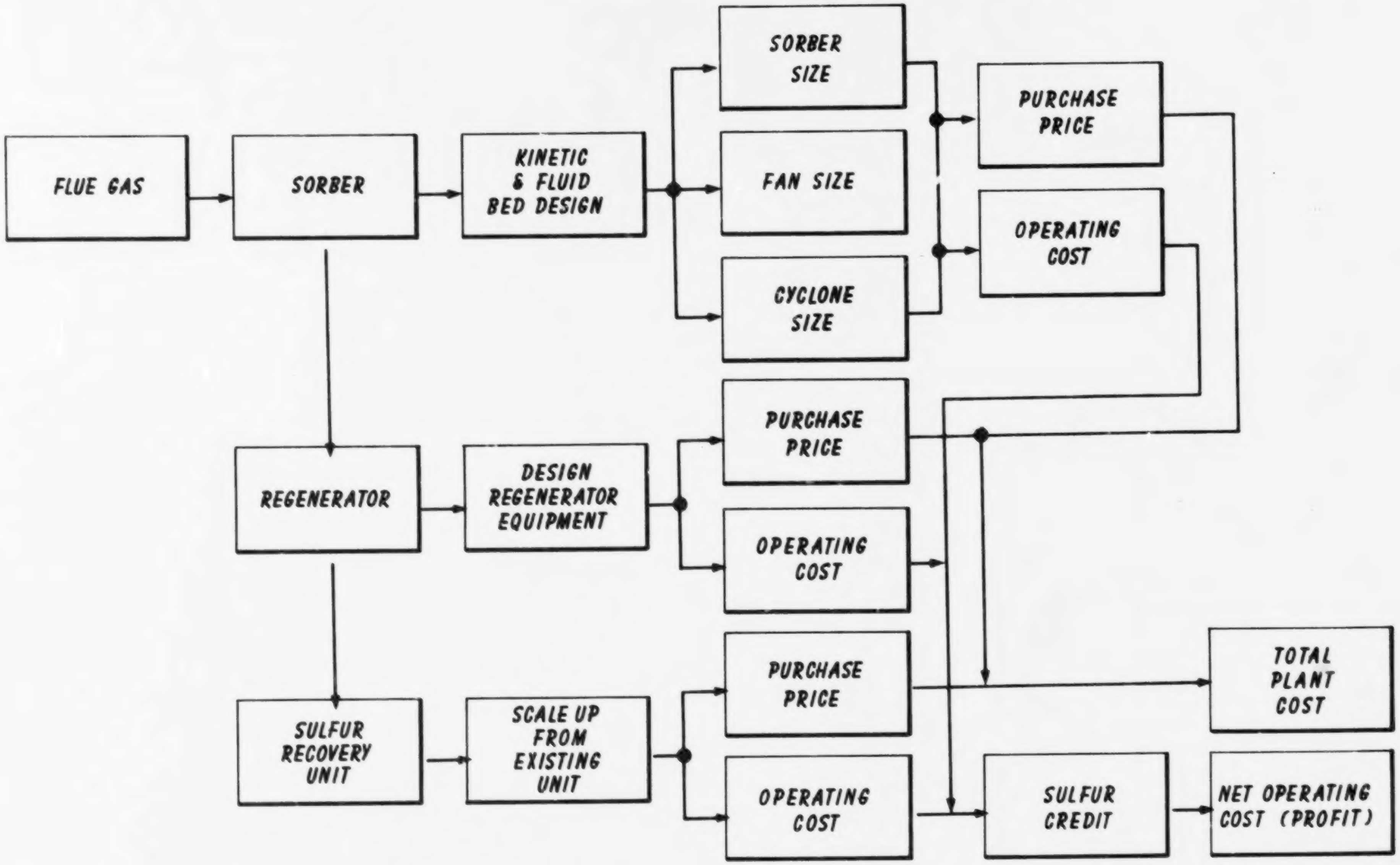
FLUE GAS
SORBER
KINETIC & FLUID BED DESIGN
SORBER SIZE
FAN SIZE
CYCLONE SIZE
PURCHASE PRICE
OPERATING COST
REGENERATOR
DESIGN REGENERATOR EQUIPMENT
PURCHASE PRICE
OPERATING COST
SULFUR RECOVERY UNIT
SCALE UP FROM EXISTING UNIT
PURCHASE PRICE
OPERATING COST
TOTAL PLANT COST
SULFUR CREDIT
NET OPERATING COST (PROFIT)

ECONOMIC STUDY CONCEPT

FIGURE 21

4.2.1 Sorber Design

The most essential piece of equipment used in the sorption step is the sorber, which is composed of a cylindrical shell, elliptical heads, and a gas distributor plate. The type of sorber chosen to be used in making economic studies of dry metal oxide sulfur recovery processes was the fluidized bed.

The fluidized bed model used for the sorber design is based on the bubbling bed model proposed by Kunii and Levenspiel (KU-007, KU-008). This simple three-region model for the gas flow through fluidized beds views uniformly sized bubbles surrounded by clouds and followed by wakes rising through an emulsion of downward moving solids. Interchange of gas occurs continuously between the bubble, cloud-wake, and emulsion regions. The bubble diameter is calculated using equations given by Kato and Wen (KA-004).

The sorber vessel dimensions to be determined were the sorber diameter, height, and shell thickness. The minimum fluidization velocity, U_{mf}, is calculated from equations given by Leva (LE-004). Values of the ratio of superficial gas velocity, U_o, to minimum fluidization velocity, U_{mf}, along with the flue gas flow rates specified by HEW for typical power plant sizes, are used as input parameters to a computer program which sets the required sorber diameter.

The second sorber dimension to be determined is the total vessel height, which is obtained by adding the expanded bed height to the freeboard height. The freeboard height is the height that must be added to the expanded bed height to minimize entrainment losses. The minimum total height was set at one half the vessel diameter to minimize gas distribution problems.

Given the extent of conversion, reaction rate constant (K_r), particle diameter (d_p) and some physical properties of both the gas and solid, the expanded bed height (L_f) can be calculated using the following equation.

$$\ln \frac{C_{Abo}}{C_{Abi}} = -K_r \int_o^{L_f} \frac{\theta dl}{U_b} \qquad (29)$$

where

$$\theta = \gamma_b + \cfrac{1}{\cfrac{K_r}{K_{bc}} + \cfrac{1}{\gamma_c + \cfrac{1}{\cfrac{K_r}{K_{ce}} + \cfrac{1}{\gamma_e}}}}$$

C_{Abi} = concentration of "A" in the inlet gas stream, g-moles/cm^3

C_{Abo} = concentration of "A" in the bubble at the top of the bed, g-moles/cm^3

K_{bc} = interchange coefficient between bubble and cloud, sec^{-1}

K_{ce} = interchange coefficient between cloud and emulsion, sec^{-1}

K_r = reaction rate constant, cm^3 gas/cm^3 solid-sec

l = height of bed above distributor plate, cm

L_f = height of expanded bed, cm

U_b = bubble velocity, cm/sec

γ_b = fraction of solids in bubble

γ_c = fraction of solids in cloud

γ_e = fraction of solids in emulsion

Equation (29) was solved by numerical integration using an iterative method where l was increased until the value for L_f

was obtained. It was found that a limit on the maximum and minimum bubble size was needed for calculating L_f for large fluidized beds.

The third sorber dimension to be determined was the sorber shell thickness. The shell thickness, t, was calculated using Equation (30) from methods set forth in the American Petroleum Institute Standard 650 (AM-001).

$$t = \frac{P_d D_s}{2SE} + C = 2.22 \times 10^{-4} D_s + 0.159 \qquad (30)$$

In Equation (30), P_d is the maximum design pressure, for which a value of 5 psig was used; D_s is the sorber diameter calculated as described earlier; S is the maximum allowable tensile stress, for which a value of 15,000 lb/in² was used; E is the joint efficiency factor, for which a value of 0.75 was used; and C is the corrosion allowance, for which a value of 1/16 in. was used.

The total pressure drop, which is equal to the pressure drop through the fluidized bed plus the pressure drop across the gas distributor plate, must be known in order to determine power requirements and utility costs. Using Equation (31) from Leva (LE-004) the pressure drop across the fluidized bed, ΔP(atm), was calculated.

$$\Delta P = (9.66 \times 10^{-4})(L_f)(1-\varepsilon_f)(\rho_s-\rho_g) \qquad (31)$$

In Equation (31), L_f is the expanded bed height from Equation (29), ρ_s and ρ_g are the densities of the solids and gas, respectively, and ε_f is the bed voidage at expanded height.

In order to prevent channeling effects, Zenz and Othmer (ZE-001) recommended that the pressure drop across the distributor plate be approximately 40% of the pressure drop through the fluidized bed. The distributor plate pressure drop was designed to be within a range of ± 10% of one-third of the fluidized bed pressure drop. The distributor plate was assumed to have holes one-half inch in diameter to limit bubble size growth.

The terminal velocity, U_t, must be compared with the superficial gas velocity, U_o, to determine the extent of entrainment of sorbent particles from the top of the sorber. Equation (32) was used to calculate the terminal velocity.

$$U_t = \left[\frac{\pi\ d_p\ g_c\ \rho_s}{2.28\ C_D\ \rho_g}\right]^{\frac{1}{2}} \tag{32}$$

In Equation (32) d_p is the particle diameter in cm, g_c is 980 cm/sec^2, ρ_s and ρ_g are the solid and gas densities in g/cm^3, and C_D is the drag coefficient.

A computer program, FLUBED, was written to calculate the sorber physical dimensions (height, diameter, and shell thickness) along with the total pressure drop through the system and the terminal velocity. An example of the computer output is given in Table X for the case of a 1400 MW power plant handling 2.5 million SCFM of flue gas using copper oxide as the sorbent.

4.2.2 Draft Fan and Driver Design

It has been shown by Prater and Antonacci (PR-001) that the cost of fans may be estimated from the wheel diameter. The wheel diameter was calculated from the inlet flow rate, fluid density, and pressure rise. The design method is described in detail in T.M. 004-009-Ch12. The type of fan chosen for use in cost estimating was a 1200 RPM, double width, double inlet fan. This type of fan is typical of large power plant installations.

TABLE X: SORBER PHYSICAL DIMENSIONS

```
                                     INPUT FOR FLUIDIZED BED


FLOW RATE (SCFM)                      2500000.000      DENSITY OF SOLID (LBS/FT**3)                100.000
PARTICLE DIAMETER (INCHES)                  .0300      INLET CONCENT. (MOLE PERCENT)                .00300
REACTION RATE (1/SEC)                    97.50000      OUTLET CONCENT. (MOLE PERCENT)               .00015
RATIO- SUPERFICIAL TO MIN. VEL.             9.000      VOL. WAKE / VOL. BUBBLE                        .320
TEMPERATURE (DEG. F.)                     613.000      FRACTION OF SOLIDS IN BUBBLE                   .000
INLET PRESSURE (PSIA)                      14.700


                                     OUTPUT FROM FLUIDIZED BED


FLOW RATE (ACFM)                      5155171.000      INITIAL BUBBLE DIAMETER (FEET)                 .205
DIAMETER OF BED (FEET)                    136.583      FINAL BUBBLE DIAMETER (FEET)                   .326
HEIGHT OF BED (FEET)                        2.675      INITIAL BUBBLE VEL. (FT/SEC)                  7.041
HEIGHT OF VESSEL (FEET)                    68.291      FINIAL BUBBLE VEL. (FT/SEC)                   7.523
THICKNESS OF SHELL (INCHES)                  .427      MIN. MASS FLUX (LBS/HR-FT**2)                89.422
BED PRESSURE DROP (IN. WATER)               4.283      MIN. FLUID VOIDAGE                             .458
DISTR. PRESS. DROP (IN. WATER)              1.441      MIN. FLUID VEL. (FT/SEC)                       .652
TOTAL PRESS. DROP (IN. WATER)               5.724      HOLES/IN.**2 IN DISTR. PLATE                  1.055
OUTLET PRESSURE (PSIA)                     14.493      PARTICLE TERMINAL VEL. (FT/SEC)              11.835
WEIGHT OF SORBENT (LBS)                327088.130      SUPERFICIAL VELOCITY (FT/SEC)                 5.866
FRACTION OF SOLIDS IN CLOUD                 2.731      FRACTIONS OF BUBBLES IN BED                    .846
FRACTION OF SOLIDS IN EMULSION             -2.619
```

The input electrical power required to drive the fan was calculated in order to choose an appropriate electric motor (driver). The horse power rating of the motor must be matched to the maximum horsepower that the fan might require under any flow conditions at the rated speed. This rating is usually about 35% more than the required fan horsepower. Hence, the motor horsepower is given in Equation (33) where BHP is the brake horsepower.

$$MHP = 1.35(BHP) \tag{33}$$

A computer program, FANCST, was written to calculate the sizes of the draft fan and driver. An example of the computer output is given in Table XI. The program is described in T.M. 004-009-Ch23.

4.2.3 Sorbent Fines Collector (Cyclone) Design

The most widely used type of dust-collection equipment is the cyclone separator. A standard cyclone operating with 98% removal efficiency as described by Perry (PE-001) and Bradley (BR-005) was designed using inputs of flow rate and allowable pressure drop.

The cyclone diameter was calculated from a given gas density, flow rate and specified pressure drop (see T.M. 004-009-Ch15A). The remaining cyclone dimensions were then calculated from relationships given by Perry (PE-001) as shown in Figure 22. The inlet rectangular duct was assumed to be one-half a cyclone diameter (Dc/2) long. The outlet duct was assumed to protrude one-half a cyclone diameter (Dc/2). A computer program, CYCLON, was written to calculate the cyclone dimensions. An example of the output is given in Table XII.

TABLE XI: COPPER OXIDE SORBER

```
                                                                              26 JUN 1969
PAGE  7

                                    INPUT VARIABLES FOR FAN COST

  COST INDEX AS OF MAY 5,1969           279.100      TOTAL FAN CAPACITY (ACFM)          5155171.000
  FAN SPEED (RPM)                      1200.000      AIR DENSITY (LBS/FT**3)                   .036
  OVERALL EFFICIENCY                       .850      FAN PRESSURE DROP (IN. WATER)           10.724
  NUMBER OF FAN UNITS                        1.


                                FAN AND DRIVER MOTOR OUTPUT PARAMETERS


                                   INDIVIDUAL FAN UNIT PARAMETERS

  FAN CAPACITY (ACFM)               5155170.999      WHEEL DIAMETER (INCHES)                 91.910
  DRIVER BRAKE HORSEPOWER             10211.362      FAN COST (DOLLARS)                      44245.
  ACTUAL DRIVER HORSEPOWER            14322.974      MOTOR COST (DOLLARS)                   147006.
  FRACTIONAL CAPACITY PER FAN             1.000      EACH FAN UNIT COST (DOLLARS)           191251.

  KILOWATTS REQUIRED BY DRIVER(S)      7614.752      COST - ALL FAN UNITS (DOLLARS)         191251.
```

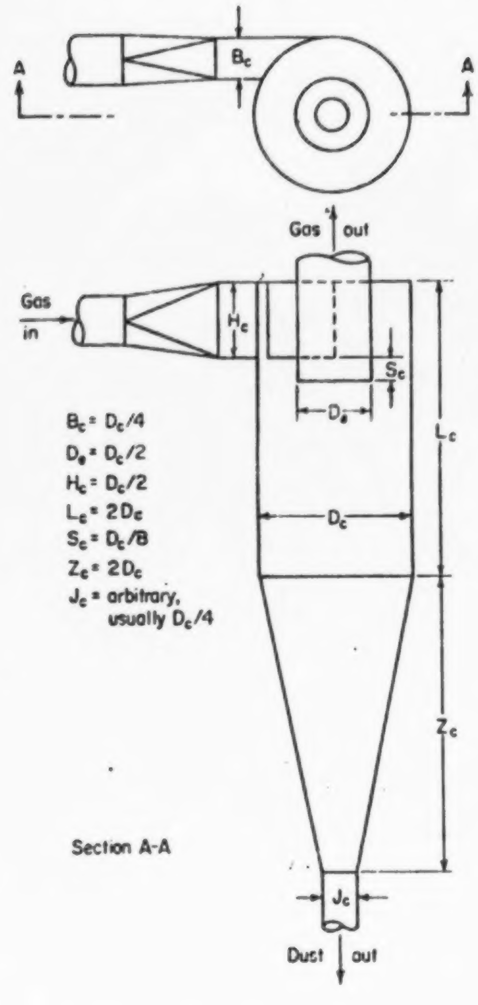
A
A
B_c
Gas out
Gas in
H_c
S_c
D_e
L_c
D_c
Z_c
J_c
Dust out
$B_c = D_c/4$
$D_e = D_c/2$
$H_c = D_c/2$
$L_c = 2D_c$
$S_c = D_c/8$
$Z_c = 2D_c$
J_c = arbitrary, usually $D_c/4$
Section A-A

Figure 22: Cyclone Separator Proportions

Perry, J. H., Chemical Engineers Handbook, 4th Ed., McGraw-Hill, 1963.

TABLE XII: COPPER OXIDE SORBER

```
                                                                                  26 JUN 196
PAGE  5
                                    INPUT PARAMETERS FOR CYCLONE

   CYCLONE REMOVAL EFFICIENCY (%)          98.000         PRESSURE DROP (INCHES WATER)           5.000
   FLUID DENSITY (LBS/FT**3)                 .038         SOLID DENSITY (LBS/FT**3)            100.000
   VISCOSITY (LBS/FT-SEC)                .0000113         WALL THICKNESS (INCHES)                 .250
   EFFECTIVE TURNS                          3.500         CURRENT COST INDEX                   279.100
   INPUT FLOW RATE (ACFM)             5155171.000         NUMBER OF CYCLONES                        4.

                                    OUTPUT PARAMETERS FOR CYCLONE

                                    INDIVIDUAL CYCLONE PARAMETERS

   INPUT FLOW RATE (ACFM)             1288792.700         INLET VELOCITY (FT/SEC)               73.969
   CYCLONE DIAMETER (FEET)                 48.202         CYCLONE WEIGHT (LBS)              363394.790
   PART. SIZE (MICRONS)- 99.% EFF.         59.800         COST OF EACH CYCLONE (DOLLARS)       139578.
   PART. SIZE (MICRONS)- 50% EFF.          35.370

   TOTAL COST OF ALL CYCLONE UNITS        558312.
```

4.3 REGENERATION UNIT DESIGN

The equipment required for the regeneration step consists of a regenerator, draft fans and cyclones. The design and sizing of these pieces of equipment is discussed in the following sections.

4.3.1 Regenerator Design

The gas-solids contactor for the regenerator was designed using the fluidized bed model discussed in Section 4.2.1. The same parameters had to be calculated for the regenerator fluidized bed as for the sorber fluidized bed. However, the required flow rate for the regenerator had not been specified as it had for the sorber. The required flow rate was calculated from the sorbent circulation rate. The sorbent circulation rate was calculated from a material balance around the sorber according to Equation (34), where G_s is the gas feed rate to the sorber in lb moles/hr.,

$$G_s(Y_{1s} - Y_{2s})M_{SO_3} = S(X_1 - X_2) \qquad (34)$$

$Y_{(1,2)s}$ is the mole fraction of sulfur oxides (entering, leaving) the sorber, S is the sorbent circulation rate in lb/hr, M is the molecular weight, and $X_{(1,2)}$ is the sorbent loading (entering, leaving) the sorber in lb.SO_2/lb.sorbent. The sorbent loading factor, X_1, was determined from the extent of conversion data found in the experimental program as described in Section 3.4.4.

The required flow rate, G_R, for the fluidizing medium was then calculated from the sorbent circulation rate S using the following equation.

$$G_R(Y_{1R} - Y_{2R})M_{SO_3} = S(X_1 - X_2) \qquad (35)$$

In Equation (35), the Y's are again the mole fraction of sulfur oxides entering and leaving, and the X's are again the sorbent loading factors It was assumed that the sorbent was only 90% regenerated and that the gas leaving the regenerator contained approximately 6 mole% SO_3, which is a sufficient concentration for operating a contact sulfuric acid plant. From the required flow rate of fluidizing medium, G_R, the regenerator vessel dimensions were calculated using the fluidized bed model computer program FLUBED. Since explicit kinetic rate data were not available for the regeneration step, residence times based on a few regeneration experiments were used to determine a reasonable value for K_r (regeneration) for the fluidized bed model program. An example of the computer output is given in Table XII.

4.3.2 Draft Fan and Driver Design

The same procedure was followed for sizing the draft fans required for the regenerator as was used on the sorber. An example of the computer output for the regenerator fan calculations is given in Table XIV.

4.3.3 Sorbent Fines Collector (Cyclone) Design

The same procedure was followed for sizing the cyclones required for the regenerator as was used on the sorber. An example of the computer output for the cyclone calculations is given in Table XV.

4.4 TOTAL CAPITAL INVESTMENT COST

The basis of computing the capital investment cost is the purchase price of the major pieces of equipment (see T.M. 004-009-Ch11). To the purchase price is added amounts of money to account for the erection cost, piping cost, instrument cost, etc. These items are added as a percent of purchase price. Several investigators (LA-004, HA-002, AR-001) have shown how percentages of the purchase price may be applied to cover the cost of erection, instrumentation, etc. The modified percentage factors given by Lang

TABLE XIII

COPPER XOIDE REGENERATION PHYSICAL DIMENSIONS

```
                                  INPUT FOR FLUIDIZED BED


FLOW RATE (SCFM)                    111500.000        DENSITY OF SOLID (LBS/FT**3)            100.000
PARTICLE DIAMETER (INCHES)              .0300        INLET CONCENT. (MOLE PERCENT)         10.00000
REACTION RATE (1/SEC)                10.00000        OUTLET CONCENT. (MOLE PERCENT)         1.00000
RATIO- SUPERFICIAL TO MIN. VEL.         9.000        VOL. WAKE / VOL. BUBBLE                   .320
TEMPERATURE (DEG. F.)                1377.000        FRACTION OF SOLIDS IN BUBBLE              .000
INLET PRESSURE (PSIA)                  14.700


                                  OUTPUT FROM FLUIDIZED BED


FLOW RATE (ACFM)                    394029.950        INITIAL BUBBLE DIAMETER (FEET)            .229
DIAMETER OF BED (FEET)                  43.110        FINAL BUBBLE DIAMETER (FEET)              .328
HEIGHT OF BED (FEET)                     2.343        INITIAL BUBBLE VEL. (FT/SEC)             5.328
HEIGHT OF VESSEL (FEET)                 21.555        FINIAL BUBBLE VEL. (FT/SEC)              6.310
THICKNESS OF SHELL (INCHES)               .250        MIN. MASS FLUX (LBS/HR-FT**2)           40.074
BED PRESSURE DROP (IN. WATER)            7.036        MIN. FLUID VOIDAGE                        .465
DISTR. PRESS. DROP (IN. WATER)           2.361        MIN. FLUID VEL. (FT/SEC)                  .500
TOTAL PRESS. DROP (IN. WATER)            9.397        HOLES/IN.**2 IN DISTR. PLATE              .483
OUTLET PRESSURE (PSIA)                  14.361        PARTICLE TERMINAL VEL. (FT/SEC)         14.207
WEIGHT OF SORBENT (LBS)              53525.159        SUPERFICIAL VELOCITY (FT/SEC)            4.500
FRACTION OF SOLIDS IN CLOUD              1.567        FRACTIONS OF BUBBLES IN BED               .767
FRACTION OF SOLIDS IN EMULSION          -1.326
```

TABLE XIV

COPPER OXIDE REGENERATOR

```
                          INPUT VARIABLES FOR FAN COST

COST INDEX AS OF MAY 5,1969          279.100       TOTAL FAN CAPACITY (ACFM)          394029.950
FAN SPEED (RPM)                     1200.000       AIR DENSITY (LBS/FT**3)                  .022
OVERALL EFFICIENCY                      .850       FAN PRESSURE DROP (IN. WATER)          14.397
NUMBER OF FAN UNITS                       1.


                    FAN AND DRIVER MOTOR OUTPUT PARAMETERS


                        INDIVIDUAL FAN UNIT PARAMETERS

FAN CAPACITY (ACFM)               394029.950       WHEEL DIAMETER (INCHES)                90.840
DRIVER BRAKE HORSEPOWER             1047.772       FAN COST (DOLLARS)                     42938.
ACTUAL DRIVER HORSEPOWER            1520.960       MOTOR COST (DOLLARS)                   16903.
FRACTIONAL CAPACITY PER FAN            1.000       EACH FAN UNIT COST (DOLLARS)           59841.

KILOWATTS REQUIRED BY DRIVER(S)      781.337       COST - ALL FAN UNITS (DOLLARS)         59841.
```

TABLE XV

COPPER OXIDE REGENERATOR

```
                                INPUT PARAMETERS FOR CYCLONE

CYCLONE REMOVAL EFFICIENCY (%)          98.000          PRESSURE DROP (INCHES WATER)            5.000
FLUID DENSITY (LBS/FT**3)                 .022          SOLID DENSITY (LBS/FT**3)             100.000
VISCOSITY (LBS/FT-SEC)               .00001830          WALL THICKNESS (INCHES)                  .250
EFFECTIVE TURNS                          3.500          CURRENT COST INDEX                    279.100
INPUT FLOW RATE (ACFM)              394029.950          NUMBER OF CYCLONES                         4.


                                OUTPUT PARAMETERS FOR CYCLONE


                                INDIVIDUAL CYCLONE PARAMETERS


INPUT FLOW RATE (ACFM)               98507.487          INLET VELOCITY (FT/SEC)                96.784
CYCLONE DIAMETER (FEET)                 11.650          CYCLONE WEIGHT (LBS)                21228.051
PART. SIZE (MICRONS)- 98.% EFF.         30.430          COST OF EACH CYCLONE (DOLLARS)          8154.
PART. SIZE (MICRONS)- 50% EFF.          17.999

TOTAL COST OF ALL CYCLONE UNITS         32614.
```

(LA-004) were used in this study. These factors are given in Table XVI. Although the factors have been criticized as being non-realistic, the Lang factors are still recommended for use in preliminary design cost estimation.

The purchase costs of the fluidized bed contacter, along with the associated cyclones and draft fans, were estimated (see T.M. 004-009-Ch14, Ch15A) for both the sorber and regenerator. The cost of the sorber, regenerator, and cyclones was conviently estimated on the basis of weight of steel required knowing the vessel dimensions. Approximate costs per pound for fabricated steel vessels and the purchase price of steel were taken from cost information supplied by the Graver Tank Company, (f.o.b. Houston, Texas).

The fluidized bed contactors were composed of the following parts:

1. Cylindrical shell (including support)
2. Two elliptical heads
3. Gas Distributor plate
4. Vessel lining-insulation material

The purchase price of the contactor was estimated to be the sum of the costs of the individual pieces of equipment. The cost of the first three parts was determined by the weight of steel required. The cost of the insulation material was obtained from Perry (PE-001).

The size and purchase price of the draft fans were estimated and they compared quite well with the draft fans being used in the city power plants in Austin, Texas.

Also included in the total capital investment for the sulfur removal process was an initial sorbent cost of $1/lb.

The cost data used in this study were updated to current price levels using the Marshall-Stevens cost index factors published

TABLE XVI

INSTALLATION COST FACTORS

NO.	ITEM	LANG FACTOR
1.	Purchased Equipment	1.00
2.	Erection Labor	.25
3.	Foundations and Platforms	.18
4.	Piping	.76
5.	Instruments	.15
6.	Insulation	.08
7.	Electrical	.10
8.	Buildings	.25
9.	Land and Yard Improvements	.13
10.	Utilities	.40
11.	Engineering and Construction	.66
12.	Contractor's Fee	.19
13.	Contingency	.59
14.	Working Capital	10% Fixed Capital

in "Chemical Engineering". The use of these cost index factors is described by Aries and Newton (AR-001).

4.5 GROSS ANNUAL OPERATING COST

The gross annual operating cost for a given process is the sum of all direct, indirect, and fixed charges (AR-001). These costs include such items as labor, plant overhead, utilities, depreciation and insurance. These costs are further defined in Table XVII.

The utility costs (power requirements) were calculated from the total pressure drop through the process. The pressure drop calculations were discussed in Section 4.2.1. Labor costs were estimated using the guidelines set forth by HEW. The heat requirement for the process was calculated from an overall process heat balance.

It was found that the sorber had a small heat credit which was applied to the requirements of the regenerator, thus lowering the amount of heat to be purchased to operate the regenerator. A detailed description of the heat balance calculations is given in T.M. 004-009-Ch26. Other operating costs were determined using percentage factors supplied by HEW. Also included in the operating cost was an attrition loss of 0.05% of the sorbent circulation rate.

4.6 RESULTS

TRACOR estimated the total capital investment and gross annual operating cost along with an overall heat and material balance for the following plants using the two most promising single metal oxide sorbents indicated by thermodynamic and kinetic screening.

Plant Type	Flue Gas Million SCFM	Size MW	Concentration Inlet (ppm)	Concentration Outlet (ppm)
Large Power Plant	2.5	1400	3000	150
Medium Power Plant	0.5	220	3000	300
Smelter Gas Plant	0.02	--	29000	5000

TABLE XVII

COMPONENTS OF GROSS ANNUAL OPERATING COST

DIRECT COSTS	INDIRECT COSTS	FIXED COSTS
Raw Matl's and Chemicals	Payroll Burden	Depreciation
Direct Labor	Plant Overhead	Taxes
Supervision	Packaging & Shipping	Insurance
Maintenance	Waste Disposal	
Plant Supplies		
Utilities		

For the largest power plant, the sorber was designed with several units linked in parallel for efficient use of available space, to allow for operating flexibility, and to decrease the required vessel diameter.

A summary of the results of the economic calculations for the best sorbent for each plant type are given in Table XVIII. An example of the simplified process flow sheet for the CuO process for the large plant is given in Figure 23. Process flowsheets describing all of the above mentioned sulfur oxide removal processes are given in Section 8.2.5 along with their respective heat and mass balances. Cost estimation output for the above plants using copper and iron oxide sorbents is given in Section 8.2.4

The total capital investment for either the copper oxide or iron oxide process for a 1400 MW power plant processing 2.5 million SCFM is $8 million ($6/KW) and the gross annual operating cost is $3 million (0.03¢/KWH). It is recognized that there are other costs that will arise when a more detailed study is done. Some of the possible costs are given in the following list.

1. The regeneration temperature may require the use of stainless steel materials.
2. Costly utility tie-ins due to plant location could occur.
3. Special heat exchange equipment may be required.
4. Sulfur product credit may vary according to market areas.
5. Special valves may be required to regulate gas flow.

The required capital investment for the sulfur oxide removal processes studied by TRACOR, through only a preliminary estimate, appears to be a reasonable one. The operating cost is in the same range as the potential sulfur by-product credit, approximately $3-4 million assuming $35 ton sulfur. In summary, the dry metal oxide sulfur recovery process appears to be economically feasible based on the information derived from this study.

TABLE XVIII

SUMMARY OF COST ESTIMATES FOR THE COPPER OXIDE AND IRON OXIDE PROCESSES

Process Sorbent	Total Capital Investment $ Million			Gross Annual Operating Cost $ Million		
	Large Power Plant	Medium Power Plant	Smelter Gas Plant	Large Power Plant	Medium Power Plant	Smelter Gas Plant
CuO	8.25	1.88	0.351	2.63	0.647	0.238
Fe_2O_3	8.01	1.76	0.279	2.53	0.627	0.226

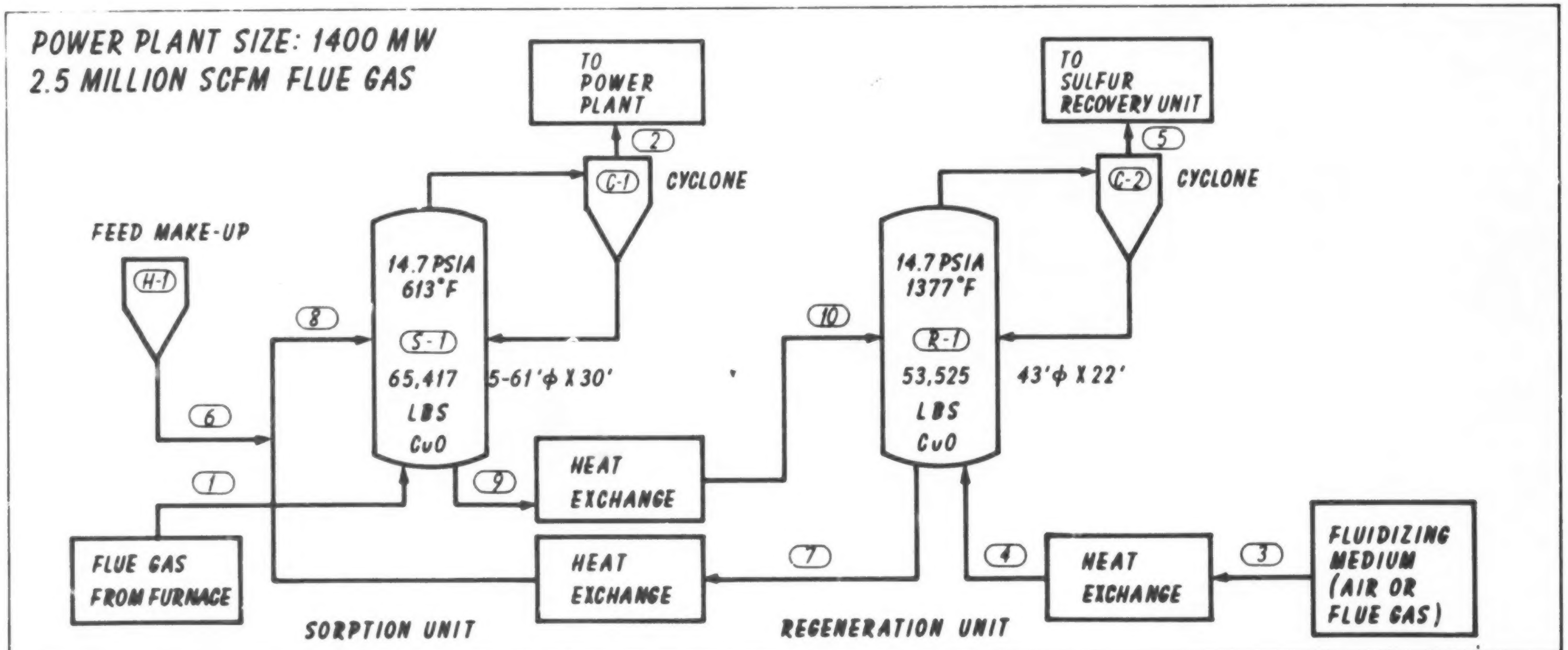
POWER PLANT SIZE: 1400 MW
2.5 MILLION SCFM FLUE GAS
TO POWER PLANT
2
C-1
CYCLONE
TO SULFUR RECOVERY UNIT
5
C-2
CYCLONE
FEED MAKE-UP
H-1
8
6
1
FLUE GAS FROM FURNACE
14.7 PSIA
613°F
S-1
65,417
LBS
CuO
5-61'φ X 30'
9
HEAT EXCHANGE
HEAT EXCHANGE
10
7
14.7 PSIA
1377°F
R-1
53,525
LBS
CuO
43'φ X 22'
4
HEAT EXCHANGE
3
FLUIDIZING MEDIUM (AIR OR FLUE GAS)
SORPTION UNIT
REGENERATION UNIT

COMPONENT / STREAM	①	②	③	④	⑤	⑥	⑦	⑧	⑨	⑩
SO_2, MLB/HR	75.86	3.79	0.17	0.17	0.17					
SO_3, MLB/HR	-	-	-	-	90.09					
N_2, MLB/HR	8285.66	8285.66	371.61	371.61	371.61					
CO_2, MLB/HR	2555.39	2555.39	114.61	114.61	114.61					
H_2O, MLB/HR	515.58	515.58	23.12	23.12	23.12					
O_2, MLB/HR	353.99	335.98	15.07	15.07	15.07					
NO, MLB/HR	5.93	5.93	0.26	0.26	0.26					
TOTAL GAS, MLB/HR	1179241	1170233	524.84	524.84	614.93					
CuO, MLB/HR						0.12507	240.22	240.22	150.68	150.68
$CuSO_4$, MLB/HR							19.91	19.91	199.54	199.54
TOTAL SOLID, MLB/HR						0.12507	260.13	260.13	350.22	350.22
ENTHALPY, MM BTU/HR	1689.81	1680.44	-	194.43	224.41	-	54.28	20.76	30.14	80.43

M = 1000
MM = 1,000,000
ENTHALPY DATUM - 60°F

TRACOR
AUSTIN TEXAS

PROCESS FLOWSHEET DATE - JUNE 30, 1969

A6-164-37

FIGURE 3 PROCESS FLOWSHEET FOR THE COPPER OXIDE PROCESS

5. SUMMARY

The purpose of TRACOR's study for NAPCA was to determine which metal oxides were best suited to the removal of sulfur oxides from flue gases by chemical reaction.

The thermodynamic requirements for efficient sulfur oxide removal and product regeneration were thoroughly investigated. The requirements for the sulfur removal process were determined from the specified outlet concentration of SO_2 in the flue gas and from the requirements of sulfur recovery processes. The specifications were that the logarithm of the equilibrium constant for the decomposition reaction must be less than -3.82 at the sorption temperature and greater than -2.0 at the regeneration temperature. In order to calculate the equilibrium constants, thermodynamic properties of interest were compiled using the Univac 1108 computer for 629 compounds. Properties for about 40% of the compounds had to be estimated. Additional descriptive data such as thermal stability properties were also compiled and used in the thermodynamic screening process. Sixteen thermodynamically favorable sorbents were selected as a result of the screening process. The potential sorbents were the oxides of titanium, zirconium, hafnium, vanadium, chromium, iron, cobalt, nickel, copper, zinc, aluminum, tin, bismuth, cerium, thorium, and uranium.

The kinetic studies were carried out to determine which of the 16 potential sorbents reacted fast enough with SO_2 to be economically feasible. The oxides were prepared in a kinetically active form by calcining a salt which decomposed to the oxide at a low temperature. The sorbents were identified and characterized using x-ray diffraction methods, BET surface area determinations, and chemical analysis. The rate data were collected using an isothermal gravimetric technique whereby weight gain of SO_2 was recorded as a function of time. The experiments were carried out in a simulated flue gas atmosphere.

It was found that six of the potential sorbents had a significant rate of reaction with SO_2. The other sorbents either failed to react or took several hours to achieve a measureable weight gain. An economically feasible residence time is on the order of minutes rather than hours. An economically feasible reaction rate constant, K_r, was found to be greater than 10 sec^{-1}. The oxides of copper, chromium, iron, nickel, cobalt, and cerium had reaction rate constants within this range. Copper and iron oxides were selected as the best potential sorbents, since the other sorbents were complicated by such factors as undefined stoichiometry of the sorption reaction, initial formation of a product layer which slowed the reaction, and low SO_3 partial pressure over the sorption product.

Finally, preliminary design and economic studies were made for a sorber-regenerator system based on a fluidized bed model for the gas-solid contactor The bubbling bed model of Kunii and Levenspiel (KU-007, KU-008) was used, with inputs from the thermodynamic and kinetic studies, to design and size the gas-solid contactor. Draft fans and cyclones were also designed and sized. The capital investment required for the process was estimated based on the purchase prices of the major pieces of equipment with amounts of money added to account for such things as erection costs, piping costs, and instrument costs. The percentage factors given by Lang (LA-004) were used to account for these installation costs.

The gross annual operating costs were determined from percentage factors supplied in HEW guidelines and from power and heat requirements determined from heat and material balances for the process. The metal oxides, CuO and Fe_2O_3, were found to have promise as potential sorbents for an economically feasible sulfur removal process. The preliminary cost estimate of the required capital investment for the dry metal oxide sulfur removal process was \$8 million, and the annual operating cost was estimated to be \$3 million for a 1400 MW power plant.

6. REFERENCES

AM-001 AMERICAN PETROLEUM INSTITUTE STANDARD 650, THIRD EDITION, AMERICAN PETROLEUM INSTITUTE. DIVISION OF REFINING, 1271 AVE. OF AMERICAS, NEW YORK, NEW YORK.(JULY,1966).

AR-001 R. S. ARIES, R. D. NEWTON, CHEMICAL ENGINEERING COST ESTIMATION, MCGRAW-HILL, NEW YORK, (1955).

BR-005 D. BRADLEY, THE HYDROCYCLONE, PERGAMON PRESS, NEW YORK (1965).

DE-006 J. F. DEMPSEY, ED., REMOVAL OF SO2 FROM FLUE GAS, FINAL REPORT, CONTRACT NO. PH 86-67-51, AVCO SPACE SYSTEMS DIVISION, WILMINGTON, MASS., (1967).

ER-001 E. ERDOS. THERMODYNAM. PROP. OF SULFITES,FIRST COMMUN. IN 'COLLECTION CZECHOSLOV. CHEM. COMMUN.,PRAGUE,VOL.27,PP.1428,1437(1962).

GR-002 S. J. GREGG, K. S. W. SING, ADSORPTION, SURFACE AREA AND POROSITY, ACADEMIC PRESS, NEW YORK (1967)

HA-002 W. E. HAND, 'FROM FLOW SHEET TO COST ESTIMATE', PETROLEUM REFINER, VOL. 37, NO. 9, PP. 331-4, (1958).

JA-001 JANAF THERMOCHEMICAL TABLES,THE DOW CHEMICAL CO.,MIDLAND,MICHIGAN, AUG.,1965.

KA-004 K. KATO, C. Y. YEN, 'BUBBLE ASSEMBLAGE MODEL FOR FLUIDIZED BED CATALYTIC REACTORS,' OFFICE OF COAL RESEARCH, PAPER NO. VIII, CONTRACT 14-01-0001-497, (SEPTEMBER, 1968).

KU-001 O. KUBASCHEWSKI, ET AL . METALLURGICAL THERMOCHEMISTRY, PERGAMON PRESS 4TH EDITION (1967).

KU-007 D. KUNII, O. LEVENSPIEL, 'BUBBLING BED MODEL FOR KINETIC PROCESSES IN FLUIDIZED BEDS,' I & E C PROCESS DESIGN AND DEVELOPMENT, VOL. 7, NO. 4, PP. 481-91 (OCT. 1968).

KU-008	D. KUNII, O. LEVENSPIEL, 'BUBBLING BED MODEL FOR THE FLOW OF GAS THROUGH A FLUIDIZED BED,' I & E C FUNDAMENTALS, VOL. 7, NO. 3 PP. 446-52 (AUG. 1968).
KU-009	D. KUNII, O. LEVENSPIEL, FLUIDIZATION ENGINEERING, JOHN WILEY AND SONS, INC., NEW YORK, (1969).
LA-001	KALORISCHE ZUSTANDGROESSEN IN 'LANDOLT BOERNSTEIN',SPRINGER-VERLAG, BERLIN,VOL.2,PART4(1961).
LA-002	W. LATIMER, J. AM. CHEM. SOC., VOL. 73, P. 1480 (1951).
LA-004	H. J. LANG, 'SIMPLIFIED APPROACH TO PRELIMINARY COST ESTIMATION', CHEMICAL ENGINEERING, JUNE (1948).
LE-004	MAX LEVA, FLUIDIZATION, MCGRAW-HILL BOOK CO., NEW YORK, (1959).
MA-006	D. S. MACIVER, P. H. EMMETT, J. AM. CHEM. SOC., VOL. 60, P. 824 (1933).
NB-003	F,ROSSINI,ET AL. SELECTED VALUES OF CHEM. THERM. PROPERTIES, NATL. BUREAU OF STANDARDS, CIRCULAR 500, (1952).
NB-005	SELECTED VALUES OF CHEM. THERM. PROPS., NATNL. BUR. STDS., TABLES FOR FIRST 34 ELEMENTS IN STD. ORDER OF ARRANGEMENT. TN 270-3 (1968).
PE-001	J.H.PERRY. CHEMICAL ENGINEERING HANDBOOK,MCGRAW HILL BOOK CO.,INC., 4TH EDITION(1953).
PR-001	N. H. PRATER, D. W. ANTONACCI, 'ESTIMATE FORCED-DRAFT FAN COSTS,' HYDROCARBON PROCESSING AND PETROLEUM REFINER, VOL. 40, NO. 7, PP. 129-39 (1961).
PR-002	E. A. PRODAN, M. M. PAVLYUCHENKO, 'HETEROGENEOUS CHEMICAL REACTIONS', NAUKA I TEKHNIKA, MINSK, U.S.S.R., P. 20, (1965).

TR-010	THIS VALUE HAS BEEN SELECTED AS THE BEST OF SEVERAL DIFFERENT REPORTED VALUES. SEE TECHNICAL MEMORANDUM 004-009-CH18
WE-002	C. Y. WEN, IND. AND ENG. CHEM., VOL. 60, NO. 9, PP. 34-54 (1968).

7. ABSTRACTS OF TECHNICAL MEMORANDUMS

7.1 Technical Memorandums on Thermodynamic Studies and Preliminary Screening

7.1.1 Technical Memorandums on Estimation of Heat of Formation

T.M. 004-009-Ch1 describes the selection of Erdös' method as the best method for estimation of heat of formation at 25°C and shows how the estimated heats compare with some accepted values.

T.M. 004-009-Ch1A describes in detail the computational method used for estimating heats of formation and its derivation. The heats of formation of the sulfites, titanates, aluminates, chromates, ferrates, vanadates, wolframates, and molybdates for thirty cations estimated from the heats of formation of their sulfates and carbonates are given along with the errors involved in the correlation.

7.1.2 Technical Memorandum on Estimation of Absolute Entropy

T.M. 004-009-Ch5 is a discussion of the selection of Latimer's method as the best for estimation of absolute entropies. A mathematical description of the method, necessary constants for estimating entropies, a comparison of estimated and accepted values, and the correlation errors are given.

7.1.3 Technical Memorandums on Estimation of Heat Capacity

T.M. 004-009-Ch4 is concerned with the selection of the best method for estimating heat capacity as a function of temperature. A comparison of estimated and accepted values for each of the methods studied is given. The uncertainty in equilibrium partial pressures due to errors in heat capacity is also discussed.

T.M. 004-009-Ch9 presents the computational method used to estimate mixed metal oxide heat capacities, describes calculation of the errors involved, and compares estimated and known mixed oxide heat capacities.

T.M. 004-009-Ch13 describes in detail the computational method used to estimate heat capacities of metal sulfides. Estimated and known values are compared. A general mathematical description and derivation for heat capacity estimations of carbonates, sulfates, sulfides and mixed oxides, and the errors involved is given in T.M. 004-009-Ch13A.

7.1.4 Technical Memorandums on the Effect of Errors in Estimated Thermodynamic Properties

T.M. 004-009-Ch2 is a discussion of the uncertainties in calculated equilibrium partial pressures caused by errors in heat of formation and absolute entropy. The uncertainty in calculated equilibrium partial pressures due to errors in estimated heat capacity is discussed in T.M. 004-009-Ch4.

7.1.5 Technical Memorandum on Conflicting Reported Thermodynamic Data

T.M. 004-009-Ch18 is a discussion of conflicting reported values for thermodynamic properties and an explanation of the choices made for accepted values. Conflicting data for 57 compounds were examined. The memorandum is based on 116 references.

7.1.6 Technical Memorandums on Thermal Stability Studies

T.M. 004-009-Ch7 discusses the determination of the most thermodynamically stable form for metal oxides having several oxidation states.

T.M. 004-009-Ch8 gives the results of an extensive literature search concerning the thermal stability of metal sulfates, formation of sulfates by catalytic oxidation of SO_2 and reductive decomposition of sulfates. The memorandum is based on 67 references.

T.M. 004-009-Ch3 is a short discussion of the literature found in early months of the contract concerning sulfite decomposition.

T.M. 004-009-Ch16 gives the results of a comprehensive literature survey and the correlation of all thermodynamic data concerning the interaction of metal oxides and SO_2. The subjects of adsorption with sulfite formation, sulfite decomposition and disproportionation, adsorption on catalytic effective oxides, catalytic oxidation of SO_2, sulfate decomposition, and price and availability of metal oxides are treated.

7.1.7 Technical Memorandum on the Price and Availability of Metal Oxides

T.M. 004-009-Ch6 presents in tabular form data concerning the price per ton, amount of production, amount of consumption, and amount stockpiled for the metal oxides or metals of interest as potential sorbents. The data were obtained mainly from publications of the U. S. Bureau of Mines.

7.1.8 Technical Memorandums on Preliminary Screening of Metal Oxides and Mixed Metal Oxides

T.M. 004-009-Ch16 describes the correlation of thermal data and other information and the selection of 16 potential metal oxide sorbents on the basis of these data.

T.M. 004-009-Ch22 describes the thermodynamic screening process for the "mixed metal oxides." T.M. 004-009-Ch25 gives the results of a theoretical study of the chemistry of the mixed oxides plus a discussion of the problems involved in conducting an experimental program for the mixed metal oxides.

7.1.9 Technical Memoramdum on Computer Programs

T.M. 004-009-Ch23 describes the computer programs written to store, retrieve, correlate, estimate, and print thermodynamic data. It also describes programs written for data analysis of experimentally obtained surface area and kinetic data. Finally, it gives a description of the programs used in the economic feasibility studies to design and size equipment and estimate costs.

7.2 Technical Memorandums on the Kinetic Studies Experimental Program

7.2.1 Technical Memorandums on Design and Operation of Experimental Equipment

T.M. 004-009-Ch10 describes the temperature calibration of the differential thermal analysis apparatus. The calibration was done by recording thermograms of high purity metals with well-defined melting points.

T.M. 004-009-Ch20 is a detailed description of the apparatus designed and built at TRACOR to simulate the composition of flue gas. The gas mixing apparatus is used in connection with the thermal analysis apparatus.

T.M. 004-009-Ch24 describes the apparatus constructed for determining nitrogen adsorption isotherms used for calculation of specific surface area by the BET method.

7.2.2 Technical Memorandums on Collection of Experimental Data and Presentation of Results

T.M. 004-009-Ch24 describes the experimental procedure and methods of data analysis used to determine BET surface areas for metal oxide sorbents.

Bimonthly Progress Report No. 8 gives a complete discussion of the experimental program up to April 30 including a detailed description of the kinetic studies. Compound preparation, compound characterization, surface area determinations, kinetic data collection apparatus and methods, and kinetic data analysis are discussed. Experimental results are tabularized for the metal oxide sorbents.

7.3 Technical Memorandums on Economic Feasibility Studies

7.3.1 Technical Memorandums on Equipment Design, Size, and Purchase Price

T.M. 004-009-Ch19 describes the design of the fluidized bed sorber based on the bubbling bed model of Kunii and Levenspiel. The model allows calculation of the bed height from data on SO_2 removal efficiency, reaction rate constant, particle diameter, and gas and solid physical properties.

T.M. 004-009-Ch14 describes the method used to calculate the sorber purchase price on the basis of the weight of steel required for the cylindrical shell, elliptical heads, and the gas distributor plate. Insulation costs were also included.

T.M. 004-009-Ch15 and the revision T.M. 004-009-Ch15A describe the determination of purchase costs for cyclone dust collectors. The cost was estimated on the basis of weight of steel required which was determined from the vessel dimensions. The vessel dimensions were calculated from gas density, flow rate, and pressure drop.

T.M. 004-009-Ch21 gives the computational procedure for estimating the purchase price of forced-draft fans such as those used to move air through power boilers. The technique is based on estimating the cost of the fan and adding the cost of an electric motor driver.

7.3.2 Technical Memorandums on the Estimation of Capital Investment and Operating Cost

T.M. 004-009-Ch26 describes the determination of heat and material balances around the sorber-regenerator system. These balances are necessary to determine sorbent circulation rate and heat requirements so that operating costs can be estimated.

T.M. 004-009-Ch11 describes the calculation of the Total Capital Investment and the Gross Annual Operating Cost for the sorber-regenerator system. The procedures used are consistent with those outlined in the General Guidelines supplied by the NAPCA. The capital investment is computed from the purchase prices of the major pieces of equipment. The gross operating cost consists of direct, indirect, and fixed costs which are described in detail.